
Doctoral Dissertations

Student Theses and Dissertations

Spring 2015

Dynamic behavior of operational wind turbines considering aerodynamic and seismic load interaction

Mohammad-Amin Asareh

Follow this and additional works at: https://scholarsmine.mst.edu/doctoral_dissertations



Part of the [Civil Engineering Commons](#), and the [Sustainability Commons](#)

Department: Civil, Architectural and Environmental Engineering

Recommended Citation

Asareh, Mohammad-Amin, "Dynamic behavior of operational wind turbines considering aerodynamic and seismic load interaction" (2015). *Doctoral Dissertations*. 2375.

https://scholarsmine.mst.edu/doctoral_dissertations/2375

This thesis is brought to you by Scholars' Mine, a service of the Missouri S&T Library and Learning Resources. This work is protected by U. S. Copyright Law. Unauthorized use including reproduction for redistribution requires the permission of the copyright holder. For more information, please contact scholarsmine@mst.edu.

DYNAMIC BEHAVIOR OF OPERATIONAL WIND TURBINES CONSIDERING
AERODYNAMIC AND SEISMIC LOAD INTERACTION

by

MOHAMMAD-AMIN ASAREH

A DISSERTATION

Presented to the Faculty of the Graduate School of the
MISSOURI UNIVERSITY OF SCIENCE AND TECHNOLOGY

In Partial Fulfillment of the Requirements for the Degree

DOCTOR OF PHILOSOPHY IN CIVIL ENGINEERING

2015

Approved by
William P. Schonberg, Advisor
Jeffery S. Volz
Genda Chen
Mohamed ElGawady
K. Chandrashekhara

© 2015

Mohammad-Amin Asareh

All Rights Reserved

PUBLICATION DISSERTATION OPTION

This dissertation consists of the following three papers, formatted in the style used by the Missouri University of Science and Technology, listed as follows:

Paper 1 (pages 18-44), M.A. Asareh, I. Prowell, J. Volz, and W. Schonberg, “A computational platform for considering the effects of aerodynamic and seismic load interaction for multi-megawatt utility scale horizontal axis wind turbines,” is under review in Earthquake Engineering and Engineering Vibrations, 2014.

Paper 2 (pages 45-73), M.A. Asareh, W. Schonberg, and J. Volz, “Effects of seismic and aerodynamic load interaction on the power generation and structural response of multi-megawatt utility scale horizontal axis wind turbines,” is under review in Renewable Energy, 2015.

Paper 3 (74-110), M.A. Asareh, W. Schonberg, and J. Volz, “Fragility analysis of a 5-MW NREL wind turbine considering aero-elastic and seismic interaction using finite element method,” is under review in Finite Elements in Analysis and Design, 2015.

ABSTRACT

With the advancements in the wind energy production industry, the demand for a cost effective and safe design of wind turbine structures is growing rapidly. The wide deployment of wind turbines in locations with high seismic hazard has lead engineers to take into account a more comprehensive seismic design of such structures. In response to the need for a computational tool that can perform coupled simulations of wind and seismic loads, a seismic module has been developed for the publicly available National Renewable Energy Laboratory (NREL) code, FAST, at the first step of this research. This achievement allows engineers working in this industry to directly consider interaction between seismic and other environmental loads for turbines with a freely available simulation tool. The first paper details the practical application and theory of these enhancements and provides examples for the use of different capabilities. The platform is then used to show the suitable earthquake and operational load combination with the implicit consideration of aerodynamic damping by estimating appropriate load factors.

In the next step, the developed platform is used to evaluate the effects of aerodynamic and seismic load coupling on the power generation and structural dynamics behavior of wind turbines. Various turbine operation scenarios such as (i) normal operational condition, (ii) idling, and (iii) earthquake induced emergency shutdown are simulated to show the differences in generated power and dynamic response of wind turbine structures. The effects of aerodynamic damping and pitch control system are presented which show reduction in the resulting design demand loads.

In the last step, a finite element model of the turbine which is calibrated with the previously implemented code is used to evaluate the fragility of wind turbines under seismic and wind excitation. This is obtained by the assessment of nonlinear dynamic behavior of a 5-MW NREL wind turbine considering different earthquake and wind intensities using the finite element model. Engineering Demand Parameters (EDP) and Intensity Measures (IM) are then obtained from Incremental Dynamic Analysis (IDA) and used to assess the probability of exceeding different Damage States (DS) using fragility curves.

ACKNOWLEDGMENTS

Although this dissertation is individual work, I could have never reached the heights and explored the depth without the help and support of many people.

Firstly, I would like to thank my Advisors Dr. Schonberg and Dr. Volz for instilling in me the qualities of being a good engineer who can plan for an objective and organize tasks and times in advance to achieve the goals.

Secondly, I would like to express my sincere gratitude to Dr. Ian Prowell who introduced me to this topic and in the one year time period that we worked together, I accomplished what one can achieve in a lifetime. I would also like to thank my committee members Dr. Chen, Dr. Elgawady, and Dr. KC for their continuous support and valuable advice and guidance during my study.

Lastly, I would like to thank my friends and family for their love, encouragement, friendship, and support during my PhD years here in Missouri S&T. Without their support I would not have been as successful and proud of myself as I am today. This work is dedicated to my parents who raised me to have a love towards science and research and supported me in all my pursuits.

I would also want to gratefully acknowledge the support of National Renewable Energy Laboratory (NREL) that provided the grant with contract No. DE-AC36-08GO28308, and the help of Dr. Jason Jonkman as the technical monitor for developing seismic module for FAST.

TABLE OF CONTENTS

	Page
PUBLICATION DISSERTATION OPTION.....	iii
ABSTRACT.....	iv
ACKNOWLEDGMENTS	v
LIST OF ILLUSTRATIONS.....	ix
LIST OF TABLES.....	xii
SECTION	
1. INTRODUCTION	1
1.1. EXISTING GUIDELINES IN THE WIND ENERGY INDUSTRY	4
1.2. PREVIOUS RESEARCH ON WIND TURBINE MODELING.....	5
1.2.1. Simple Models	6
1.2.2. Full System Models	6
1.3. LITERATURE ON SEISMIC BEHAVIOR OF WIND TURBINES	8
1.4. RESEARCH OBJECTIVES	13
1.5. ORGANIZATION OF THE DISSERTATION.....	14
REFERENCES	16
PAPER	
I. A COMPUTATIONAL PLATFORM FOR CONSIDERING AERODYNAMIC AND SEISMIC LOAD INTERACTION FOR MULTI-MEGAWATT UTILITY SCALE HORIZONTAL AXIS WIND TURBINES	18
ABSTRACT.....	18
1. INTRODUCTION	19
2. SIMULATION PLATFORM DESCRIPTION	22
2.1. GROUND MOTION APPLICATION	23
2.2. MOTION HANDLING.....	24
2.2.1. Baseline Correction.....	25
2.2.2. Target response spectral matching.....	27
3. EFFECTS OF AERODYNAMIC DAMPING ON SEISMIC RESPONSE	30
4. IMPLICIT CONSIDERATION OF AERODYNAMIC DAMPING IN SEISMIC AND WIND LOAD COMBINATIONS.....	33

4.1. SELECTED GROUND MOTIONS AND WIND LOADS.....	34
4.2. SIMULATION RESULTS	35
5. CONCLUSIONS.....	42
REFERENCES	43
II. EFFECTS OF SEISMIC AND AERODYNAMIC LOAD INTERACTION ON THE POWER GENERATION AND STRUCTURAL RESPONSE OF MULTI- MEGAWATT UTILITY SCALE HORIZONTAL AXIS WIND TURBINES	45
ABSTRACT.....	45
1. INTRODUCTION	46
2. DEVELOPMENT OF SEISMIC MODULE FOR FAST	49
3. NORMAL OPERATION WITHOUT CONSIDERATION OF EARTHQUAKE LOADS	51
4. SCALING AND SELECTION OF GROUND MOTIONS	56
5. WIND TURBINE OPERATION WITH CONSIDERATION OF EARTHQUAKE LOADS	58
6. DISCUSSION AND CONCLUSION	68
7. ACKNOWLEDGEMENT	70
REFERENCES	71
III. FRAGILITY ANALYSIS OF A 5-MW NREL WIND TURBINE CONSIDERING AERO-ELASTIC AND SEISMIC INTERACTION USING FINITE ELEMENT METHOD	74
ABSTRACT.....	74
1. INTRODUCTION	75
2. PROPERTIES OF 5-MW NREL WIND TURBINE.....	78
3. SELECTED GROUND MOTIONS AND AERODYNAMIC LOADS FOR NONLINEAR ANALYSIS.....	85
4. NONLINEAR DYNAMIC ANALYSIS	87
5. FRAGILITY ANALYSIS OF THE 5-MW WIND TURBINE.....	100
6. CONCLUSIONS.....	105
7. ACKNOWLEDGEMENT	107
REFERENCES	108
SECTION	
2. CONCLUSIONS AND FUTURE WORK	111

APPENDICES

A. SEISMIC MODULE INPUT FILE DESCRIPTION.....	116
B. ABAQUS-AERODYN-FAST LINK THROUGH MATLAB	135
VITA.....	150

LIST OF ILLUSTRATIONS

Figure	Page
SECTION	
1.1 Top 10 cumulative wind capacity at the end of 2013.	2
1.2 Trends in increasing wind turbine size.....	2
1.3 Turbine failure due to earthquake loading in Japan and New Zealand.....	4
 PAPER I	
1 Logical flow for initialization for of seismic shaking module functionality.....	23
2 Baseline correction application on the 5-MW turbine using seismic module.	26
3 Target, initial, and the matched response spectra for the applied motion.....	28
4 Initial and modified ground motion before and after response spectral matching.....	28
5 Effect of spectral matching on tower moment demand for each elevation.....	29
6 Tower top acceleration for operational and idling condition in both directions under seismic excitation.....	31
7 Amplitudes of the tower top acceleration for idling and operational conditions of the turbine in both directions.....	32
8 Spectral displacement with 5% damping for the earthquake ensemble.....	35
9 Mean of the maximum of SRSS of the moments in fore-aft and side-side direction considering the 44 ground motions in idling condition.....	36
10 Maximum of the SRSS of the moments in fore-aft and side-side direction considering the 44 ground motions in idling condition.....	38
11 Comparison of linear combination of operational and earthquake loads.....	39
12 Comparison of 0.75 combination of operational and earthquake loads.....	40
 PAPER II	
1 Mean generated power and torque for different wind speeds for normal operational conditions without earthquake.....	52
2 Mean Pitch angle with respect to different mean wind speed levels.....	54
3 Maximum of Base shear and moment in both directions of wind turbine for 50 wind conditions.....	55
4 Maximum moment demand in different elevations of the tower for tested wind speeds.....	56

5	Maximum acceleration and displacement in different elevations of the tower for tested wind speeds.....	57
6	Sample of the generated power for different operational conditions.....	59
7	Mean of the generated power for three operational conditions with and without the consideration of earthquake loads.....	60
8	Mean of the generated power for different wind and earthquake intensities for running condition.....	62
9	Mean of the generated power for different wind and earthquake intensities for emergency shutdown.....	62
10	Mean of the maximum of the SRSS of moment and shear for 44 earthquakes and different wind speeds for the three operational conditions.....	63
11	Mean of the maximum of SRSS of moment demand for 44 earthquake simulations for four wind speeds for different operational conditions.....	65
12	Maximum of SRSS of base moment for different earthquake intensities and wind speeds in idling mode.....	66
13	Maximum of SRSS of base moment for different earthquake intensities and wind speeds in running mode.....	66
14	Maximum of SRSS of base moment for different earthquake intensities and wind speeds in emergency shutdown mode.....	67

PAPER III

1	Configuration of the developed finite element model.....	80
2	Tower fore-aft and side-side 1 st and 2 nd mode shapes.....	82
3	Graphical representation of the pushover analysis for the finite element model.....	83
4	Base moment and top displacement relationship for pushover analysis.....	84
5	Maximum base moment of 5-MW turbine for 44 earthquake motions and three wind speeds.....	88
6	Peak tower top displacement for 44 earthquake simulations in three wind scenarios.....	90
7	Peak rotation for 44 earthquake simulations in three wind scenarios.....	91
8	Residual deformation for 44 earthquake simulations in three wind scenarios.....	91
9	Peak stress for 44 earthquake simulations in three wind scenarios.....	92
10	Displacement time history of earthquake #18 applied with different magnification factors to the base of the turbine model in wind speed 2.5 m/s.....	93
11	Peak base moment for 44 earthquakes with various amplifications for wind speed 2.5 m/s.....	94

12	Tower top displacement for earthquake #7 with wind speed of 7 m/s in terms of different magnification factors	95
13	Peak displacement in terms of different elevations of the tower for earthquake #10 and wind speed 9 m/s	96
14	Buckling of the tower for all simulations with different earthquake intensities and wind speeds	97
15	IDA curves for maximum rotation relative to the spectral acceleration for 10 m/s wind speed.....	98
16	Mean of the IDA curves for maximum rotation relative to the spectral acceleration for all wind speed.....	99
17	Fragility Curve for different damage states of the 5-MW NREL wind turbine for 2.5 m/s wind speed.....	102
18	Fragility curve in with respect to spectral acceleration and wind intensity for DS ₅	103
19	Fragility curve in with respect to spectral acceleration and wind intensity for DS ₂	103
20	Fragility curve in with respect to spectral acceleration and wind intensity for DS ₄	104

LIST OF TABLES

Table	Page
SECTION	
1.1 Previous contributions on the work done in the field of modeling seismic and wind response of wind turbines.....	13
PAPER I	
1 General specifications of the 5-MW NREL Wind Turbine	26
2 Characteristics of the ground motion used to perform the analysis	37
3 Difference (%) in tower moment between load combinations.....	41
PAPER II	
1 Coefficients for Eq. (7) for finding mean of the generated power in running and emergency shutdown conditions	61
2 Increase in shear and moment demand from the presence of earthquake in comparison with normal operation of wind turbine.....	64
PAPER III	
1 Structural properties of the 5-MW NREL Wind Turbine	79
2 Natural frequencies of different modes for four models	82
3 SRSS values of engineering demand parameters for 44 earthquakes and 7 m/s wind speed.....	90
4 Damage states considered for fragility analysis.....	102

SECTION

1. INTRODUCTION

During the last decades the demand for sustainable energy production has led to a plethora of innovative technological solutions. The forecast of the fuel shortage in the near future combined with the negative environmental impacts caused by the use of traditional electricity production methods forced all those involved in the energy production field to start exploring new directions in energy production. The so-called clear energy sources (e.g. the wind and solar) recently became the basic subjects of these investigations. Among the latter efforts, specialized infrastructure, the so-called wind farms, aiming to produce energy from the wind play a predominant role on the scene of clear energy production. As a matter of fact, wind farms are composed of families of wind turbines supported on steel towers [1]. The strong drive to exploit wind energy has recently led to consideration of new types of locations for wind turbines. A major concern for wind farm installation in these sites is the long-term reliability of the support structures.

The beginning of the 21st century has seen a rapid growth in wind power with a world-wide capacity approaching 100 GW. Within the U.S., at the end of 2013, the installed capacity of wind power was over 61 GW. Wind power accounts for about 4.2% of the electricity generated within the U.S. and according to DOE the wind energy generated is going to reach 20% by the year 2030 [2]. Figure 1.1 shows the growth of capacity in wind energy production in different countries. With this growth, wind turbines are being installed in sites prone to high seismic hazard. As shown in figure 1.2, the turbines are increasing in size which makes these structures more vulnerable to lateral loads. Until recently, seismic demand has received little attention in comparison to other types of extreme loads for wind turbines. The matter is further motivated by the increase in size and mass of the newer wind turbines, where seismic loading, not wind or fatigue, may control the design of the supporting structure.

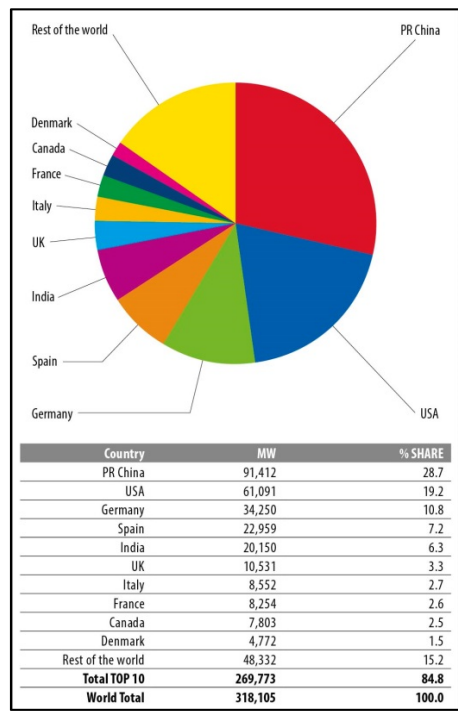


Figure 1.1 Top 10 cumulative wind capacity at the end of 2013 [2]

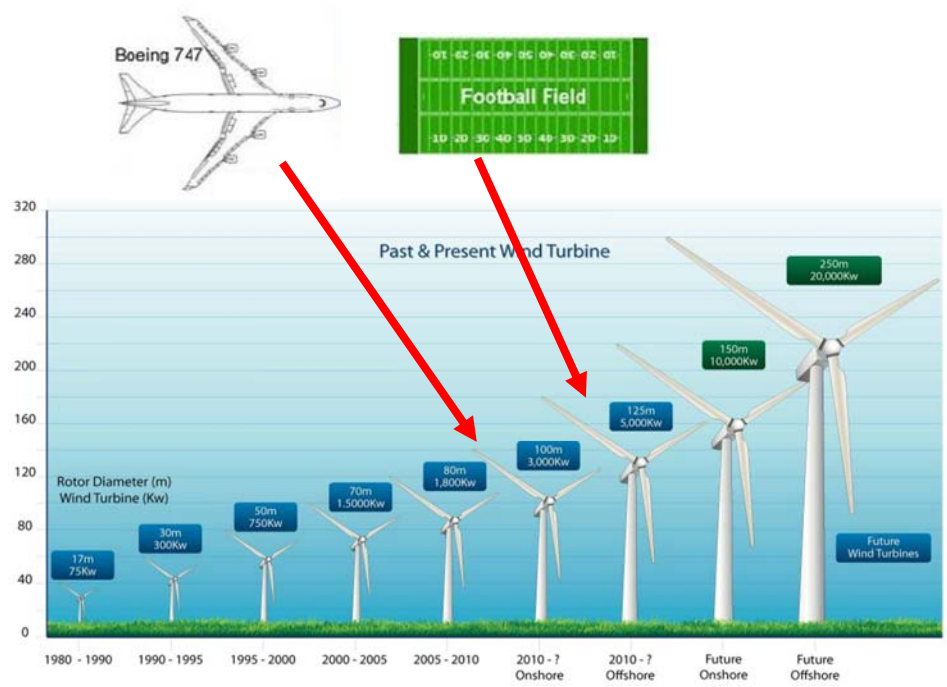


Figure 1.2 Trends in increasing wind turbine size [2]

Contemporary turbine design standards provide only a simple method for seismic analysis that idealizes the structure as a Single Degree of Freedom (SDOF) system and using frequency domain analysis to calculate ground motion forces [3-5]. Existing research shows that there are significant discrepancies between a SDOF approach and improved modeling methodologies. Improved methods include the turbine rotor, among other additions that arise due to consideration of aerodynamic forces acting on the turbine rotor which are believed to be critically important and cannot be directly incorporated into a SDOF model [6-7].

Unlike any other building structure, wind turbines can have various dynamic movements during operation that require specific considerations that might be unfamiliar to civil engineers. Due to the active control systems mounted on the blades in modern utility scale wind turbines, the dynamic behavior of the turbine system changes in real time. As a result, the structural response of a turbine can show significant variability in different simulation conditions that have to be accounted for, which is not an issue to be considered in other civil engineering structures. Research shows that extreme loads vary depending on the operational state of the turbine [8], which cannot be considered with simplified models. Of particular concern for turbine structures is ensuring that the turbine tower does not fail during simultaneous seismic and aerodynamic loading. However, modeling approaches used by previous researchers that include aerodynamics [6, 7] cannot directly predict tower failure because they rely on a simple linear multi-body dynamics representation of the turbine structure. Investigations of varying detail have been conducted to directly consider tower buckling and failure, but to date, all have ignored aerodynamics and operational states of the turbine [9-11].

Figure 1.3 shows some of the damages in wind turbine structure towers due to recent earthquakes in Japan and New Zealand. Tower failure caused by high seismic forces has caused the structure to completely collapse. In some cases the loss of strength in the soil has caused residual tilts in the tower which will considerably effect the energy production.



Figure 1.3 Turbine failure due to earthquake loading in Japan and New Zealand

1.1. EXISTING GUIDELINES IN THE WIND ENERGY INDUSTRY

Certification guidelines for wind turbines prescribe that the response for all extreme loads including seismic loading is elastic [3-5]. Four main documents exist that provide direct guidance for seismic loading of wind turbines. Guidelines for Design of Wind Turbines (Risø-DNV) [5], provides the most general suggestion. In this document, the wind turbine is represented by a concentrated mass on top of a vertical rod which is the combination of rotor, nacelle, and a quarter of the tower mass, and by using frequency-domain analysis with a specific response spectrum, the loads set up by the ground motion will be determined.

The Germanischer Lloyd (GL) [4] guidelines first suggest that either local building codes should be applied or in the absence of specific provisions, the American Petroleum Institute (API) [12] recommendations are to be applied. The investigation of earthquake generated loads in this guideline is based on the combination of the wind loads and an earthquake acceleration with a recurrence period of 475 years [5]. Earthquake load is to be combined with standard wind load conditions in a load combination with load factor equal to one.

The International Electrotechnical Commission (IEC) guidelines [3] mentions that the design level earthquake is prescribed as a 475 year return period event and the

resulting loads must be superimposed with the maximum of operating loads or emergency shutdown loads with a unit safety factor. A simplified estimate of the seismic load is provided in Annex C of this guideline, which suggests the use of a design response spectrum from local building code adjusted to a damping of 1% to find the design response acceleration based on the first natural frequency of the tower [13]. There are no recommendations on how to deal with nonlinearity or buckling of the components of the turbine in the three previously mentioned guidelines.

A systematic effort by a joint committee commissioned by the American Wind Energy Association (AWEA) and the American Society of Civil Engineers (ASCE) has resulted in publishing a document that provides recommended practices for design and permitting of large wind turbines support structures [14]. This document provides guidance on calculating seismic loads for large wind turbines with consideration of the above mentioned industry guidelines in conjunction with applicable U.S. building codes. It is suggested that operational and earthquake loads be combined as an absolute sum with a load factor of 0.75. Seismic ground motion values are determined from ASCE 7-10 [15] and spectral response acceleration parameters should be based on 1% of damped values while parked and 5% of the damped value while the turbine is under operational conditions. The ASCE/AWEA document begins to address nonlinear response. For buckling analysis, it is mentioned that a procedure that considers geometric and material nonlinearity with imperfections in the shell's initial shape would be acceptable but no other details are provided.

1.2. PREVIOUS RESEARCH ON WIND TURBINE MODELING

Existing literature regarding modeling wind turbines for seismic loading is divided between two types of models; models that focus on the tower by accounting for the mass of the nacelle and rotor as a point mass at the top of the tower; and models that describe the full turbine including the nacelle and rotor with some level of detail. Simplified models are attractive as they remove the complexity of modeling the rotor. The simplified approach casts the turbine as a SDOF system and may be unreliable for modeling behavior that arises from modes other than the first tower mode.

In contrast, full system models increase complexity of interpreting the results. The

additional overhead is rewarded by model flexibility. Existing full system models attempt to incorporate all possible factors to seismic risk including aerodynamic loads, rotor dynamics, soil-structure interaction, electrical system dynamics, and other sources. A full system model further has the benefit of prediction of component loads instead of only tower loads. Since there is no systematically documented experience of seismically induced failure in wind turbines, designers cannot be certain how a turbine might fail in a seismic event. It is generally assumed that the tower and foundation are the critical components for seismic loading. Full systems models can help evaluate component loads not included in a simple tower based model.

1.2.1. Simple Models. As previously discussed, both Risø National Laboratory [5] and the IEC Annex C [3] provide simplified procedures for estimating seismic loading of a wind turbine. The difference between these two procedures is subtle. The Risø procedure uses a simplified model to determine the first tower natural period that could prove useful for estimation during design iterations. The IEC assumes that the first natural period is known based on existing analysis. Both procedures then use this first natural period to extract the design response acceleration from a design response spectrum. The Risø procedure then leaves the designer free to select an appropriate method to translate the design response acceleration into seismic loads where the IEC procedure prescribes that this acceleration be translated into a base shear and moment as described in section 3.1. Some other existing research on wind turbines includes the analysis of wind turbines as a SDOF system neglecting the effects of rotor dynamics in frequency domain, which will be discussed in the next sections of this document.

1.2.2. Full System Models. Full system models that consider aerodynamic and seismic effects are analyzed in frequency domain and time domain. Frequency-domain methods are typically favored in design due to their ease of implementation. Time-domain analyses have a higher computational demand and are often used in analysis of structures, rather than in their design. Time-domain analyses are increasingly being used in the wind turbine industry. Aside from the time domain being time consuming and heavy computational requirements, full system models are evaluated using two methods. First one is a combined modal and multi-body dynamics formulation to simulate the dynamic behavior of the turbine in the time domain. The structural dynamics of the wind

turbine are represented using a limited-degree-of-freedom modal model. This approach is less time consuming than the second approach which is the finite element (FE) approach. The disadvantage of using modal combination approach is that the structure is modeled using elastic beam elements with reduced degrees of freedom. For a more detailed analysis that could consider nonlinearities and stress analysis through different components of the system, FE method has to be considered.

Current well known computational tools that use modal combination approach and are capable of coupling seismic and aerodynamic loads are GH Bladed which is produced by Garrad Hassan (GH), and the FAST code [16] which is maintained by the National Renewable Energy Laboratory (NREL). Both GH Bladed and the FAST code have been validated by Germanischer Lloyd for calculating operational loads associated with typical load cases.

GH added a seismic module to GH Bladed in response to demand for estimation of loading at seismically active sites. GH Bladed does not model the turbine using a finite element method due to computational complexity, but instead uses a limited-degree-of-freedom modal model. Modal calculations are conducted in the time domain for the major components of the turbine. The resulting forces for each mode are then calculated at the component interfaces. GH Bladed has two methods for simulating seismic loading. The first method is to use recorded acceleration time histories. The second method uses an iterative procedure to produce a synthetic acceleration time history with an elastic response spectrum that closely resembles a specified design response spectrum. To further increase flexibility, the user is able to specify a foundation stiffness to account for soil and foundation influences on the structural response. The end result is a comprehensive package that is able to simulate seismic response of a turbine in the time domain with any specified level of damping in combination with other load sources. This approach allows the designer to explore numerous loading scenarios and obtain a detailed understanding of the resulting structural loads.

The FAST code [16] uses a combined modal and multi-body dynamics formulation to simulate the dynamic behavior of a turbine. The equations of motion are solved using standard multi-body dynamics formulations for elements whose flexibility is determined by the summation of mode shapes provided by the user. Prior to work

presented in this dissertation, the FAST code did not directly provide a facility to simulate seismic loading. Instead, a generic framework was provided that allows the user to provide a custom-developed loading routine to be imposed at the base of the turbine. This dissertation details appropriate additions to the FAST code so that it is capable of providing a full system model for seismic loading.

1.3. LITERATURE ON SEISMIC BEHAVIOR OF WIND TURBINES

The growth of wind power has led to an interest in addressing seismic loading of wind turbines. Early publications (Bazeos et al., 2002 [10]; Lavassas et al., 2003 [11]) considering seismic loading of wind turbines focused on loading of the tower based on simplified models that lumped the nacelle and rotor as a point mass. Gradually interest shifted from these simple models to more refined models that also consider loads for turbine components other than the tower (Ritschel et al., 2003[17]; Witcher, 2005 [6]; Haenler et al., 2006 [18]; Zhao and Maißer, 2006 [19]).

Somewhat unique, but worthy of note, is a 1984 publication considering seismic loads in combination with wind loads for a wind turbine rotor (Hong, 1984) [20]. This work develops a set of analytical equations describing the statistical distribution of blade response parameters. Seismic input motion is considered as white-noise, filtered to approximate the shaking transmitted by the tower, in each of three orthogonal directions at the hub. The effects and interaction with tower vibrations are neglected in this study. Based on the proposed formulation, it is concluded that turbulence is a larger contributor to fatigue for wind turbine blades than earthquake loads.

In 2002, another attempt to quantify the dynamics of wind turbines due to seismic loading was published (Bazeos et al., 2002) [10]. This publication presented extensive finite element modeling of a prototype 450-kW turbine with a 38 meter tall steel tower designed for installation in Greece. The tower was modeled in detail using shell elements as well as by a simpler model that used beam-column elements. Both models addressed the rotor and nacelle by adding a point mass at the top of the tower and used a viscous damping of 0.5%. Time history analyses of the two models were conducted and compared. The results from the two models showed good agreement, but the more detailed model was required for buckling analysis. Soil structure interaction (SSI) was

investigated using springs, dampers, and added mass. The main outcome of the SSI analysis was to show a significant decrease in the frequencies at which the second and third tower bending modes occurred due to base fixity. The analysis concluded that seismic loading did not produce design driving loads.

An early publication considering both earthquake and wind loads was published by Kiyomiya et al. (2002) [21]. First the relative probabilities of wind speed and earthquake acceleration are examined. Based on appropriate probability distributions for each, it is concluded that likelihood of concurrent extrema is small enough to be neglected. In the case of a large and rare earthquake it is found that the highest likely wind speed is the mean wind speed. A simplified beam-column model with a lumped mass for the nacelle and rotor mass at the hub height with an assumed equivalent viscous damping of 2% is used to simulate the turbine structure. The wind is applied as a static point load at the hub height. Additionally, a FE mesh is used to model the soil and foundation. Simulations are conducted using a recording of the Hyougoken-Nanbu earthquake obtained at a depth of 82 m below Port Island. A resulting tower base demand of 1.5 times the demand from a storm condition is found for the simulated earthquake, but is found to be below the capacity of the simulated tower. It is concluded that the turbine has sufficient strength to resist the earthquake without damage. Suggestions for further research support the work presented in this dissertation to allow consideration of dynamic wind loads in parallel with earthquake loads.

In 2003, a detailed finite element investigation was published of 1-MW turbine with a 44 m tall steel tower and 52 m rotor diameter designed for installation in Greece (Lavassas et al., 2003) [11]. The seismic loading in this investigation was based on a multimode linear analysis which used a design response spectrum from Eurocode 3 for a site in seismic zone II with rocky soil. The authors concluded seismic stresses were 60 percent lower compared to those developed by extreme wind loads for this level of seismicity. Again the rotor and nacelle were simplified to a point mass at the top of the tower. The authors speculate that seismic design could become critical in regions with higher seismic hazard and less favorable soil conditions.

Windrad Engineering published an analysis that considers seismic loads for components other than the turbine tower (Ritschel et al., 2003) [17]. The publication first

looks at the seismic loads produced by a modal analysis of a simple distributed mass cantilever beam model of a 2.5-MW Nordex N80 wind turbine with an 80 m rotor diameter and 60 m hub height. This modal approach produced seismic loads that closely matched the contemporary IEC approach [3] based on a synthetic input time history with a peak ground acceleration (PGA) of 0.3 g. Realizing that such a model was incapable of properly addressing component loads, a full system model with 28 degrees of freedom was developed using FLEX5 by mapping ground acceleration through a coordinate transformation into effective external nodal forces. The FLEX5 model produced lower moment demand at the base of the tower compared to both the IEC approach and the modal approach using the same synthetic earthquake time history. The loads approached parity toward the top of the tower. At the top of the tower the seismic load from FLEX5 slightly exceeded both the IEC approach and the modal approach. The difference was not significant and it was concluded that the existing design loads were sufficient. The vertical seismic excitation caused higher bearing loads than those from extreme wind conditions. Vertical excitation was also found to induce tilt vibration in the nacelle. This investigation concluded that seismic loads in the blades were about 70% lower than those caused by the 50-year wind loads.

Witcher (2005) [6] presents an overview of the GH Bladed seismic module in conjunction with some preliminary results for loading of a 2-MW upwind machine with an 80 m diameter rotor and a 60 m tower. The results show the response in three load cases: continuous operation throughout the earthquake; emergency shutdown initiated during the earthquake; and parked throughout the earthquake. The difference in the resulting maximum moment demand at the base of the tower for the three load cases was compared for a time and frequency domain calculation. Only a 2.9% increase in the maximum moment demand was observed in the time domain compared to the demand from the frequency domain. A fourth load case considered the turbine parked while subjected to an earthquake in combination with high winds. This case resulted in a 79% increase in moment demand for a time domain simulation from that calculated using a modal simulation. This result is used to highlight the importance of time domain simulations to account for aero-elastic interaction.

In collaboration with Peter Maißer and Jingyan Wu, Xueyong Zhao presents what

was termed a hybrid MBS for modeling turbine dynamics (Zhao and Maißer, 2006 [19]; Zhao et al., 2007 [22]). The technique is detailed in the 2007 publication [22] by providing the theoretical development, showing resulting mode shapes, and variation in natural frequencies as a function of rotor speed for a 600-kW turbine with a 43 m diameter rotor and a 52 m tower. This introduction is followed by an extension of the technique to include seismic loading and soil structure interaction [19]. The rotor, which was initially modeled with three flexible blades, was simplified to a rigid disk when considering seismic loading. The soil structure interaction was addressed by connecting the turbine base to a rigid support with translational and rotational springs and dampers whose properties were derived based on assumed soil properties. The response of a 1.5-MW turbine subjected to turbulent wind with a mean velocity of 10.16 m/s and an earthquake acceleration time history with a maximum acceleration of 0.06 g is calculated using this model. The low PGA is consistent with a minor or very distant earthquake. Negligible impact was observed for the tower base shear and bending moment. In contrast, oscillation in the lateral reaction force of the main bearing was significantly increased. This observation is similar to that of Ritschel et al. (2003) [17] regarding vertical loads in the main bearing.

Ishihara and Sawar (2008) [23] completed a study on seismic demands for two different sizes of wind turbines (400-kW and 2-MW). Initially two modeling techniques are explored: one that places the rotor and nacelle mass into a single lumped mass; and a second that included mass and stiffness distribution of the nacelle and rotor. It is concluded that for first mode response both models provide good representations, but when the second and higher modes are considered the lumped mass model diverges from the more representative model. Presented results show that, for the 2-MW turbine, second mode and higher responses are important and contribute significantly. Based on calculated demand, a semi-analytical approach to estimate shear and moment demand is proposed. It is shown that for the two studied turbines, moment is well modeled by the approach, but greater disagreement exists for the shear results. It is concluded that since moment generally governs design of the turbine tower that the approach is a useful tool for understanding seismic loads for wind turbines.

More recently, an extensive investigation into the seismic response of a 1.65- MW

Vestas turbines was constructed (Nuta, 2010) [9]. In this work a full shell model of the turbine tower was constructed using the modeling package ANSYS. Effects such as mesh refinement and connection detail modeling were explored. In the model the rotor and nacelle are lumped as two point masses near the top of the tower. The mass representing the rotor was offset to account for eccentricity. Consistent with this approach, aerodynamics are not considered and only the parked state of the turbine is simulated. Modeling procedures were validated against experimental results from the 2004 shake table test conducted at UCSD on a 65-kW Nordtank turbine and showed good general agreement in lower frequency response, but lacked some of the higher frequency content that was experimentally recorded (Prowell et al., 2009) [24]. Once the modeling procedure and the mesh of the 1.65-MW Vestas turbine were validated, an incremental dynamic analysis (IDA) was conducted using 20 records composed of 2 horizontal components from 10 earthquakes. Using the IDA results fragility curves were developed for the magnification factor, peak ground velocity (PGV), and PGA intensity measures (IM). Finally, the procedure is applied for two specific sites, one in Western and one in Eastern Canada. Table 1.1 shows a chronological overview of the research done on the seismic behavior of wind turbines in the past few decades which were explained in this section. The work done in this research begins to include the methods used by previous researchers, and use them to consider new methodologies in finding aspects of the dynamic response of wind turbines that have not been focused on in the work of others.

Table 1.1 Previous contributions on the work done in the field of modeling seismic and wind response of wind turbines

Reference	Year	Simplified Model	Modal Combination Model	FE Model	Aerodynamics	Seismic Loads	Nonlinearities
Hong et al.	1984	✓	✗	✗	✗	✓	✗
Bazeos et al.	2002	✓	✗	✓	✗	✓	✓
Kiyomiya et al.	2002	✓	✗	✓	✗	✓	✓
Lavassas et al.	2003	✓	✗	✗	✗	✓	✗
Ritschel et al.	2003	✓	✓	✗	✓	✓	✗
Witcher et al.	2005	✗	✓	✗	✓	✓	✗
Zhao and Maißer	2006	✓	✓	✗	✓	✓	✗
Ishihara and Sawar	2008	✓	✗	✗	✗	✓	✗
Nuta et al.	2011	✓	✗	✓	✗	✓	✓
Prowell et al.	2012	✓	✓	✓	✓	✓	✗
Asareh et al.	2015	✓	✓	✓	✓	✓	✓

1.4. RESEARCH OBJECTIVES

The objective of this study is to advance the methodologies in finding the detailed response of a full-system wind turbine under coupled seismic and aerodynamic loading. This will include assessing the behavior of turbine structure under different operational states when subjected to simultaneous wind and earthquake loading. The objective can be achieved by focusing on the following key factors: 1) Consideration of aerodynamic loads of the blades into the response of the whole system, 2) Investigating the effects of aerodynamic damping on the structural response, 3) Developing simplified methods to implicitly consider aerodynamics in the seismic response of wind turbines, and 4) Using finite element models to evaluate tower failure and buckling analysis using nonlinear models which take into account different intensity measures, damage measures, and damage states. To date, the factors described have not been concurrently considered in the limited work in the published research. In the first stages of this research, a seismic module is developed to be used for coupled aerodynamic and seismic analysis on two or three bladed wind turbines. The module is then used to evaluate the effects of

aerodynamic damping and implicit consideration of this damping on dynamic response of the structure. Different load combinations from suggested codes and guidelines are tested with considering coupled and uncoupled simulations in the next stage of this research. Power generation of wind turbines considering seismic loads and different operational conditions are also assessed using the developed seismic module. In the final stages, research will incorporate nonlinear behavior of the turbine tower. Although multi-body dynamics models that are used in recent wind turbine computational tools may be adequate for preliminary design, a more detailed structural finite element model is necessary to enhance the verification of the final design. The proposed research at that point will mainly focus on the investigation of fragility of wind turbine towers subjected to combined seismic and wind loading. Incorporating a high fidelity analysis model that considers the interaction and coupling between turbine components and loads may result in reduction of the cost of energy and improve reliability for the wind turbine systems and lead to technological advances in the wind energy industry.

1.5. ORGANIZATION OF THE DISSERTATION

The first step of this research is to modify and update the FAST [16] code, which is publicly available in the National Renewable Energy Laboratory (NREL). A module was developed using FORTRAN coding that can apply user defined or synthetically generated motion by incorporating a damped oscillator at the base of the turbine tower. The module also includes subroutines for motion handling procedures such as baseline correction and target response spectrum matching analysis. The FAST code uses modal combination approach and assigns beam elements for tower and blades with limiting the degrees of freedom. This code can be linked to NREL's AeroDyn [25] program to calculate aerodynamic forces on the blades and consider the operational condition of a wind turbine. This code is used for evaluating the linear response of wind turbines considering seismic and aerodynamic load interaction for observing the effects of aerodynamic damping and implicitly considering aerodynamics in the seismic response of wind turbines. Paper I will include a description of the developed module followed by examples of different subroutines that can be used for different motion characteristics. It will also contain results from the observation of aerodynamic damping in the response of

wind turbines and how to implicitly consider this damping with the seismic response of these structures.

In paper II, power generation of the turbine is evaluated by considering simultaneous aerodynamic and seismic loads in different operational conditions of wind turbines. This is also done using the seismic module that was compiled with FAST.

Next step of the research is to create the analysis approach using finite element method to conduct simulations that can directly capture the failure of the turbine tower simultaneously with aerodynamic loads and operational state of the turbine which is presented in paper III. This approach will go beyond the current state-of-the-art by considering nonlinear structural response, which is currently neglected. By considering material and geometrical nonlinearities, simulations will be able to predict damage instead of only determining extreme demand. The observations from this procedure can be compared with the linear response achieved from the beam model in FAST to investigate the effects of nonlinearity in the system.

Using this approach, simulations will be systematically conducted to investigate the probability of various response states of the turbine as a function of demand parameters for combined wind and seismic events. With the results of linear and nonlinear analysis for seismic and aerodynamic interaction in the operational conditions of the turbine in hand, the final step is to identify demand parameters that are high quality estimators of damage to the turbine tower based on the refined modeling approach. Based on the results achieved by simulations using various wind fields and earthquake motions, fragility curves and probability of failure for the turbine can be developed and analyzed. The proposed research will generate results that describe damage states as a direct outcome to a realistic description of behavior under extreme loading which to date does not exist.

REFERENCES

- [1] M. Molinari, M. Pozzi, D. Zonta, L. Battisti, "In-field testing of a steel wind turbine tower," in *Structural Dynamics and Renewable Energy*, Volume 1, Springer, p. 103-112. 2011.
- [2] S. Lindenberg, B. Smith, K. O'Dell, "20% wind energy by 2030," *National Renewable Energy Laboratory (NREL)*, US Department of Energy, Renewable Energy consulting Services, Energetics Incorporated, 2008.
- [3] IEC, "IEC 61400-1 Ed. 3: Wind Turbines - Part 1: Design Requirements," *International Electrotechnical Commission*: Geneva, Switzerland. 2005.
- [4] GL, "Guidelines for the certification of wind turbines," *Germanischer Lloyd*: Hamburg, Germany. 2003.
- [5] Risø-DNV, "Guidelines for Design of Wind Turbines," *Wind Energy Department of Risø National Laboratory and Det Norske Veritas*: Copenhagen, Denmark. 2001.
- [6] D. Witcher, "Seismic analysis of wind turbines in the time domain," *Wind Energy*, 8(1): p. 81–91, 2005.
- [7] I. Prowell, "An experimental and numerical study of wind turbine seismic behavior," *Thesis Dissertation*: University of California, San Diego, 2011.
- [8] I. Prowell, A. Elgamal, C. Uang, J. Jonkman, "Estimation of seismic load demand for a wind turbine in the time domain," in *European Wind Energy Conference*: Warsaw, Poland, 2010.
- [9] E. Nuta, "Seismic analysis of steel wind turbine towers in the Canadian environment," *Thesis Dissertation*: University of Toronto, 2010.
- [10] N. Bazeos, G.D. Hatzigeorgiou, I.D. Hondros, H. Karamaneas, D.L. Karabalis, D.E. Beskos, "Static, seismic and stability analyses of a prototype wind turbine steel tower," *Engineering Structures*, 24(8): p. 1015–1025, 2002.
- [11] I. Lavassas, G. Nikolaidis, P. Zervas, E. Efthimiou, I.N. Doudoumis, C.C. Baniotopoulos, "Analysis and design of the prototype of a steel 1-MW wind turbine tower," *Engineering Structures*, 25(8): p. 1097–1106, 2003.
- [12] API-PR-2A, "Recommended practice for design and construction of fixed offshore platforms," *American Petroleum Institute*: Washington, DC, USA, 2000.

- [13] I. Prowell, P. Veers, "Assessment of wind turbine seismic risk: Existing literature and simple study of tower moment demand," *Sandia National Laboratories*: Albuquerque, NM, 2009.
- [14] N.A. Agbayani, "A Technical Overview of ASCE/AWEA RP2011: Recommended Practice for Compliance of Large Land-based Wind Turbine Support Structures," in *Structures Congress 2014*: ASCE, pp. 1759-1770, 2014.
- [15] ASCE-7-10, "Minimum design loads for buildings and other structures," in *American Society of Civil Engineers*, Reston, Virginia, 2010.
- [16] J.M. Jonkman, M.L. Buhl Jr., "FAST user's guide," *National Renewable Energy Laboratory (NREL)*, Golden, CO, 2005.
- [17] U. Ritschel, I. Warnke, J. Kirchner, B. Meussen, "Wind turbines and earthquakes," *World Wind Energy Association*, Cape Town, South Africa, 2003.
- [18] M. Haenler, U. Ritschel, I. Warnke, "Systematic modelling of wind turbine dynamics and earthquake loads on wind turbines," *European Wind Energy Conference and Exhibition*: Athens, Greece, 2006.
- [19] X. Zhao, P. Maisser, "Seismic response analysis of wind turbine towers including soil-structure interaction," *Journal of Multi-Body Dynamics*, **220**(1): p. 53-61. 2006.
- [20] R.C.-Y. Hong, "Response of a wind turbine blade to seismic and turbulent wind excitations," *Thesis Dissertation*: University of Illinois at Urbana-Champaign, 1984.
- [21] O. Kiyomiya, T. Rikiji, P.H. Van Gelder, "Dynamic response analysis of onshore wind energy power units during earthquakes and wind," in *Proc. 12th International Offshore and Polar Engineering Conference*, pp. 520-526, 2002.
- [22] X. Zhao, P. Maißer, J. Wu, "A new multibody modelling methodology for wind turbine structures using a cardanic joint beam element," *Renewable Energy*, **32**(3): p. 532-546, 2007.
- [23] T. Ishihara, M.W. Sawar, "Numerical and theoretical study on seismic response of wind turbines," *European Wind Energy Conference and Exhibition*, Brussels, Belgium: European Wind Energy Association, 2008.
- [24] I. Prowell, M. Veletsos, A. Elgamal, J. Restrepo, "Experimental and numerical seismic response of a 65 kW wind turbine," *Journal of Earthquake Engineering*, **13**(8): p. 1172-1190, 2009.
- [25] D.J. Laino, A.C. Hansen, "User's guide to the wind turbine aerodynamics computer software AeroDyn," *National Renewable Energy Laboratory (NREL)*, Golden, CO, 2002.

PAPER

I. A COMPUTATIONAL PLATFORM FOR CONSIDERING AERODYNAMIC AND SEISMIC LOAD INTERACTION FOR MULTI-MEGAWATT UTILITY SCALE HORIZONTAL AXIS WIND TURBINES

ABSTRACT

With the advancements in the wind energy production industry, the demand for a cost effective and safe design of wind turbine structures is growing rapidly. The wide deployment of wind turbines in locations with high seismic hazard has lead engineers to take into account a more comprehensive seismic design of such structures. Turbine specific guidelines usually use simplified methods and consider many assumptions to combine seismic demand with the other operational loads affecting the design of these structures. As the turbines increase in size and capacity, the interaction between seismic loads and aerodynamic loads becomes even more important. In response to demand for an open platform capable of conducting coupled simulations of wind and seismically induced loads, research modifications that added these capabilities to the FAST code are improved for public release. This achievement allows researchers worldwide to directly consider interaction between seismic loads and other load sources for turbines with a freely available simulation platform. This paper details the theory and practical implementation of these innovations and demonstrates illustrative examples for different capabilities. The platform is then used to show the suitable earthquake and operational load combination with the implicit consideration of aerodynamic damping by estimating appropriate load factors.

Keywords: renewable energy; horizontal axis wind turbines; aerodynamic-seismic load interaction; aerodynamic damping; coupled simulations

1. INTRODUCTION

In the past few decades, forecasts on the depleting source of fossil fuels along with the harmful environmental effects caused by the use of these sources in generating electricity, such as the production of waste materials or carbon emissions, has forced those involved in the energy production industry to start searching for alternative methods. Among these is the wind energy which has been considered as one of the most safe and reliable sources of renewable energy. In the US, the installed capacity of wind power at the end of 2013 was up to 61 GW which accounted for 4.2% of the energy produced. According to the predictions in the DOE report made by Lindenberg (2009), by the end of the year 2030, the capacity of wind power would rise up to 300 GW which will be 20% of the electricity produced. This is done by taking into account new technology in the wind industry, and using the complete potential of offshore wind that is available in the east and west coastlines of the US.

The power that can be produced by horizontal axis wind turbines is proportional to the wind speed and the diameter of the rotor as indicated in Hau and Von Renouard (2013). Therefore, in order to increase the capacity of wind turbines, rotor diameter needs to increase in size since there is no control over wind speed and environmental conditions. By increasing the rotor diameter, the mass of the top of the turbine tower increases which will result in higher seismic loads and will affect one of the design deriving parameters of these structure which is the tower bending moment. As a coincidence most of the areas with high potential of wind resources, also have a high seismic hazard. One of these areas is the Pacific Rim which includes countries such as China, Japan, and the west coast of the United States. This makes the consideration of seismic and aerodynamic load interactions for these structures even more important.

Currently, limited work is available regarding seismic design of wind turbines and the work usually includes simplified models and various assumptions for obtaining seismic demands. Early publications done by Bazeos, et al. (2002) and Lavassas, et al. (2003) include considerations of seismic loading of wind turbines focusing on loading of the tower based on simplified models assuming the nacelle and rotor as a lumped mass on top of the tower for a prototype 450-kW, and 1MW turbines with a 38 m, and 44 m tall

steel tower designed for installation in Greece, respectively. The authors speculate that seismic design could become critical in regions with higher seismic hazard and less favorable soil conditions. Ritschel, et al. (2003) conducted simulations for a 2.5-MW Nordex N80 wind turbine with an 80 m rotor diameter and 60 m hub height using a full system model with 28 degrees of freedom in FLEX5 by mapping ground acceleration through a coordinate transformation into effective external nodal forces. This investigation concluded that seismic loads in the blades were about 70% lower than those caused by the 50-year wind loads. Witcher (2005) presented an overview of the GH Bladed seismic module for a 2 MW upwind wind turbine with 80 m rotor diameter and 60 m tower height and considers the response of the structure in three different load cases of parked, operational, and earthquake induced emergency shutdown. The significance of time domain analysis and the effects of aerodynamic damping were emphasized in this work. More recently, Prowell, et al. (2009) conducted experimental work on a 65 KW Nordtank wind turbine using the large high performance outdoor shake table available in University of California at San Diego. Earthquake motions were applied in two horizontal directions and the modal characteristics and dynamic behavior of this turbine was obtained. Numerical simulations were also done in the FAST program in the three different loading cases described previously which agreed very well with the experimental results. This work also concluded that the importance of considering seismic demand increases as the turbines grow in size and capacity.

Turbine specific guidelines such as IEC (2005), GL (2003), and Risø-DNV (2001) provide direct guidance for seismic design of wind turbines. However, in all documents wind turbines are represented in frequency domain and treated as a single degree of freedom (SDOF) system and the structure is assumed to be linear in extreme load cases. Some of these guidelines even rely on local building codes in the absence of specific provisions. Structural design codes such as ASCE-7-10 (2010) do not combine wind and earthquake loads in load combinations and it is the maximum of the two if they are mentioned in a load combination. However turbine specific design codes such as IEC (2005) or GL (2003) consider a combination of seismic and operational loads together using load factors of one. The ASCE/AWEA (2012) document which is the most recent document in the field of design and recommendations for large onshore wind turbine

support structures, begins to address analysis done in time domain and also uses load factors of 0.75 for both seismic and operational loads in load combinations and indicates that load factors of one for both loads is an overestimation in the design of such structures.

In this paper, a seismic module is developed for the FAST simulation code developed by Jonkman and Buhl Jr (2005) as a modification to the previous work done by Prowell (2011). The developed seismic module has the capability to apply predefined seismic ground motion or generate synthetic motion in three translational coordinates to the base of the turbine structure in forms of acceleration, velocity, and displacement. Beyond these capabilities, motion handling procedures such as baseline correction and response spectral matching can be performed on the desired input ground motion which minimizes the likelihood that preprocessing of earthquake records will be required. This module was tested to the previous versions and experimental verifications and they are in good agreement and examples of each capability are described. Finally, the simulation platform is used to show the effects of aerodynamic damping in coupled simulations. Load combinations for independent earthquake and aerodynamic loading are described with different load factors and a suitable combination that better estimates the aero-elastic seismic coupling is defined for consideration of a more cost effective and efficient design.

2. SIMULATION PLATFORM DESCRIPTION

FAST is an aero-elastic computer aided engineering tool developed by Jonkman and Buhl Jr (2005) in the National Renewable Energy Laboratory (NREL). This platform uses a combined modal and multi-body dynamics formulation to simulate two or three bladed horizontal axis wind turbine behavior in time domain by solving the equations of motion using a standard dynamics formulation with elements whose flexibility is determined by summing user defined mode shapes for different components. The two fore-aft and side-side tower mode shapes and the two flap-wise and one edge-wise blade mode shapes are given to the program in terms of sixth order polynomials with the zeroth and first terms set as zero to closely define the cantilevered shape of the components. FAST can be compiled with the AeroDyn code developed by Laino and Hansen (2002) that uses blade element momentum theory to calculate the aerodynamic loads in time domain and apply them to the blade elements. Early versions of FAST did not have the capabilities to consider seismic loads in the analysis of wind turbines. Prowell (2011) used a basic formulation that considered the two horizontal and one vertical earthquake motion in forms of acceleration, velocity, and displacement to the base of the turbine as the earthquake force.

In a comprehensive project done in this research by Asareh and Prowell (2011), seismic simulation capabilities are implemented through a module with different routines for reading seismic input, generating synthetic motion, applying baseline correction, and conducting response spectral matching. This module can be compiled in FORTRAN along with the FAST program and is available for public use in the NREL webpage. The desired simulation details are defined through an input file with a similar format to existing configuration files which are required in FAST. Figure 1 shows the logical flow used to apply desired ground motion to the base of the structure. The parameter SeismicMode is responsible for identifying the desired type of motion. If this parameter is set to 1 the program will load the user-defined ground motions given by the user and if it is set to 2, the program will generate synthetic motion according to the variables specified in the input file. User provided motions can be given in terms of acceleration, velocity, or displacement with a scaling factor defined in the seismic input file. If

desired, residual displacement or velocity can be removed by applying baseline correction. The developed spectral matching subroutine allows modification of the input motion to a specific spectrum defined by the user. The most common logical flow, appropriate when the provided motion needs no specific modifications, is indicated by a thick line in Figure 1. The seismic module is validated with previous versions which were calibrated and verified by experimental analysis done in Prowell, et al. (2011).

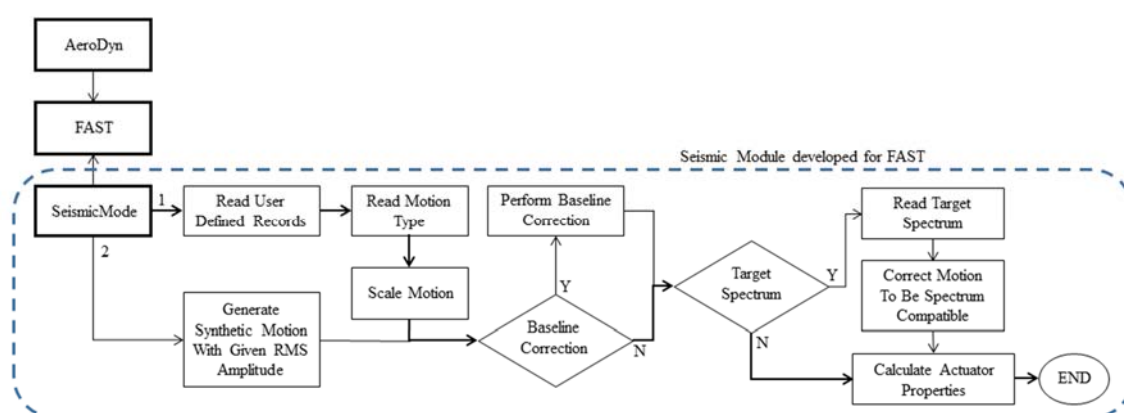


Figure 1. Logical flow for initialization for of seismic shaking module functionality

2.1. GROUND MOTION APPLICATION

Time histories are formatted using two columns, time and value (acceleration, velocity, or displacement). This approach enables the specification of input histories without the need for re-sampling and even allows the use of a non-constant time steps. The time history is simply linearly interpolated to a constant time step that matches that used in the simulation. The user defined or generated synthetic motion is given to the FAST program by releasing the degree of freedom in the desired translational direction at the base of the turbine tower and replacing it with a damped actuator. According to the properties of the actuator which can also be specified in the seismic input file, the motion

is applied as earthquake force in the desired direction in each time-step. The stiffness (K) and damping (C) coefficients of the actuator can be obtained by using the following equations:

$$K = m\omega^2 \quad (1)$$

$$C = 2m\omega\xi \quad (2)$$

where m is the total mass of the turbine including the nacelle, rotor, and the platform, ξ is the actuator damping ratio, and ω is the angular frequency of the actuator. A value of 60 to 70 percent for the oscillator damping and an actuator frequency of approximately 10 times the highest frequency of the turbine model is suggested. A simulation time step of 1/10 of the period of the oscillator is a good starting value. A smaller time step may be necessary for particularly energetic input motions. The force time history is calculated using the displacement and velocity of the motion at each time step using the following equation:

$$F = K(X - D) + C(\dot{X} - V) \quad (3)$$

In Equation 3, X and \dot{X} are the desired displacement and velocity; D and V are the realized displacement and velocity respectively. In addition to user-defined motion, generation of synthetic motion is possible. First a sequence of random numbers with zero mean and unit variance is generated using two seed numbers. If specified, an initial and final ramp is used to shape the generated synthetic motion to more closely resemble an earthquake. The ramp file format matches that of the input motion and can be specified with any time step. The time series is then scaled so that the resulting root-mean-square (RMS) amplitude matches that specified by the user. A simple recursive, single-pole, low-pass filter with exponential smoothing is applied to attenuate high frequency content that cannot be reproduced by the model. The applied motion can be saved for later analysis by outputting the appropriate variables in the simulation.

2.2. MOTION HANDLING

Two types of motion handling are provided. The first method of motion modification is baseline correction, in which residual velocity or displacement is removed. The second modification procedure is used to adjust the motion to conform to

a target response spectrum. As shown in Figure 1, both user-defined and synthetic motions can make use of these features.

2.2.1. Baseline Correction. Numerically calculated displacement from many accelerograms shows a large value of drift due to various sources, including numerical error and measurement noise. If the input motion shows residual displacement or velocity, baseline correction is frequently used to remove these artifacts. In the modified FAST code, baseline correction is performed by first numerically integrating the prescribed motion to calculate displacement. A second order polynomial is then fit using least squares to the calculated displacement. The polynomial is subtracted from the displacement time history to eliminate residual drift. Finally, the updated velocity and acceleration are calculated from the corrected displacement time history by numerical differentiation.

For an illustrative example the 5-MW NREL utility scaled wind turbine is selected and the properties of this structure are implemented in the FAST input files. This model is intended to serve as a standard model for conceptual studies of modern wind turbines. Some of the properties of this turbine are shown in Table 1 and the complete description is available in Jonkman, et al. (2009). For demonstrating the effectiveness of baseline correction procedure, a synthetic motion with a 50 second duration and 0.5 m/s^2 RMS amplitude, with appropriate initial and final ramping values, was applied in the wind parallel horizontal direction to the base of the turbine using the seismic module. Two simulations were conducted, one without taking into account baseline correction and the other with using the baseline correction subroutine. Simulation is conducted in 600 seconds time duration with synthetic ground motion applied at the beginning of 400 seconds. Application of the synthetic motion time history is delayed to allow initial transient behavior to diminish. As seen in Figure 2 the simulation without baseline correction results in a final velocity of 2 m/s and a displacement of 68 m. While the acceleration remains considerably close to the initial acceleration, the application of baseline correction successfully eliminated these undesirable artifacts. It is suggested that baseline correction be performed when motion is synthetically generated.

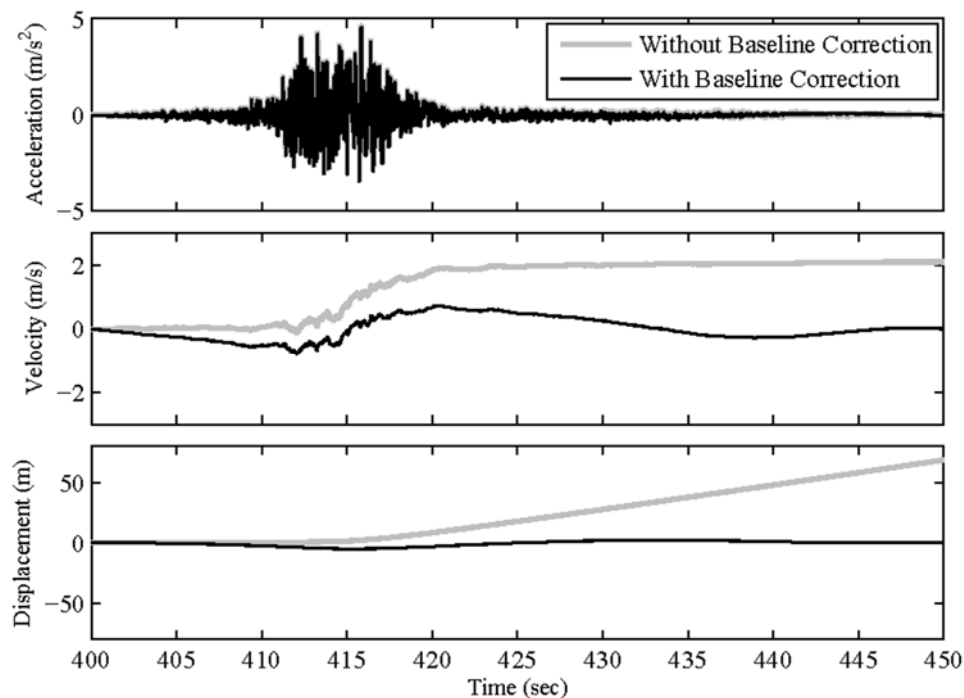


Figure 2. Baseline correction application on the 5-MW turbine using seismic module

Table 1. General specifications of the 5-MW NREL Wind Turbine

Property	Description
Rated power	5-MW
Rated Wind Speed	11.4 m/s
Tower Height	87.6 m
Mass of Rotor	111,000 kg
Mass of Nacelle	240,000 kg
Mass of Tower	347,460 kg
1 st Tower Fore-Aft Freq.	0.32 Hz
1 st Tower Side-Side Freq.	0.31 Hz
2 nd Tower Fore-Aft Freq.	2.90 Hz
2 nd Tower Side-Side Freq.	2.93 Hz

2.2.2. Target Response Spectral Matching. In some cases, input acceleration must be modified according to a specific response spectrum. Spectral matching is used to modify a time history to produce, within acceptable tolerance, the desired response spectrum. The 2009 version of RspMatch, documented by Atik and Abrahamson (2010), is now directly integrated in the seismic module of the FAST code. Tapered cosine wavelets are strategically added to the input acceleration time history to remove the discrepancies (misfits) between the spectral response of the input motion and the target response. This approach improves numerical efficiency, eliminates the need for additional baseline correction, and improves preservation of non-stationary characteristics of the original motion when compared to earlier strategies.

The 90 degree component of the 1989 Loma Prieta Earthquake, recorded at the Gilroy Array is used to illustrate the influence of using spectral matching in comparison to simply linearly scaling a motion. Figure 3 shows initial response spectrum and results of spectral matching to conform to a design spectrum for Imperial Valley considering soil type B and a site with one second spectral response acceleration (S_1) of 0.36 g and a short period spectral response acceleration (S_s) of 0.91 g that was calculated according to the specifications of ASCE-7-10 (2010). Both the considered design spectrum and the recorded motion have a pseudo spectral acceleration (PSA) of 0.42 m/s^2 at the first natural frequency of the turbine (0.31 Hz or 3.22 seconds in terms of period). By using spectral matching the difference between the desired response spectrum and that produced by the input motion is effectively eliminated. Figure 4 illustrates the effects of spectral matching on the motion time history. In the case of the selected motion the high frequency content exceeds that of the design spectrum (Figure 3) and is attenuated, noticeable as a reduction in the peak ground acceleration (Figure 4).

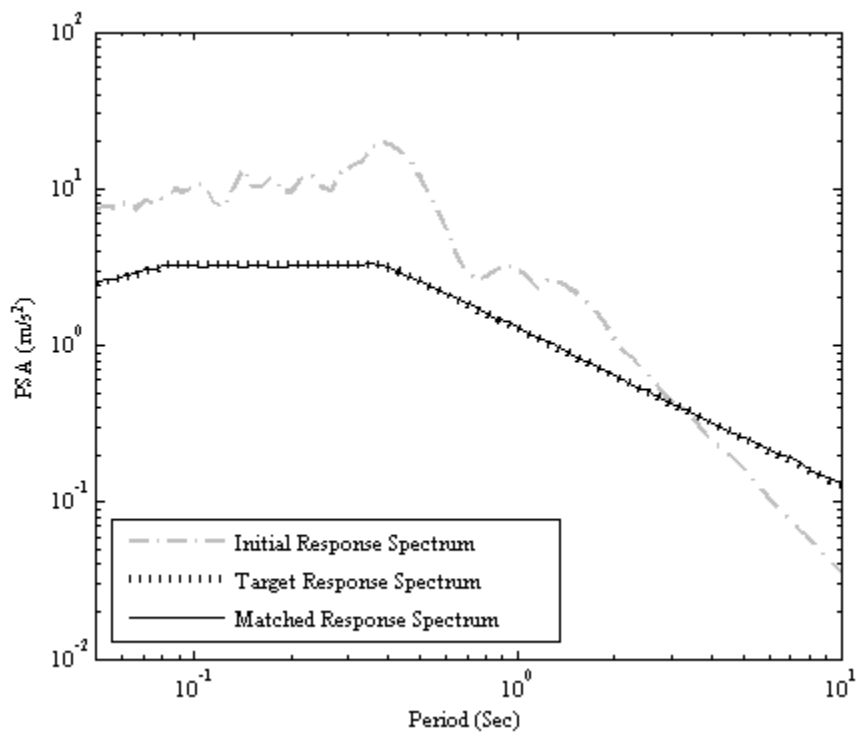


Figure 3. Target, initial, and the matched response spectra for the applied motion

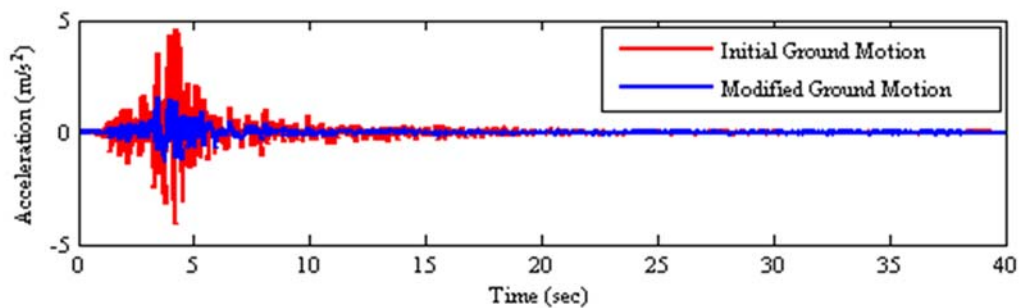


Figure 4. Initial and modified ground motion before and after response spectral matching

Two simulations are conducted where earthquake excitation from both before and after spectral matching is applied in the fore-aft direction (parallel to the wind direction) of the 5-MW reference turbine when it is operating under a constant wind with a hub height wind speed of 12 m/s. The wind is applied to the turbine model by using the AeroDyn code compiled with FAST. The PSA at the first period of the turbine is effectively the same for two motions considered, but as illustrated in Figure 3, there is a large difference at the second period (0.34 seconds). The resulting fore-aft moment demand at the tower base, top, and 4 other elevations (19, 37, 54, and 72 meters) is shown in Figure 5 for both simulations. For civil structures it is typically assumed that the seismic response is highly dominated by the first mode, however Figure 5 clearly illustrates that the second mode plays an important role. For the motion after spectral matching the base moment demand is reduced by approximately 25%. Given this significant difference, spectral matching to a design spectrum based on a uniform hazard spectrum (UHS) may not be appropriate as the controlling events for these two ranges are likely different in terms of magnitude and distance. Instead, the conditional mean spectrum (CMS) may be more appropriate for determination of extreme loads based on spectrum compatible time histories as described in Baker (2011).

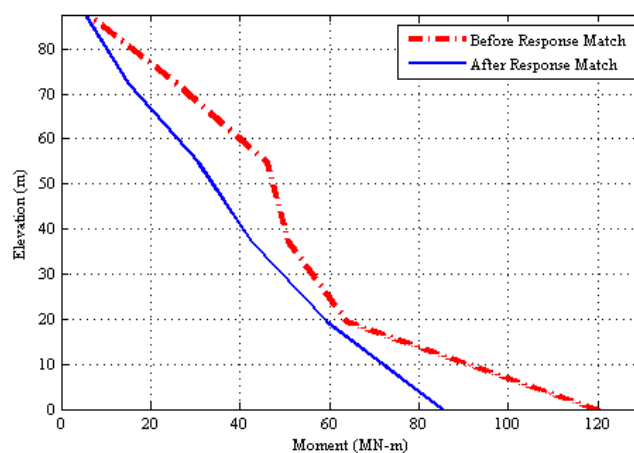


Figure 5. Effect of spectral matching on tower moment demand for each elevation

3. EFFECTS OF AERODYNAMIC DAMPING ON SEISMIC RESPONSE

Unlike conventional civil engineering structures that have single stationary state, wind turbines have multiple dynamic states which will affect the dynamic response of these structures. It is expected that operational dynamics will influence the structural response due to aerodynamic damping. Aerodynamic damping can be added to the velocity term of the equation of motion but calculating the exact amount of this type of damping is quite complex. In the work provided by Valamanesh and Myers (2014), a simplified method for calculation of aerodynamic damping is introduced. Aerodynamic damping is mainly caused by the wind velocity, and angular velocity of the rotor which will cause energy dissipation at the top of the tower in the direction of aerodynamic loading. It is also shown in Asareh and Volz (2013), that the first fore-aft tower mode shape of the structure which is the dominant mode will carry some of its contributions from the blades of the wind turbine which will cause more dissipation of the kinetic energy in the wind direction.

To show the effects of aerodynamic damping, FAST and the seismic module are used for the same 5-MW NREL wind turbine model in the two conditions of when the turbine is idled (not operating), and when the turbine is normally operational both in an event of an earthquake. The horizontal components of the Manjil, Iran 1990 earthquake were selected for this comparison. The longitudinal component in the fore-aft (X) direction of the wind turbine has a peak ground acceleration value of 0.57g and in the side-side (Y) direction 0.53g. For showing the attenuation in the dynamic response, acceleration at the top of the tower can be compared in the cases of idling and operational in both fore-aft and side-side direction. Figure 6 compares the absolute acceleration at the tower top for both of the mentioned configurations. As stated in the previous sections, earthquake loading is applied at the start of 400 seconds in the 600 second simulation to make sure that the transient vibrations of the turbine have completely diminished. The applied ground motion has 53.5 seconds duration; hence the results of the tower top acceleration are shown from the beginning of ground motion application to the end of the earthquake duration. It is observed that during the operation of the turbine the observed accelerations have a lower maximum with a faster decay than the case when turbine is

not operational in the wind direction but it almost has the same acceleration at all times in the side-side direction.

Figure 7 also shows the amplitudes of the tower top acceleration for both configurations in both directions. As can be seen the dominant frequency with highest amplitude is the first tower fore-aft and side-side natural frequency which are close to each other as stated in the wind turbine properties in Table 1. For the idling condition without the presence of aerodynamic loading, the amplitude is higher than the case of operational configuration. The difference between the amplitudes is not visible in the side-side case of the structure because of the absence of aerodynamic loading.

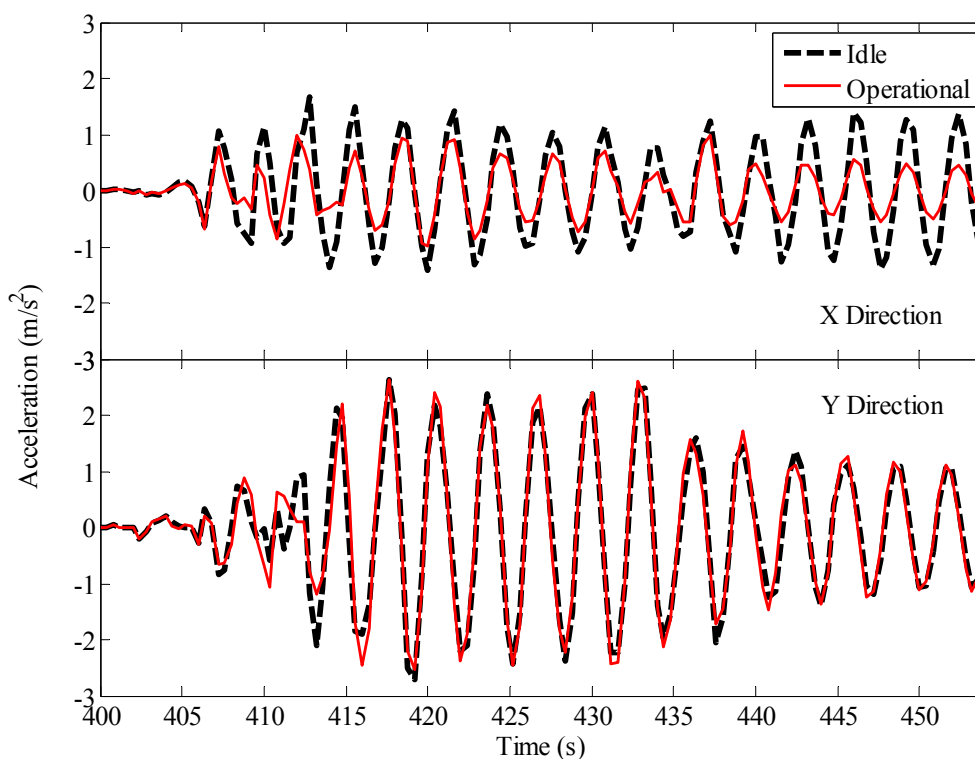


Figure 6. Tower top acceleration for operational and idling condition in both directions under seismic excitation

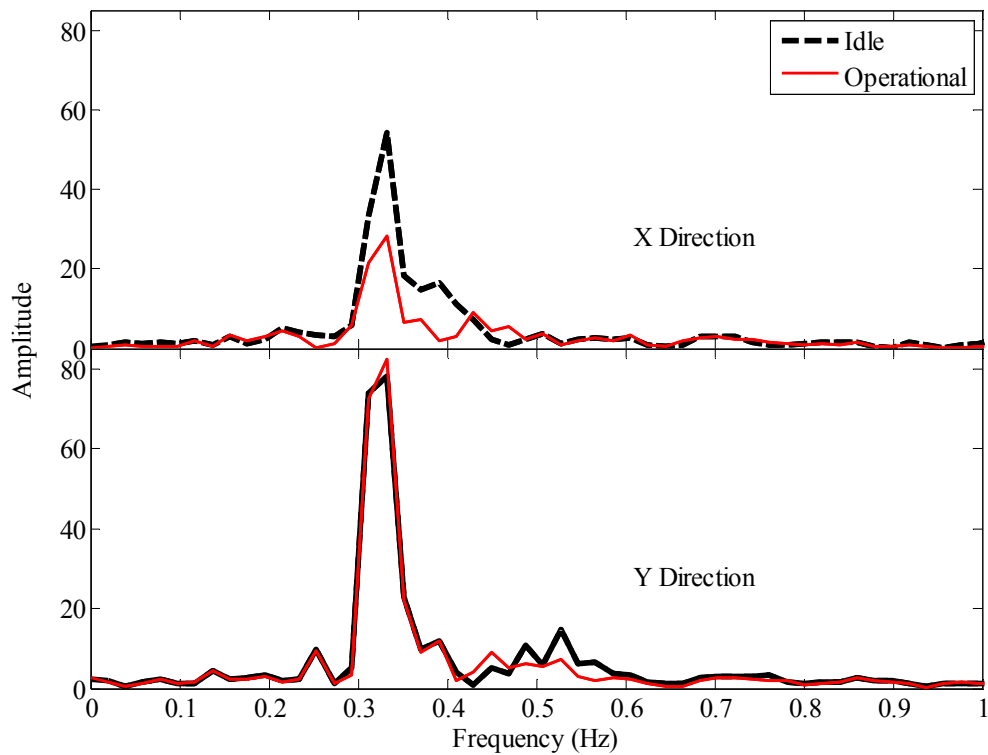


Figure 7. Amplitudes of the tower top acceleration for idling and operational conditions of the turbine in both directions

4. IMPLICIT CONSIDERATION OF AERODYNAMIC DAMPING IN SEISMIC AND WIND LOAD COMBINATIONS

Turbine specific design codes such as the previously mentioned IEC (2005), or GL (2003) use linear combinations for considering extreme earthquake and operational loads together. These guidelines use load factors of one for operational and seismic load combinations. Earthquake loads are basically calculated using simplified approaches in frequency domain finding the desired spectral acceleration according to the natural frequency of structure and multiplied by a certain proportion of the mass of the structure for the obtaining the seismic demand at the base of the tower and added to the maximum of the operational loads which is used for design of both the foundation and tower of the turbine.

In this section, attempts have been made to show that the load combinations available in these guidelines which consider independent calculations of earthquake and operational loads are an overestimation of the actual design demand in the event of extreme seismic and wind activities. This is done by considering the coupling of the loads using the seismic module platform which is added to FAST which consider direct interaction between loads. The results of coupled loads are compared with the combination of simulations that independently evaluate seismic (Q_e) and operational loads (M) of wind turbines. For independent analysis seismic loads of the 5-MW NREL turbine are obtained from the FE simulation platform OpenSees developed by Mazzoni, et al. (2006) using different critical damping ratios. The Rayleigh damping coefficients are obtained according to the first and second natural frequencies of the turbine tower which is 0.32Hz and 2.90Hz, respectively. The OpenSees model of the turbine is developed using beam elements for the tower and the blades considering different section properties of the turbine components which were available in Jonkman, et al. (2009). Mass of each section is distributed such that the model in OpenSees has the same modal properties (1st and 2nd tower natural frequencies and mode shapes) with the FAST model of the turbine. OpenSees does not have the capability to consider aerodynamic loads, thus the results can only be used for calculation of seismic loads and compared with coupled simulations in the idling condition where operational loads are not affected. A series of

independent analysis are done in FAST without any seismic loads so that they can be added to the OpenSees results and compared with the coupled simulations in operational cases of normal operation and idling of the turbine.

4.1 SELECTED GROUND MOTIONS AND WIND LOADS

The two horizontal components of the 22 far-field earthquake records provided by ATC (2009) are used for the analysis. The earthquake motions are scaled such that the mean of the square root of the sum of the squares (SRSS) for both horizontal components of each earthquake conforms with the three dimensional excitation requirements for a site with one second spectral response acceleration (S_1) of 0.55g, which is typical for sites with soil class B in Northern California. The resulting ensemble has also been scaled such that the mean of the SRSS of the spectral displacement of all 22 earthquakes matches the spectral displacement of the design displacement response spectrum at the first natural period (3.22 seconds) of the turbine structure. The displacement spectrum is used because of the long period of the structure which makes the structure to be accounted as displacement sensitive. Figure 8 shows the SRSS of the displacement spectrum of all 22 earthquakes along with the mean of the SRSS of all earthquakes and the design displacement spectrum. Table 2 shows the selected earthquake characteristics and the scale factors used. The 22 earthquakes were applied at the base of the two models in the coupled FAST and OpenSees models with the horizontal components swapped to remove any bias due to relative orientation with the wind direction making them a total of 44 simulations for operational and idling state.

For the coupled simulations in FAST and the seismic simulation module and also for the independent simulations in FAST with only considering aerodynamic loading, the turbine is subjected to a hub height mean wind speed of 11.4 m/s and an IEC turbulence level B. This is equal to the rated wind speed of the 5-MW NREL wind turbine which will produce the highest intensity of aerodynamic loads according to Asareh and Volz (2013). The wind field is generated by a stochastic, full field turbulent-wind simulator called TurbSim which was developed in NREL by Jonkman (2009). The wind field is read by AeroDyn and used in FAST to apply the aerodynamic loads to the blades of the turbine in each time-step. In total 134 analysis were done in 600 second durations which

included 88 simulations for coupled analysis using 22 earthquake motions in 2 interchangeable directions for 2 operational and idling states using the 11.4 m/s mean wind speed, 44 simulations in OpenSees considering different earthquakes on the base of the FE model, and 2 simulations in FAST with only considering the 11.4 m/s wind load without considering the earthquakes for operational and idling state.

4.2 SIMULATION RESULTS

The results of coupled and independent simulations are presented in this section. They are shown in terms of moment demand in each elevation of the tower which is one of the most design deriving parameters of this structure because the tower is mostly governed by bending loads.

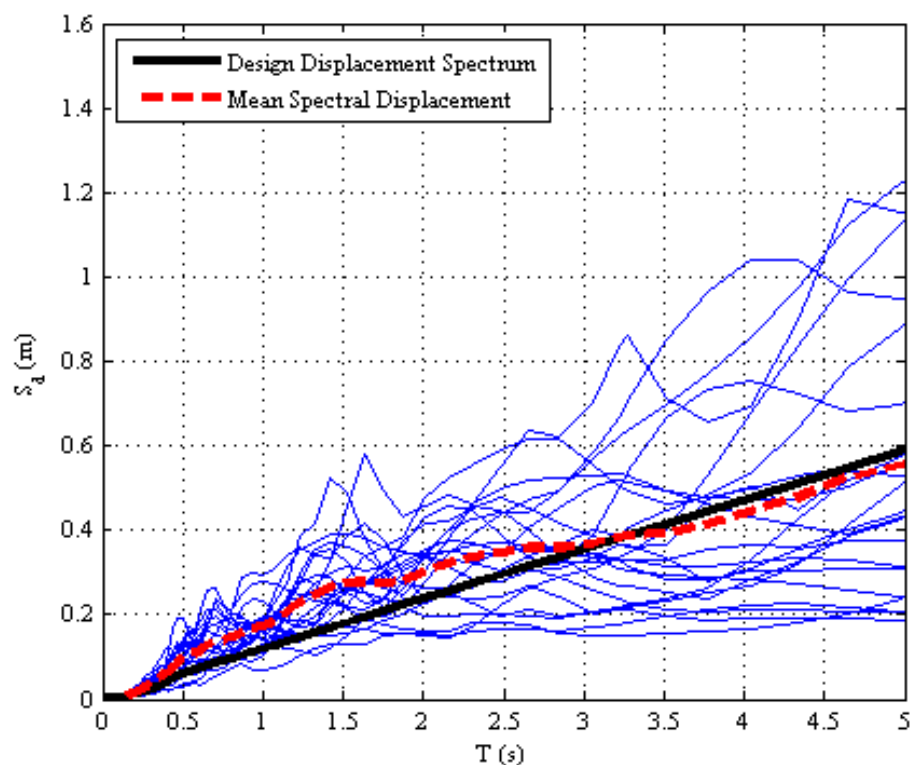


Figure 8. Spectral displacement with 5% damping for the earthquake ensemble

First, the results of coupled simulations in idling state are compared with the results obtained from OpenSees. This comparison can be done because there are no aerodynamic loads involved in the idling state and the only loads that are involved are the different earthquake loads. Figure 9 shows the mean of the maximum of the square root of sum of the squares for moment in the fore-aft and side-side directions for coupled simulations in FAST using seismic module and OpenSees with three different damping ratios of 0.5%, 1%, and 5% for all 44 earthquake motion scenarios.

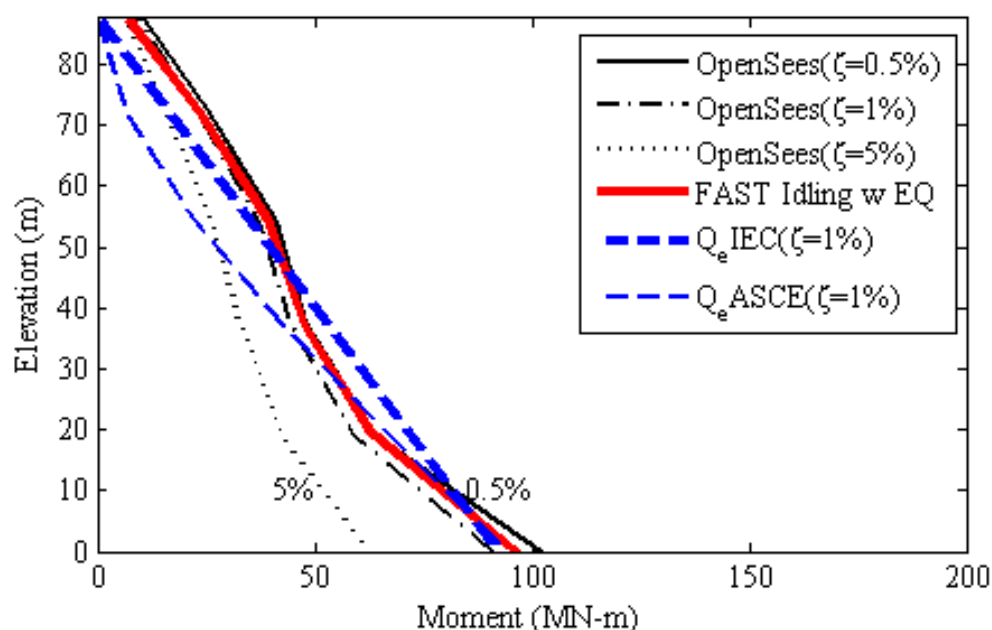


Figure 9. Mean of the maximum of SRSS of the moments in fore-aft and side-side direction considering the 44 ground motions in idling condition

Table 2. Characteristics of the ground motion used to perform the analysis

#	Motion Name	Scale Factor	SRSS PGA (g)	SRSS PGV (m/s)	SRSS PGD (m)	SRSS PSA(g) @3.22 seconds $\xi = 5\%$	SRSS PSD(m) @3.22 seconds $\xi = 5\%$
1	Northridge (1994)	0.65	0.56	0.72	0.14	0.09	0.23
2	Northridge (1994)	0.83	0.68	0.67	0.18	0.12	0.31
3	Duzce, Turkey (1999)	0.63	0.90	0.68	0.21	0.14	0.36
4	Hector Mine (1999)	1.09	0.62	0.71	0.36	0.13	0.33
5	Imperial Valley (1979)	1.31	0.72	0.70	0.36	0.32	0.83
6	Imperial Valley (1979)	1.01	0.69	0.70	0.31	0.20	0.52
7	Kobe, Japan (1995)	1.03	0.97	0.70	0.19	0.10	0.26
8	Kobe, Japan (1995)	1.10	0.46	0.67	0.16	0.13	0.33
9	Kocaeli, Turkey (1999)	0.69	0.42	0.65	0.41	0.19	0.51
10	Kocaeli, Turkey (1999)	1.36	0.46	0.73	0.64	0.13	0.33
11	Landers (1992)	0.99	0.37	0.74	0.60	0.15	0.38
12	Landers (1992)	1.15	0.76	0.73	0.28	0.08	0.21
13	Loma Prieta (1989)	1.09	0.94	0.65	0.15	0.08	0.21
14	Loma Prieta (1989)	0.88	0.75	0.64	0.23	0.13	0.32
15	Manjil, Iran (1990)	0.79	0.78	0.70	0.26	0.20	0.50
15	Superstition Hills (1987)	0.87	0.50	0.69	0.29	0.14	0.36
17	Superstition Hills (1987)	1.17	0.82	0.72	0.21	0.21	0.53
18	Cape Mendocino (1992)	0.82	0.72	0.65	0.30	0.06	0.15
19	Chi-Chi, Taiwan (1999)	0.41	0.30	0.69	0.42	0.24	0.62
20	Chi-Chi, Taiwan (1999)	0.96	0.83	0.66	0.63	0.08	0.21
21	San Fernando (1971)	2.10	0.74	0.64	0.37	0.26	0.66
22	Friuli, Italy (1976)	1.44	0.88	0.71	0.12	0.07	0.17
-	ASCE Design Response Spectrum	-	-	-	-	0.15	0.33
-	Average of 22 motions	-	-	-	-	0.15	0.33

Moment demand for this turbine is also obtained from the simplified methods in IEC (2005) using equations available in Annex C. It is also calculated using equivalent lateral force method in ASCE-7-10 (2010). These methods both take into account an efficient mass of the structure (usually the mass of the rotor and nacelle plus a proportion of the mass of the tower) and the spectral acceleration according to the first period. Figure 9 shows that the results of the analysis of coupled simulations are approximately in agreement with the results from OpenSees with the consideration of 1% damping. The

base bending moment demand also matches the bending moments achieved from simplified methods of the design codes. The differences in design code simplified methods and analysis done in time domain in FAST and OpenSees for the top elevations of the tower is because of the considerations of higher mode shapes in time domain analysis. It is also mentioned in IEC (2005) and the experimental simulations done by Prowell (2011), that the appropriate damping ratio that needs to be considered for a turbine in idling or parked condition is about 1% which agrees with the results shown in Figure 9. Figure 10 also shows the maximum of the SRSS of the moments in both directions for each elevation for FAST and OpenSees analysis in idling condition which match at a damping ratio of 1%.

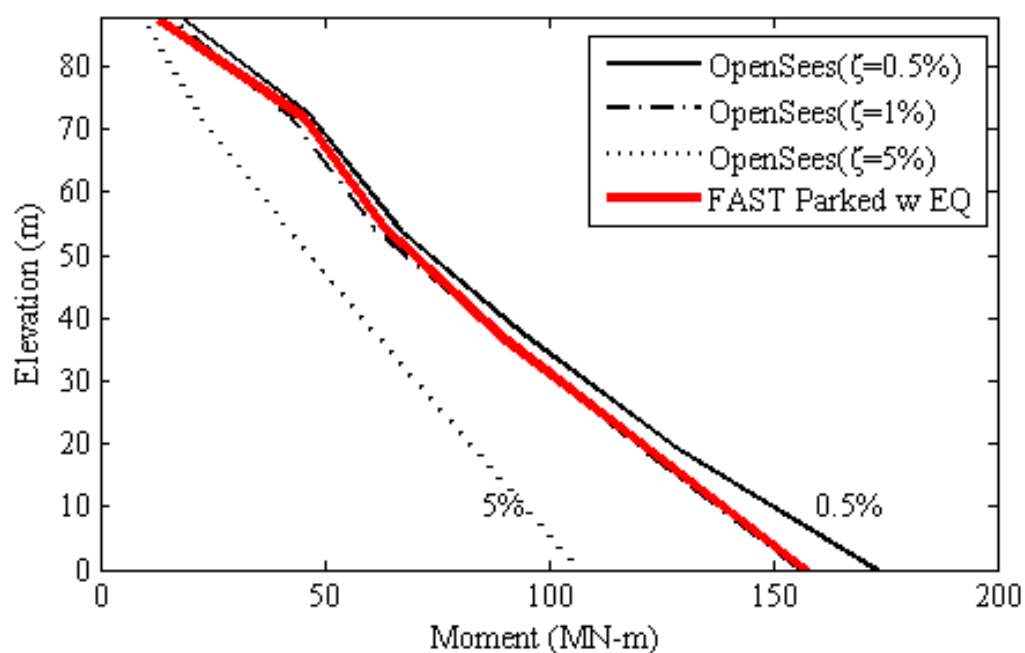


Figure 10. Maximum of the SRSS of the moments in fore-aft and side-side direction considering the 44 ground motions in idling condition

In the next step, the results of coupled simulations in operational condition of the turbine are compared with the combinations of individual simulations done in OpenSees on earthquake loads (Q_e), and FAST on wind loads (Q_o) without operating the seismic module. The load combinations considered are two linear combinations of wind and earthquake loads considering load factors of 1 and 0.75 for both earthquake and operational loadings. Figure 11 shows the comparison between coupled aerodynamic and seismic simulations in operating condition with the combination of OpenSees earthquake analysis and FAST wind simulations with load factor of one. Seismic moment demands obtained by design codes are also added to the operating loads obtained from FAST simulations only considering the operational loads (Q_o) using a load factor of one. Same results are shown for the data considering a load factor of 0.75 for both individual simulations in Figure 12.

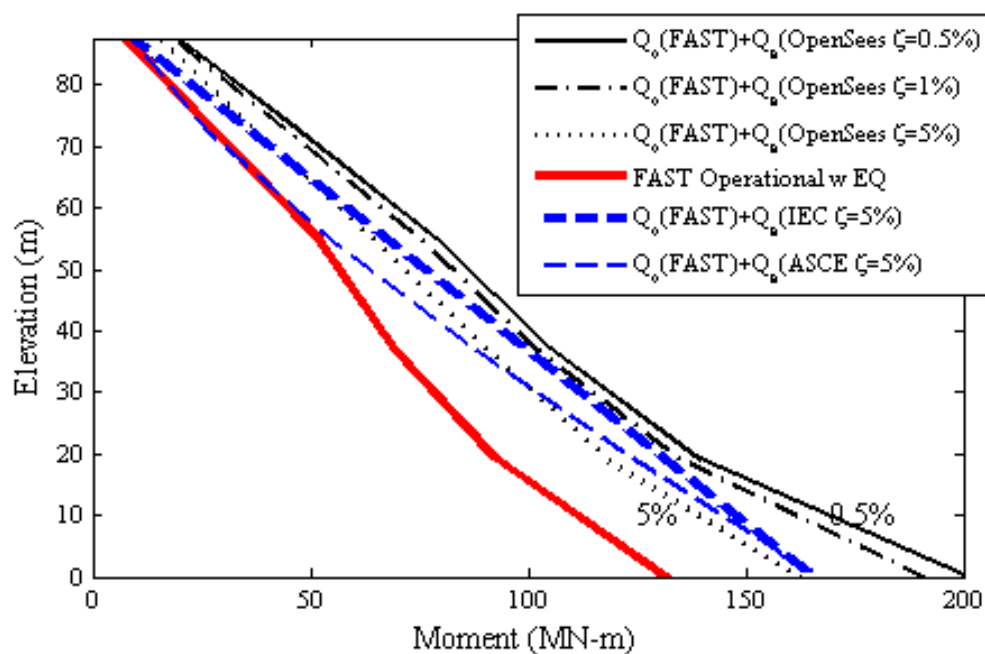


Figure 11. Comparison of linear combination of operational and earthquake loads

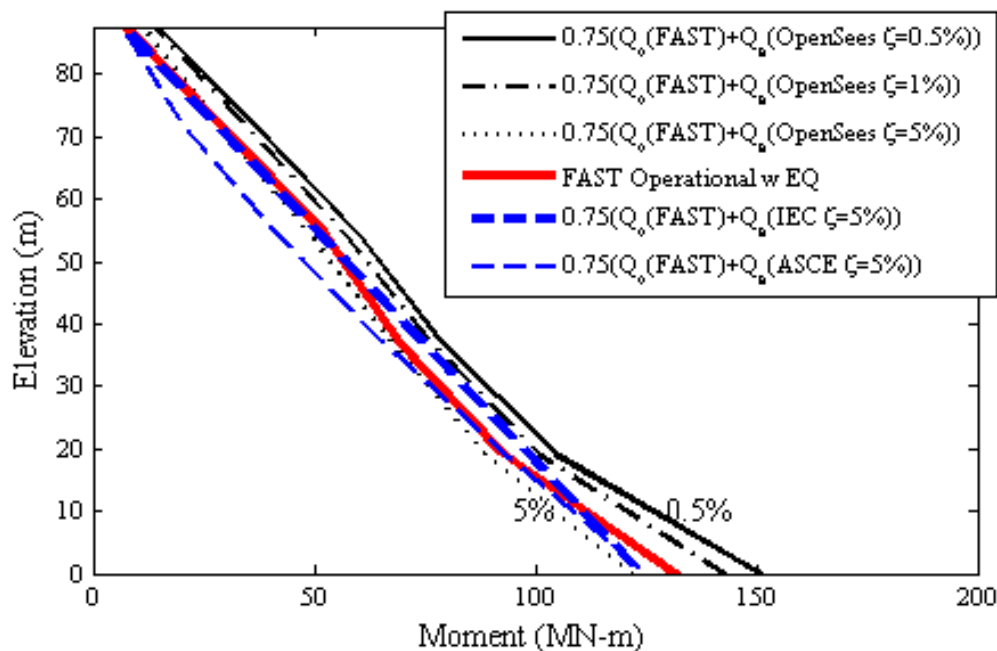


Figure 12. Comparison of 0.75 combination of operational and earthquake loads

It is observed from the results shown in Figure 11 and Figure 12 that the load combination with load factor of 0.75 is a better estimate of moment demands in tower elevations. The load combination with load factors of 1 which is proposed in the IEC (2005) guidelines is an overestimate of the loads because when the loads are considered individually, factors such as aerodynamic damping and other effects like higher mode contributions are not entirely considered. It is also seen that the appropriate damping ratio that is needed to simulate this structure in the operating condition is close to 5%. Table 3 shows the percentage of difference between the moment demand in each elevation for the coupled and individual load combinations with different load factors which also shows the 0.75 load factor to be a more optimized combination for a cost effective design. This combination is also indicated to be a better estimate in the recently published document published by the ASCE/AWEA (2012).

Table 3. Difference (%) in tower moment between load combinations

Height (m)	Operational (%)	
	(Q_c+Q_o)	$0.75(Q_c+Q_o)$
0.00	23	7
19.27	28	4
37.66	29	3
54.31	26	5
72.71	30	2

5. CONCLUSIONS

In this paper, the effects of seismic excitation along with other environmental loading conditions acting on a wind turbine structure are evaluated. A numerical procedure is developed and implemented in the FAST program that has the capabilities of applying user-defined or synthetically generated earthquake records in the translational degrees of freedom to the base of the structure. The developed seismic module can also perform baseline correction and spectral matching analysis on the desired ground motion. Numerical simulations that can be performed for different subroutines are summarized. This program is then used to evaluate the effect of aerodynamic damping on the bending moment demand of the turbine tower which is known as one of the design deriving parameters for these structures. It is observed that for the studied 5-MW NREL turbine, a total value of 1%, and 5% damping ratio will provide a good estimate for idling and operational conditions, respectively.

Linear load combinations of seismic and operational loads with two different load factors of one and 0.75 are achieved from the individual wind and earthquake simulations. These combinations are compared with the results obtained from coupled simulations. This comparison shows that the load factor of one for earthquake and wind load is an overestimation in the design of wind turbines because the effect of aerodynamic damping during the operation of structure will considerably reduce the moment demand of these structures.

REFERENCES

- [1] Asareh M-A and Volz JS (2013), "Evaluation of aerodynamic and seismic coupling for wind turbines using finite element approach," Proceedings of the ASME 2013 International Mechanical Engineering Congress and Exposition, 4B, San Diego, California, USA, V04BT04A041.
- [2] Asareh MA and Prowell I (2011), Seismic loading for FAST, National Renewable Energy Laboratory, Golden, CO.
- [3] ASCE-7-10 (2010), Minimum design loads for buildings and other structures, American Society of Civil Engineers, Reston, Virginia.
- [4] ASCE/AWEA (2012), Recommended practice for compliance of large onshore wind turbine support structures, ASCE/AWEA RP2011, Reston, VA.
- [5] ATC (2009), Quantification of building seismic performance factors, Applied Technology Council, Redwood City, CA.
- [6] Atik LA and Abrahamson N (2010), "An improved method for nonstationary spectral matching," Earthquake Spectra, 26(3): 601-617.
- [7] Baker JW (2011), "Conditional mean spectrum: tool for ground-motion selection," Journal of Structural Engineering, 137(3): 322-331.
- [8] Bazeos N, Hatzigeorgiou GD, Hondros ID, Karamaneas H, Karabalis DL and Beskos DE (2002), "Static, seismic and stability analyses of a prototype wind turbine steel tower," Engineering Structures, 24(8): 1015-1025.
- [9] GL (2003), Rules and Guidelines: Industrial Service: Guideline for the Certification of Wind Turbines, Germanischer Lloyd.
- [10] Hau E and Von Renouard H (2013), Wind turbines: fundamentals, technologies, application, economics, Springer.
- [11] IEC (2005), IEC 61400-1 Ed. 3: Wind Turbines - Part 1: Design Requirements, International Electrotechnical Commission, Geneva, Switzerland.
- [12] Jonkman BJ (2009), TurbSim user's guide: version 1.50, National Renewable energy Laboratory, Golden, CO.
- [13] Jonkman JM and Buhl Jr ML (2005), FAST user's guide, National Renewable Energy Laboratory, Golden, CO.
- [14] Jonkman JM, Butterfield S, Musial W and Scott G (2009), Definition of a 5-MW reference wind turbine for offshore system development, National Renewable Energy Laboratory, Golden, CO.

- [15] Laino DJ and Hansen AC (2002), User's guide to the wind turbine aerodynamics computer software AeroDyn, National Renewable Energy Laboratory (U.S.).
- [16] Lavassas I, Nikolaidis G, Zervas P, Efthimiou E, Doudoumis I and Baniotopoulos C (2003), "Analysis and design of the prototype of a steel 1-MW wind turbine tower," *Engineering structures*, 25(8): 1097-1106.
- [17] Lindenberg S (2009), 20% wind energy by 2030: Increasing wind energy's contribution to US electricity supply, DIANE Publishing.
- [18] Mazzoni S, McKenna F and Fenves GL (2006), Open system for earthquake engineering simulation user manual, Pacific Earthquake Engineering Research Center, Berkeley, CA.
- [19] Prowell I, Veletsos M, Elgamal A and Restrepo J (2009), "Experimental and numerical seismic response of a 65 kW wind turbine," *Journal of Earthquake Engineering*, 13(8): 1172-1190.
- [20] Prowell I (2011), An experimental and numerical study of wind turbine seismic behavior, University of California, San Diego.
- [21] Prowell I, Uang CM and Elgamal A (2011), Shake table test of a utility-scale wind turbine, Department of Structural Engineering, University of California, San Diego: La Jolla, California, USA.
- [22] Risø-DNV (2001), Guidelines for Design of Wind Turbines, Wind Energy Department of Risø National Laboratory and Det Norske Veritas, Copenhagen, Denmark.
- [23] Ritschel U, Warnke I, Kirchner J and Meussen B (2003), Wind turbines and earthquakes, World Wind Energy Association Cape Town,, South Africa.
- [24] Valamanesh V and Myers A (2014), "Aerodynamic damping and seismic response of horizontal axis wind turbine towers," *Journal of Structural Engineering*, 140(11): 04014090.
- [25] Witcher D (2005), "Seismic analysis of wind turbines in the time domain," *Wind Energy*, 8(1): 81-91.

II. EFFECTS OF SEISMIC AND AERODYNAMIC LOAD INTERACTION ON THE POWER GENERATION AND STRUCTURAL RESPONSE OF MULTI-MEGAWATT UTILITY SCALE HORIZONTAL AXIS WIND TURBINES

ABSTRACT

Horizontal axis wind turbines can experience significant time varying aerodynamic loads that has the potential to cause adverse effects on structural, mechanical, and power production. The progress in the wind industry has caused the construction of wind farms in areas prone to high seismic activity. With the advances in computational tools, a more realistic representation of the behavior of wind turbines should be performed. One of the simulation platforms was developed using the 5-MW NREL utility scale reference turbine model. The performed simulations will be used to evaluate the effects of aerodynamic and seismic load coupling on the power generation and structural dynamics behavior of this structure. Different turbine operational scenarios such as (i) normal operational condition with no earthquake, (ii) idling condition with the presence of seismic loads, (iii) normal operational condition with earthquake, and (iv) earthquake-induced emergency shutdown will be simulated with various loading conditions to show the differences in generated power and dynamic response. The results of this paper provide formulations for calculating generated power and design deriving parameters by considering different intensity measures. Moreover, the effects of aerodynamic damping and pitch control system are presented to shows reduction in the resulting design demand loads.

Keywords: horizontal axis wind turbine; aerodynamic-seismic interaction; power generation; coupled simulations; moment demand; seismic-induced emergency shutdown

1. INTRODUCTION

Common sources of energy production (i.e. carbon based resources) have been used for hundreds of years. However, they are rapidly depleting and also have significant disadvantages such as carbon emissions and the generation of hazardous waste. Another common energy production method is hydroelectric power which is known for disadvantages like high reliability on water, high construction and maintenance costs, and the potential for damage to the natural environment. For such reasons, researchers and others who are involved in the energy production industry have started exploring new and alternative energy production methods. Having advantages such as guaranteed fuel availability, no cost volatility, emission free operation, and no waste generation, wind energy has become a rapidly deployed and cost effective renewable energy method in recent decades.

According to recently published DOE report [1], the installed capacity of wind turbines in the US at the end of 2013 was up to 61 GW, which accounted for 4.2% of the energy produced in this country. It is also predicted that, by the end of the year 2030, the estimated value of energy production by wind will reach 300 GW, which will be 20% of the electricity produced. These estimations rely on taking into account new technologies in wind turbine systems and also on using the complete potential of the offshore wind energy available in the east and west shorelines of the US. The power of a wind turbine is described by the power in wind multiplied by the efficiency factor (which has the maximum of 0.59 according to the Betz limit and basic rotor momentum theory described in [2]). The power produced by wind is proportional to the third power of wind speed and the second power of the rotor diameter. Since there is no control over the environmental factor of wind speed, the method to procure more energy from the horizontal axis wind turbines is to increase the rotor diameter. This has led the designers of wind turbines to come up with a way to make lighter and cost effective wind turbines, including larger rotor diameters and alternative materials for blades [3]. As turbines become larger in size, the tower top mass increases, which will increase the tower moment and seismic demand loads when designing these structures. It is important to consider that most of the areas with high wind resources also have a high seismic hazard. These areas include the west

coast of the US and the coasts of Japan and China. Reports show damages induced by earthquakes as the turbines increase in size [4]. Turbine specific design codes such as IEC [5], GL [6], and DNV [7] have rudimentary recommendations for the consideration of wind turbines, which mostly calculate seismic force in frequency domain and consider the turbine structure to be a single degree of freedom system.

In the past few years researchers have tried to consider the importance of seismic loads for operational wind turbines, and yet the work is limited. Early publications done by Bazeos, et al. [8] and Lavassas, et al. [9] include consideration of seismic loading of wind turbines by focusing on the loading of the tower. These simplified models assume the tower top components (nacelle and rotor) to be a lumped mass for prototype 450-kW and 1MW turbines with 38 m and 44 m tall steel towers designed for installation in Greece. The authors speculate that seismic design could become critical in regions with higher seismic hazard and less favorable soil conditions. Ritschel, et al. [10] conducted simulations for a 2.5-MW Nordex N80 wind turbine with an 80 m rotor diameter and 60 m hub height using a full system model with 28 degrees of freedom in FLEX5 by mapping ground acceleration through a coordinate transformation into effective external nodal forces. This investigation concluded that seismic loads in the blades were about 70% lower than those caused by the 50-year wind loads.

Witcher [11] presented an overview of the GH Bladed [12] seismic module for a two megawatt upwind turbine with 80 m rotor diameter and 60 m tower height and considers the response of the structure in three different load cases of parked, operational, and earthquake induced emergency shutdown. The significance of time domain analysis and the effects of aerodynamic damping were emphasized in this work. Prowell and Veers [13] performed a comprehensive study the assessment of wind turbine seismic risk. Results showed that wind-driven loads can grow faster than seismic-driven loads in the absence of control systems. But for modern turbines with blade pitch control system, the dominant loads would be the seismic-driven loads as the turbine increases in size. Prowell, et al. [14] conducted experimental work on a 65 KW Nordtank wind turbine using the large high performance outdoor shake table available in University of California at San Diego. Earthquake motions were applied in two horizontal directions and the modal characteristics and dynamic behavior of this turbine was obtained. This

work also concluded that the importance of considering seismic demand increases as the turbines grow in capacity. Ishihara and Sawar [15] and Haenler [16] also studied the effects of aerodynamic and seismic loads using simplified methods. They concluded that the effects of higher modes also play an important role in the dynamic response of wind turbines. More recently, an extensive investigation into the seismic response of a 1.65-MW Vestas turbines was conducted using ANSYS by Nuta, et al. [17]. The authors developed fragility curves by performing incremental dynamic analysis and considering different intensity measures, damage measures, and damage states. However, aerodynamic loading was not considered in the analysis.

In this paper, a seismic module was developed for the publicly available wind turbine simulation tool FAST [18], which was originally developed by the National Renewable Energy Laboratory (NREL). This module can be compiled with the FAST core program for consideration of wind and earthquake load interaction. A 5-MW NREL reference wind turbine [19] was modeled using this program and analyzed using different wind and earthquake scenarios. The results obtained in this paper, are shown to evaluate power generation and structural dynamic characteristics without the involvement of earthquake at the first step. In the next steps, the normal operation of the wind turbine model in the first step is compared with three operational conditions of idling, running, and seismic induced emergency shutdown with the consideration of earthquake loads. Power generation formulations were obtained for different conditions using statistical methods in different operational scenarios considering various intensity measures from the earthquake and wind loads that were applied to the structure. The effects of pitch control system and aerodynamic damping caused by the interaction of these loads is also shown in different simulation conditions.

2. DEVELOPMENT OF SEISMIC MODULE FOR FAST

FAST (Fatigue, Aerodynamics, Structures, and Turbulence) is an open source simulation platform developed by Jonkman, et al. [18] at the National Renewable Energy Laboratory (NREL). This platform uses multi-body dynamics formulation to solve the equation of motion for a combination of flexible and rigid bodies with limited degrees of freedom for two or three horizontal axis wind turbines in time domain. The blades and tower mode shapes are given by the user as input in terms of sixth order polynomial formulations with the zeroth and first terms set to zero to closely define the cantilevered shape of the components. FAST can be compiled with the AeroDyn code developed by Laino and Hansen [20] that uses blade element momentum theory to calculate the aerodynamic loads in time domain. Wind speed, angle of attack, and drag and lift coefficients of different airfoils are used to calculate normal, tangential, and pitch moment forces that are then applied to each segment of the blades in FAST. A comparison of different wind conditions and the effect of blade pitch control system as determined by FAST is described in [21].

Seismic simulation capabilities were implemented through a module with different subroutines written in FORTRAN for FAST by Asareh and Prowell [22]. The basic concept of this module is that the base degrees-of-freedom in three translational directions can be released and replaced with a damped oscillator having stiffness and damping properties given in Eq. (1) and Eq. (2) below, where m is the total mass of the turbine including the nacelle, rotor, and the platform, ξ is the oscillator damping ratio, and ω is the angular frequency of the oscillator. The ground motion is then applied as force to the base of the turbine tower in the desired direction in each time step using the formulation shown in Eq. (3).

$$K = m\omega^2 \quad (1)$$

$$C = 2m\omega\xi \quad (2)$$

$$F = K(X - D) + C(\dot{X} - V) \quad (3)$$

In Eq. (3), X and \dot{X} are the desired displacement and velocity, while D and V are

the realized displacement and velocity, respectively. The seismic simulation module also has the capability to generate synthetic motion in the three translational directions of the base of the turbine by obtaining the desired RMS amplitude from the user. It also has subroutines that can perform motion handling analysis such as baseline correction and target response spectral matching analysis. Baseline correction is used when there are residual drifts in displacement and velocity time history due to numerical error and measurement noise and need to be removed. Target spectral matching is used when the frequency content of a specific earthquake needs to be modified to match a desired design response spectrum for a particular site or location and the method is theoretically explained in [23, 24]. The logical flow of how these subroutines work with the main program is available in [22]. Experimental studies from [14] were also used to verify this module with very good agreement between experiments and module predictions. Seismic characteristics are given as a separate input file to the FAST program. FAST program will check if any degrees of freedom at the base of the turbine are released and, if so, it will call the seismic input file that contains the ground motion input file paths (if the user provides ground motion records), type of ground motion (whether they are given in terms of displacement, velocity, or acceleration), scale factor, or the properties needed to generate synthetic motion, and other variables for baseline correction and target response spectral matching analysis.

The developed seismic module is used in all the steps in this paper to evaluate the effects of different earthquakes and wind conditions on the 5-MW NREL wind turbine model with structural properties shown in Table 1 in Paper I. This turbine is intended to serve as a standard model for conceptual studies of modern wind turbines [19]. This turbine is an upwind, three bladed, variable speed, and collective pitch control with a rotor diameter of 126 m and tower height of 87.6 m with cut-in, rated, cut-out wind speed of 3 m/s, 11.4 m/s, and 25 m/s, respectively. Cut-in speed is when the generator torque is near zero and no power is generated. Rated wind speed is the point where the pitch control system is activated and will rotate the blades so that the torque and generated power remain at a constant level at winds equal to the rated wind speed or higher. Cut-out wind speed is when the turbine shuts down in high wind speeds to prevent structure from excessive damage.

3. NORMAL OPERATION WITHOUT CONSIDERATION OF EARTHQUAKE LOADS

In the first step of this research, the normal operation of the 5-MW wind turbine is considered without any involvement from earthquake excitations. This will be used as means of comparison with other conditions to later show the effects of earthquake loads. A set of 50 wind loads were considered with different wind speeds ranging from 2 m/s to 20 m/s. Sample selection for wind is done by considering a Weibull distribution for different wind speeds and then randomly selecting 50 samples according to the distribution available. This method will ensure that selection is biased and that most of the data selected is concentrated around the rated wind speed of the turbine. Wind fields in time durations of 600 seconds according to the 50 hub-height wind speeds with an IEC turbulence level B [5] are generated using TurbSim [25], which is a stochastic, full-field, turbulent wind simulation program that has output files that can be read by AeroDyn and applied to the FAST turbine model. It is important to mention that the generated wind fields that are calculated using a specific hub-height wind speed will have a mean wind speed of the given hub-height wind speed with some fluctuations over time. These short term variations in mean wind speed in different directions through time will result in turbulence that does not have major impact on the generated power but will influence the design loading of the blades [3].

The results of the mean generated power and mean generated torque from the 50 wind speeds that were applied to the 5-MW turbine model are shown in Figure 1. It is observed that before the cut-in speed of the turbine (3 m/s) the generated power is zero, but after the rated wind speed (11.4 m/s) the turbine will reach its maximum power capacity and remain constant until the cut-out speed is reached. The blade pitch control is responsible for the constant torque that will result in constant power generation after rated wind speed is reached so that the turbine will not encounter any damage from excessive wind loads. A sixth order polynomial fit is used to calculate the turbine power generation with respect to different mean wind speeds. Eq. (4), with a coefficient of determination (R^2) equal to 0.994, shows the relation between mean generated power (MW) and wind speed (m/s).

$$P = (-1.1393 \times 10^{-5}) V^6 + (7.97023 \times 10^{-4}) V^5 - (0.02149) V^4 + (0.27742) V^3 - (1.74157) V^2 + (5.26449) V - 5.90215 \quad (4)$$

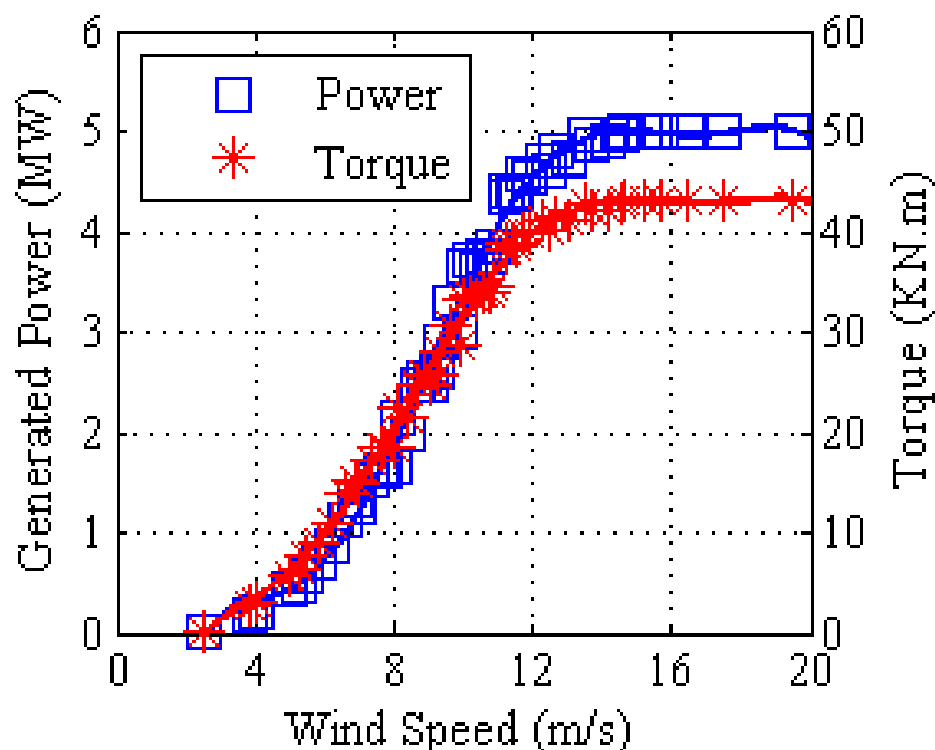


Figure 1. Mean generated power and torque for different wind speeds for normal operational conditions without earthquake

The initiation of pitch control system is shown in Figure 2 in terms of the rotation of the angle of blade in degrees. The pitch angle begins to increase after the rated wind speed of the turbine is reached. It will have to increase as the wind speed reaches near the cut-out speed of the turbine so that less aerodynamic loads are obtained from high wind speeds to obtain a constant level of torque. At the cut-out speed of the turbine, the pitch angle will reach 90 degrees, which is similar to the idling condition of the turbine when the rotor is not generating any power. Figure 3 shows the maximum shear and moment

forces for each wind scenario considered. The wind load is applied at the fore-aft (X) direction of the wind turbine. It is observed that the shear (Fy) and corresponding moment (Mx) in the side-side direction (Y) of the turbine are significantly smaller than the other forces acting in the direction of the wind. The maximum of shear force and moment, as predicted, is achieved at the rated wind speed of the turbine and have values of 1073 KN and 94.84 MN.m, respectively. As the turbine size and tower top mass increases, the period of the tower structure increases, which makes this component more flexural dominant. Therefore one of the design deriving parameters that has to be considered for a reliable and cost effective design of wind turbine towers and foundations is the maximum base moment of the structure. The maximum bending moment design capacity of the 5-MW turbine tower as calculated by the recently published recommendations for wind turbine support structures [26, 27] is about 246 MN.m, so the design demand obtained by the aerodynamic loads is significantly lower than the capacity of the tower. Forth order polynomials (using least square method) were fitted on the shear and moment data obtained and are shown in Eq. (5) and Eq. (6) for shear (Fx) and moment (My) for calculations in different wind speeds.

$$F_x \text{ (KN)} = (0.0974) V^4 - (4.439) V^3 + (62.1776) V^2 - (238.9945) V + 571.6388 \quad (5)$$

$$M_y \text{ (MN.m)} = (0.0079) V^4 - (0.365) V^3 + (5.1237) V^2 - (19.2956) V + 45.5226 \quad (6)$$

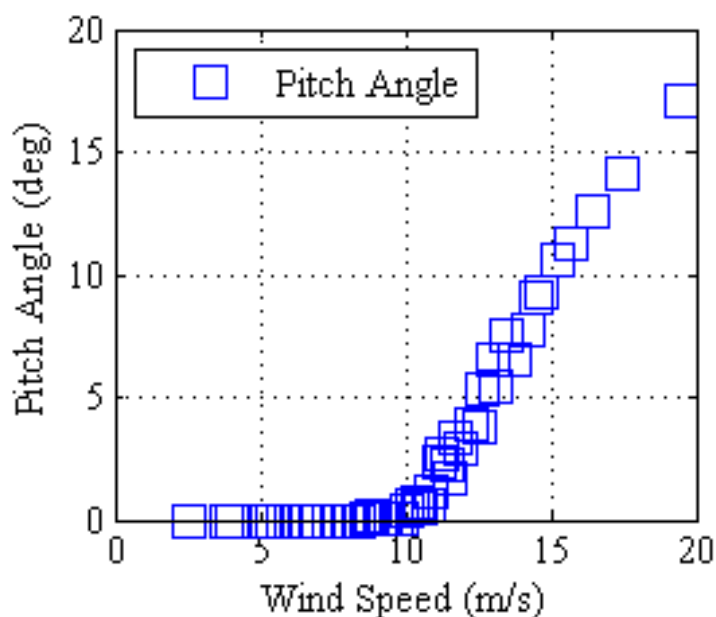


Figure 2. Mean Pitch angle with respect to different mean wind speed levels

Figure 4 illustrates the maximum moment demand in different elevations of the tower for different wind speeds in the side-side direction, which is obtained from the aerodynamic loads in the fore-aft direction. This shows that the moment demand obtained by the aerodynamic loads mainly affects the first mode shape of the tower and higher mode contributions are not involved. It is also observed that the maximum moment in different tower elevations is reached at the rated wind speed of the tower. Although the same torque is achieved to produce the desired power from the rotor, the moment demand has decreased in wind speeds higher than the rated wind speed. As mentioned before, this is caused by the pitch control system activated in the blades for speeds higher or equal to the rated wind speed. Findings from maximum acceleration and displacement in both fore-aft (X) and side-side (Y) directions with respect to tower elevations are shown in Figure 5. Acceleration diagrams show that the contribution of higher modes comes into effect as the wind speed is increased. The maximum acceleration is obtained at 57 m above the base of the turbine and is relatively higher in the direction of the applied load.

Maximum displacement obtained from the analysis is 0.51 m and occurs at the rated wind speed of the turbine.

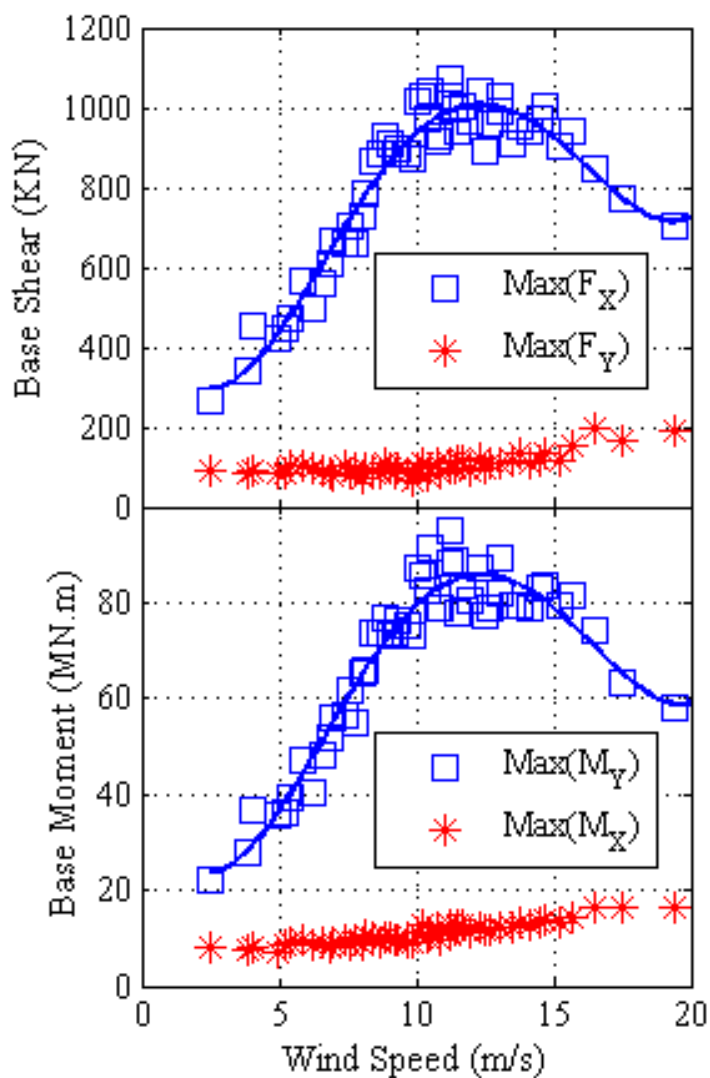


Figure 3. Maximum of Base shear and moment in both directions of wind turbine for 50 wind conditions

4. SCALING AND SELECTION OF GROUND MOTIONS

The two horizontal components of the 22 far-field earthquake records provided by ATC [28] are used for the analysis. To decrease bias in the aerodynamic and seismic coupling analysis, the two horizontal components were swapped (in X and Y direction) and recognized as two separate simulations, which made a total of 44 simulations for each wind condition. The earthquake motions were scaled such that the mean of the SRSS for both non-vertical components of every earthquake conformed to the three dimensional excitation requirements for a site with one second spectral response acceleration (S1) of 0.55g. This is typical for sites with soil class B in Northern California and was calculated using [29].

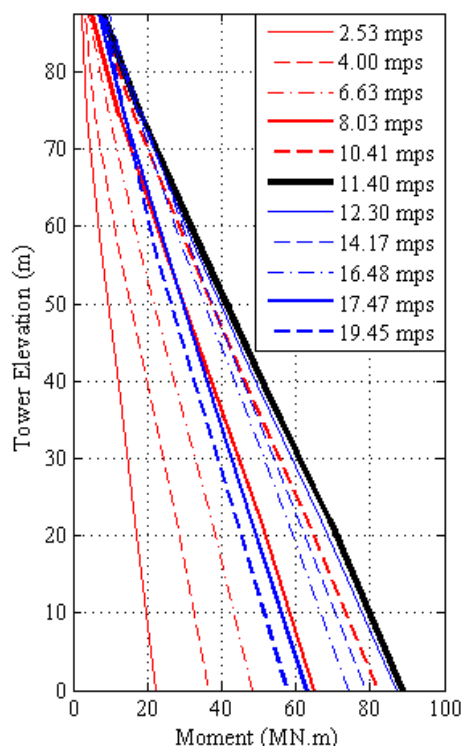


Figure 4. Maximum moment demand in different elevations of the tower for tested wind speeds

The resulting ensemble has also been scaled such that the mean of the SRSS of the spectral displacement of all 22 earthquakes matches the spectral displacement of the design displacement response spectrum at the highest natural period (3.22 seconds) of the structure. The displacement spectrum is used because of the long period of the structure which makes the structure to be accounted as displacement sensitive. The SRSS of the displacement spectrum of all 22 earthquakes along with the mean of the SRSS of all earthquakes and the design displacement spectrum are shown in Figure 8 in Paper I. The list of names of earthquakes, scaled factors, and other characteristics are available in [30].

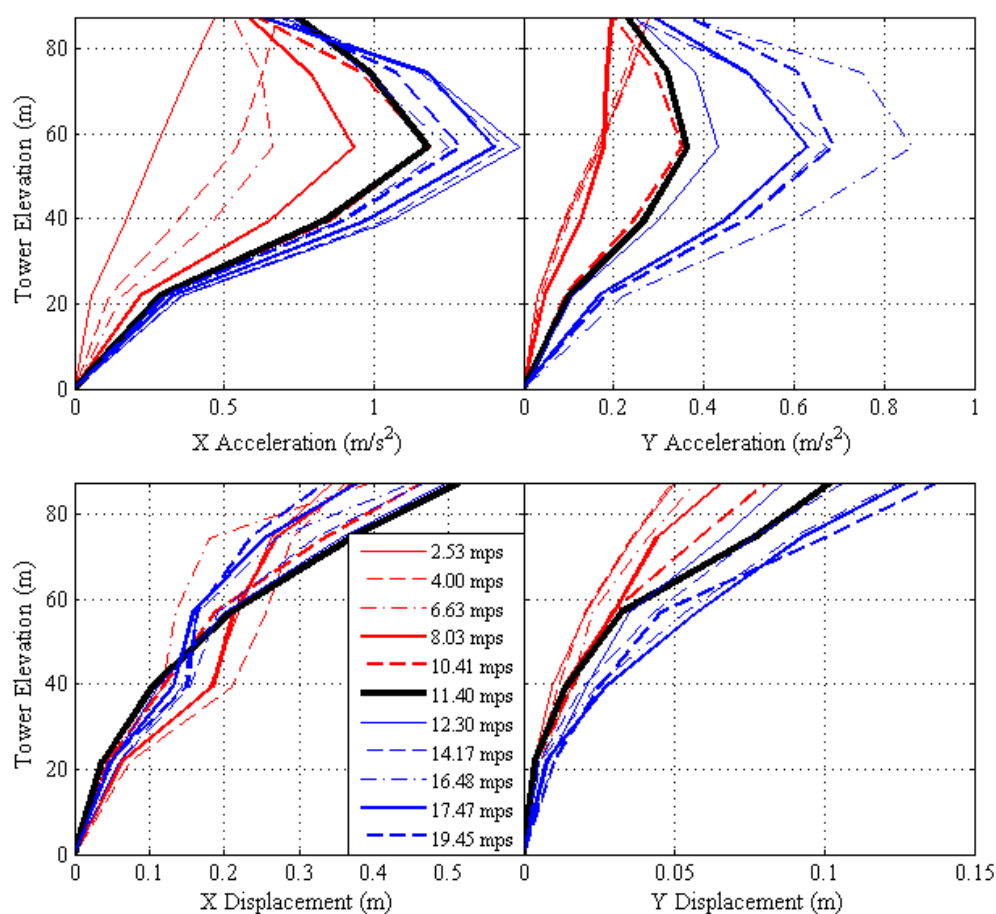


Figure 5. Maximum acceleration and displacement in different elevations of the tower for tested wind speeds

5. WIND TURBINE OPERATION WITH CONSIDERATION OF EARTHQUAKE LOADS

In the final step of this study, 44 earthquake ground motions were coupled with 30 of the wind fields ranging from 2 to 20 m/s using the developed seismic module that was compiled with FAST [22]. Simulations were done in 600 second time durations where the earthquake loads were applied at 400 seconds into the simulation. In this manner, the transient behavior of the turbine at the start of the simulation would have completely decayed and would not have intervened with the coupling simulation results. Different operation conditions of the wind turbine that were considered include (i) idling (ii) running (iii) seismic induced emergency shutdown. In the idling mode, the turbine was analyzed with blade pitch angle set to 90 degrees. In this condition the edge of the blades were faced parallel to the direction of the wind and the lift load generated from the wind was at its minimum value. This meant that the rotor was not able to rotate and there is no torque acquired to generate power. For fixed pitch turbines (where the blades don't feather), an aerodynamic break is deployed that brings the turbine into a complete stop. Idling term is only used for active pitch turbines, such as the turbine studied herein. Otherwise this condition would be known as parked condition for fixed pitch turbines. Earthquake load is predicted to be the dominant load in this operational scenario. In the running condition, the normal operation of the turbine is considered with the presence of seismic excitation. In the seismic induced emergency shutdown condition, the turbine operation is shutdown when the acceleration at the top of the tower reaches 2 m/s^2 . When this acceleration is reached, the turbine generator is shut off and the blades begin to feather (increasing the pitch angle), causing reduction in lift loads from the wind which reduces the torque load on the rotor. By reducing the torque, the blades slow down until the transition into idling condition is reached. Emergency shutdown was achieved by feathering the turbine blades at a rate of 8 degrees per second. In total, 1320 simulations with different earthquake loads and wind fields were performed for the three operation scenarios summing up to 3960 simulations for all conditions.

Figure 6 shows the generated power in time domain for one of the 1320 simulation cases from the start of the application of earthquake (400 sec), until the end of

ground motion duration for a 19.45 m/s wind speed. Generated power for the idling condition remains zero at all times during the simulation. Fluctuations can be seen in the condition where the turbine is running with earthquake applied in comparison with the case of running turbine without the effects of earthquake. The last scenario shown in the diagram is the emergency shutdown where the power would reach zero when the limit of 2 m/s^2 acceleration is reached at the top of the tower and the rotor stops generating torque. In this case, emergency shutdown is induced at time 404.54 sec during the operation of the turbine.

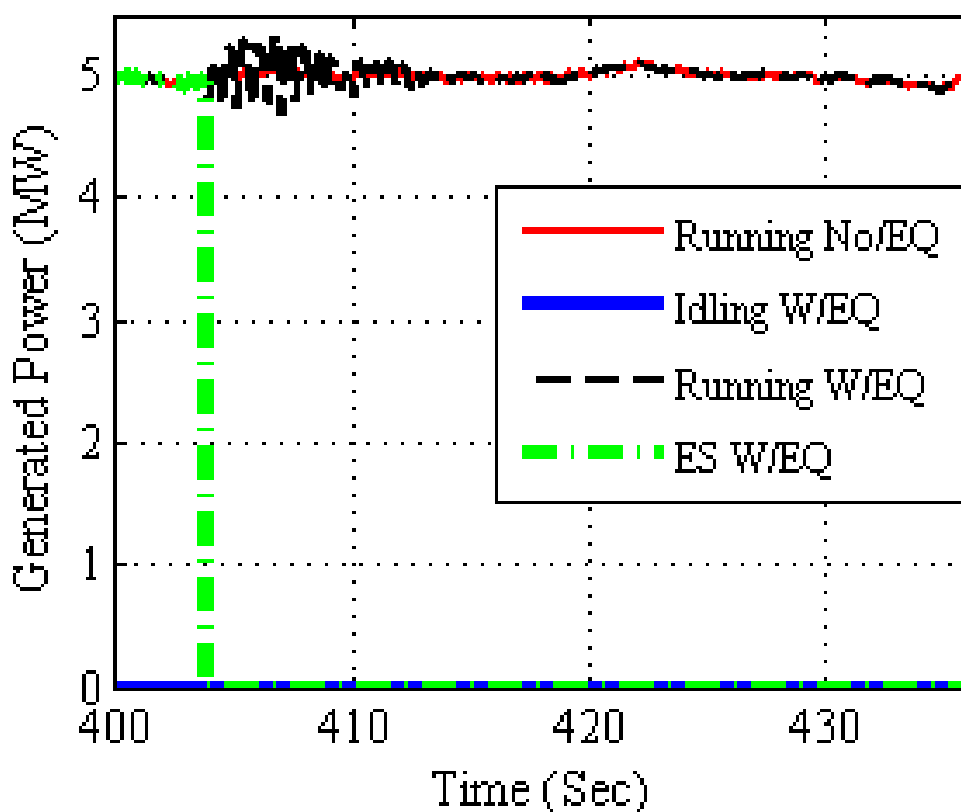


Figure 6. Sample of the generated power for different operational conditions

Figure 7 shows the mean of the generated power for 44 earthquakes and different wind conditions idling, running, and emergency shutdown condition. The results are also compared with the results of previous section without the consideration of earthquake loads for corresponding wind speeds. As suspected, no power is generated from the idling condition because the blades are completely feathered and rotor is not producing any torque for the generator. It is shown that the presence and absence of earthquake loads in the running condition will produce the desired amount of power in both cases. This is because the response of earthquake only fluctuates the power generation at the time when earthquake load is applied (as shown in Figure 6) but has no significant effect on the average of the generated power. Mean of the generated power for the case of emergency shutdown has decreased 30% in comparison with running condition with and without the consideration of earthquake.

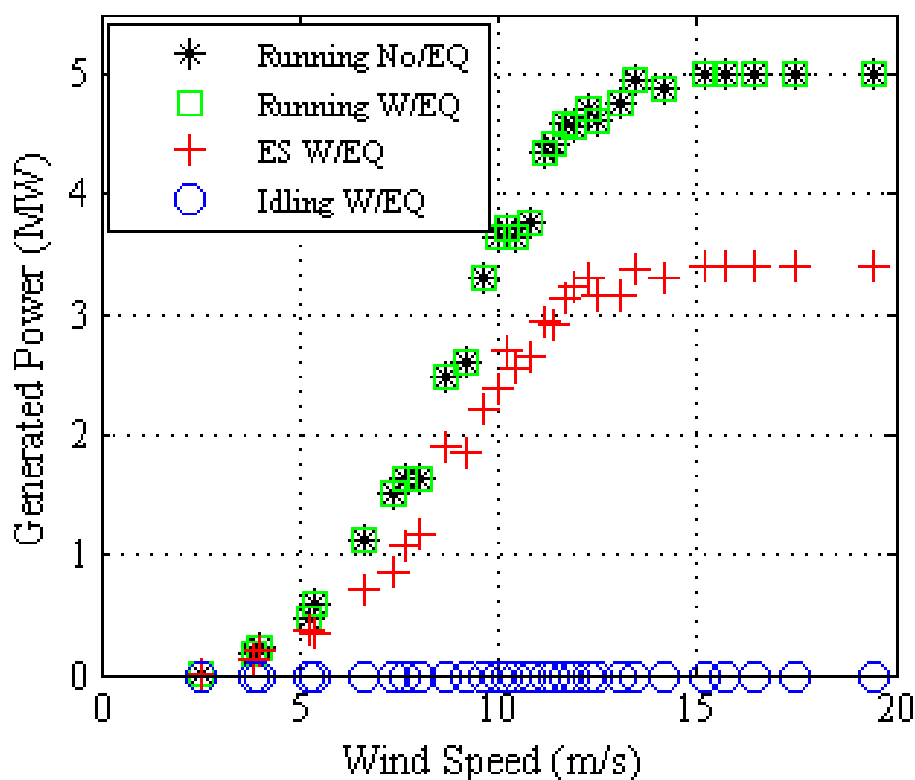


Figure 7. Mean of the generated power for three operational conditions with and without the consideration of earthquake loads

A 3D graphical representation of the relation between wind speeds, earthquake spectral displacement at the first period of structure considering 5% damping, and mean of the generated power for running and emergency shutdown is shown in Figure 8 and Figure 9, respectively. Other intensity measures of earthquake such as peak ground acceleration, velocity, displacement and spectral acceleration of the first period of the structure were also calculated for comparison. The spectral displacement was chosen to be plotted for power generation of the turbine. It is shown that for different spectral displacements for all earthquakes the power generation pattern remains relatively similar except for high wind intensities where less power is shown to be generated. The relation between these three variables are calculated according to the obtained data (with 95% confidence bounds) using Eq. (7) and considering coefficient values shown in Table 1.

$$P \text{ (MW)} = a_{00} + a_{10}V + a_{01}S_d + a_{20}V^2 + a_{11}VS_d + a_{30}V^3 + a_{21}V^2S_d + a_{40}V^4 + a_{31}V^3S_d \quad (7)$$

Table 1. Coefficients for Eq. (7) for finding mean of the generated power in running and emergency shutdown conditions

Operation	a ₀₀	a ₁₀	a ₀₁	a ₂₀	a ₁₁	a ₃₀	a ₂₁	a ₄₀	a ₃₁
Running	3.67	-2.29	0.00192	0.4425	-0.0004146	-0.02692	1.861×10 ⁻⁵	0.0005345	-7.402×10 ⁻⁸
Emergency shutdown	2.748	-1.693	-0.002583	0.3244	0.0001123	-0.01987	0.0001837	0.0003987	-6.26×10 ⁻⁶

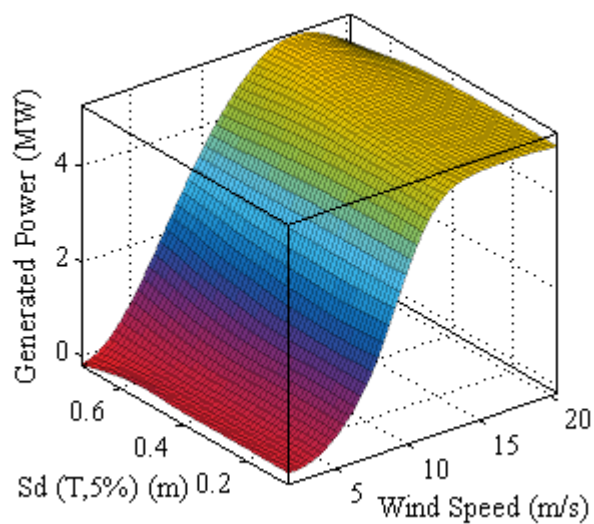


Figure 8. Mean of the generated power for different wind and earthquake intensities for running condition

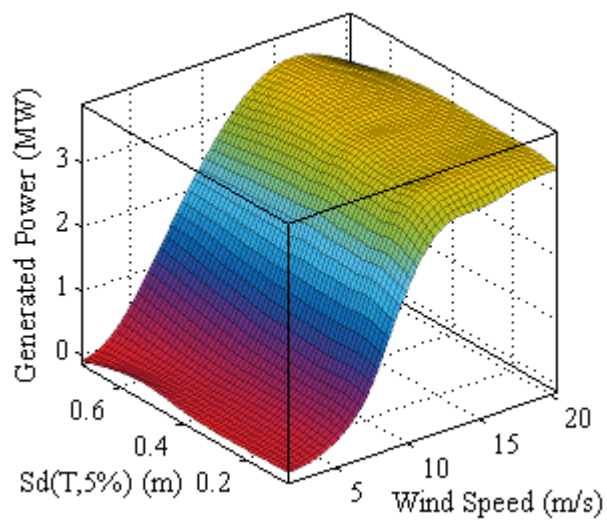


Figure 9. Mean of the generated power for different wind and earthquake intensities for emergency shutdown

The results obtained from base shear and moment in the three operational conditions are shown in Figure 10. The earthquake load is applied in both fore-aft and side-side directions, hence the mean of the maximum of square root of the sum of the squares (SRSS) for moment and shear in both directions for all 44 earthquakes analyzed over different wind fields is considered for observation. From the idling condition of the turbine where no aerodynamic loads are involved, it is concluded that the resulting shear and moment forces obtained from seismic forces are approximately 2200 KN and 100 MN.m, respectively. From the base moment and shear demand achieved in normal operation of wind turbine without consideration of earthquake, it is concluded that earthquake loads can play a significant role in the design and analysis of wind turbines.

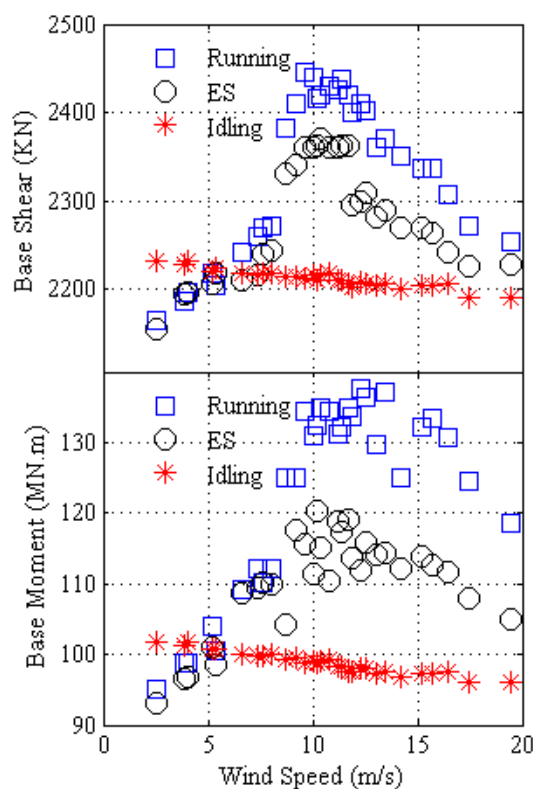


Figure 10. Mean of the maximum of the SRSS of moment and shear for 44 earthquakes and different wind speeds for the three operational conditions

Table 2 shows the increase in base moment and shear demand for running and emergency shutdown conditions with earthquake loads in relation with normal operation of the turbine described in Section 3 of this paper. There is a 95%, and 78% increase in base moment demand in running and emergency shutdown condition while the turbine undergoes seismic excitation relative to the normal operation of the turbine. Furthermore, there is an 11% moment reduction between the running and emergency shutdown condition when earthquake is present.

Table 2. Increase in shear and moment demand from the presence of earthquake in comparison with normal operation of wind turbine

Operational condition	Increase rate (%)
Shear demand (Running)	223
Shear demand (ES)	217
Moment demand (Running)	95
Moment Demand (ES)	78

The increase in base shear loads are shown to be more significant than base moment demand according to Table 2. Figure 11 shows the mean of the SRSS of maximum moment demand for 44 earthquake motions in different elevations of the tower for aforementioned operational conditions for four different wind speeds. The effects of higher modes can be seen in the simulations when seismic motion is involved in comparison with the normal operation of the turbine. It is observed that the Idling scenario gives similar moment demand because there are no aerodynamic loads present in the simulation.

In the case where wind speed is 2.53 m/s, there are no significant differences in the three load conditions because the effect of aerodynamic loading is minimal. The maximum of average moment demand is obtained when the turbine is under the effect of

rated wind speed (11.4 m/s), which is 140 MN.m which is still significantly below the base moment capacity of the turbine tower. However, in some cases of earthquakes with high spectral acceleration, larger moment was obtained but the average of the 44 earthquakes is shown herein. Another conclusion from this representation is that although the values of moment demand from wind and earthquake is similar, the simultaneous application of these load sources would result in a considerably lower value (34%) than the expected direct addition of each load. The coupling of seismic and aerodynamic loads will encounter a phenomena known as aerodynamic damping which will reduce the seismic force acting on the turbine which is thoroughly explained in [30, 31]. Figure 12, Figure 13, and Figure 14 show a 3D representation of the moment demand for idling, running, and seismic induced emergency shutdown in terms of peak ground acceleration and wind speed which are in line with what has been mentioned in this section.

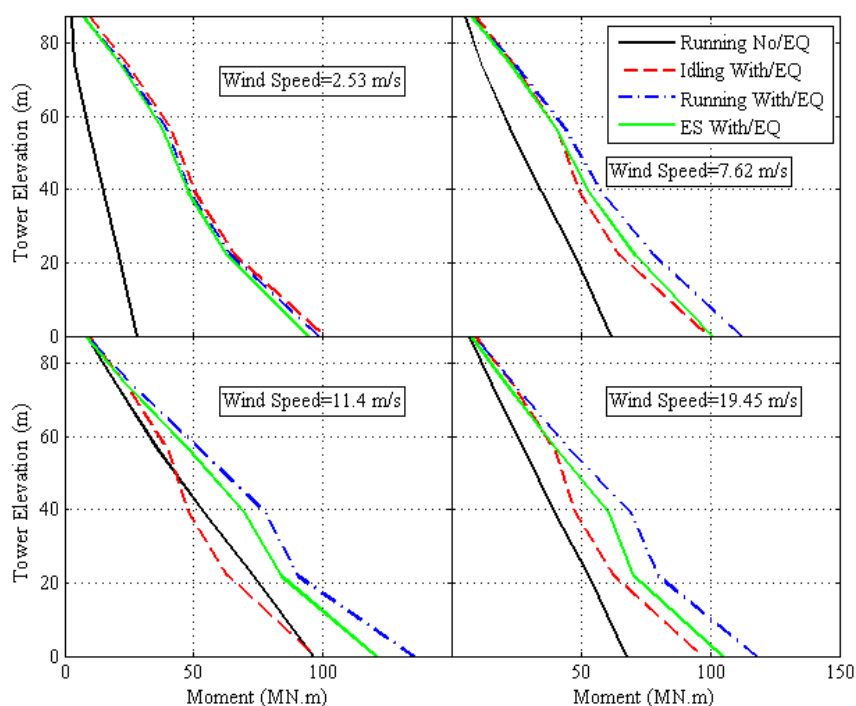


Figure 11. Mean of the maximum of SRSS of moment demand for 44 earthquake simulations for four wind speeds for different operational conditions

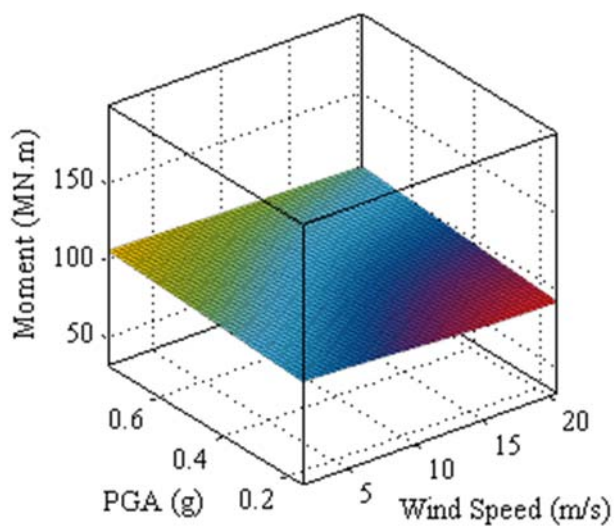


Figure 12. Maximum of SRSS of base moment for different earthquake intensities and wind speeds in idling mode

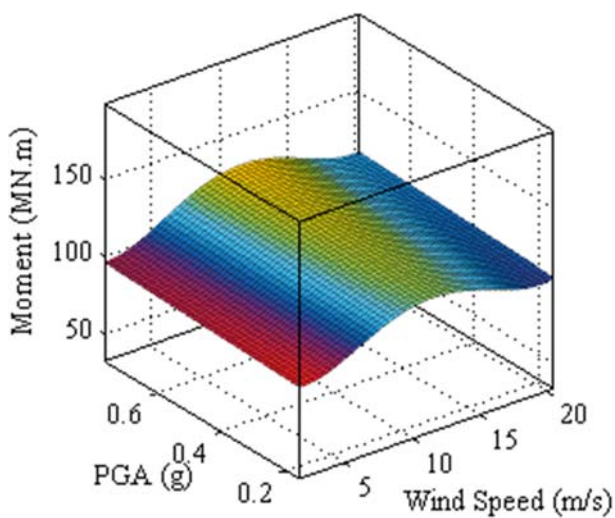


Figure 13. Maximum of SRSS of base moment for different earthquake intensities and wind speeds in running mode

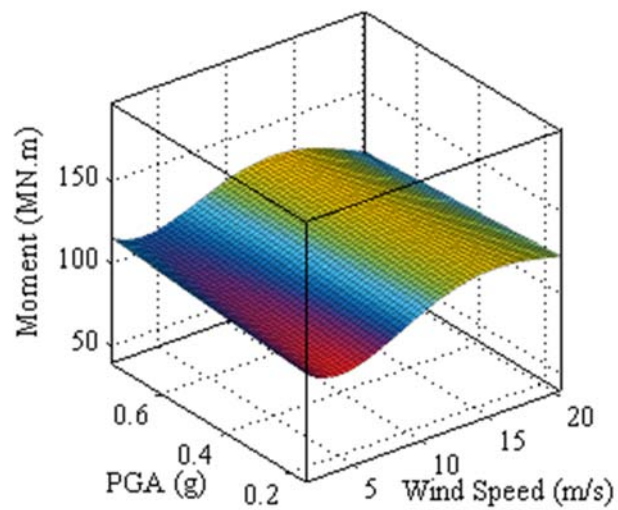


Figure 14. Maximum of SRSS of base moment for different earthquake intensities and wind speeds in emergency shutdown mode

6. DISCUSSION AND CONCLUSION

In this paper, the effects of interaction between aerodynamic and seismic loads on power generation and structural dynamic properties of a 5-MW NREL reference wind turbine in different operational conditions is discussed. It is shown that seismic loads plays an important role on the reliability and cost effectiveness of the turbine structure for turbines with high flexibility. A module is developed for FAST program to apply seismic forces to the base of the turbine structure and coupled with aerodynamic loads acting on the rotor. The turbine is analyzed in four different load cases, normal operation condition without earthquake loading, idling condition, normal operation, and seismic induced emergency shutdown with the presence of earthquake loading. Different earthquake and wind fields were considered for the simulations that were performed. Conclusions from the observations of the results in different conditions are summarized as follows:

- Power generated in normal operational condition without the consideration of seismic forces will reach the capacity of turbine at the rated wind speed of the turbine and will remain constant by controlling the constant torque produced by active pitch control system until the cut-off wind speed that will transition the turbine operation from normal to idling.
- Power generation for running mode with earthquake loads involved is the same as the normal operation of turbine without seismic loads. However a 30% decrease in power generation is observed when shutdown is triggered in the time the acceleration at the top of the tower reaches 2 m/s^2 . No power is generated in the idling case because the blades are completely feathered and rotor is not moving.
- Moment and shear forces obtained from normal operation of the turbine without earthquake loads are also evaluated and reach their maximum value at the rated wind speed of the turbine and gradually decrease as the turbine blades begin to feather.
- Moment and shear forces in the presence of earthquake loading is significantly increased in comparison with normal turbine operation without earthquake but changes in a similar pattern in relation with rated wind speed.

Moment and shear forces for the idling load case remain relatively constant at all wind speeds because no aerodynamic load is involved and the demand solely relies on earthquake forces in this condition.

- An 11% decrease in moment demand is observed in the emergency shutdown case in relation with running condition when the turbine is subjected to earthquake loads. The difference in shear loads in these two cases are relatively smaller.
- Moment demand envelopes along the elevation of the turbine tower in cases where earthquake activities are involved show the involvement of higher modes in comparison with normal operation of the turbine without seismic excitation.

Another conclusion from the results presented in this paper is that the interaction between earthquake loads and aerodynamic loads will result in a moment demand value which is 34% smaller than the addition of the loads as a linear combination which shows the effect of aerodynamic damping on seismic loads applied to the structure. This effect has resulted in moment demands smaller than the bending capacity of the turbine. However, without the consideration of this effect, moment obtained from wind and earthquake loads will in some cases pass the capacity limit of the turbine tower.

7. ACKNOWLEDGEMENT

The authors gratefully acknowledge the support of National Renewable Energy Laboratory (NREL) that provided the grant with contract No. DE-AC36-08GO28308 and the help of Dr. Jason Jonkman and Dr. Ian Prowell as the technical monitors for developing seismic module for FAST.

REFERENCES

- [1] Lindenberg S. 20% Wind Energy By 2030: Increasing Wind Energy's Contribution to US Electricity Supply: DIANE Publishing; 2009.
- [2] Hau E, Von Renouard H. Wind turbines: fundamentals, technologies, application, economics: Springer; 2013.
- [3] Ahlström A. Simulating dynamical behaviour of wind power structures. Stockholm: Royal Institute of Technology; 2002.
- [4] Ashford SA, Boulanger RW, Donahue JL, Stewart JP, Kokusho T, Lee W et al. Geotechnical quick report on the Kanto Plain region during the March 11, 2011, Off Pacific Coast of Tohoku earthquake, Japan. GEER Association Report No GEER-025a, Geotechnical Extreme Events Reconnaissance (GEER). 2011.
- [5] IEC. IEC 61400-1 Ed. 3: Wind Turbines - Part 1: Design Requirements. Geneva, Switzerland: International Electrotechnical Commission; 2005.
- [6] GL. Guidelines for the certification of wind turbines. Hamburg, Germany: Germanischer Lloyd; 2003.
- [7] Risø-DNV. Guidelines for Design of Wind Turbines. Copenhagen, Denmark: Wind Energy Department of Risø National Laboratory and Det Norske Veritas; 2001.
- [8] Bazeos N, Hatzigeorgiou GD, Hondros ID, Karamaneas H, Karabalis DL, Beskos DE. Static, seismic and stability analyses of a prototype wind turbine steel tower. Engineering Structures. 2002;24:1015–25.
- [9] Lavassas I, Nikolaidis G, Zervas P, Efthimiou E, Doudoumis I, Baniotopoulos C. Analysis and design of the prototype of a steel 1-MW wind turbine tower. Engineering structures. 2003;25:1097-106.
- [10] Ritschel U, Warnke I, Kirchner J, Meussen B. Wind turbines and earthquakes: World Wind Energy Association Cape Town,, South Africa; 2003.
- [11] Witcher D. Seismic analysis of wind turbines in the time domain. Wind Energy. 2005;8:81–91.
- [12] Bossanyi E. Bladed for windows user manual. Garrad Hassan and Partners, Bristol, UK. 2000.
- [13] Prowell I, Veers P. Assessment of wind turbine seismic risk: Existing literature and simple study of tower moment demand. Albuquerque, NM: Sandia National Laboratories; 2009.

- [14] Prowell I. An experimental and numerical study of wind turbine seismic behavior. University of California, San Diego; 2011.
- [15] Ishihara T, Sawar MW. Numerical and theoretical study on seismic response of wind turbines. European Wind Energy Conference and Exhibition. Brussels, Belgium: European Wind Energy Association; 2008.
- [16] Haenler M, Ritschel U, Warnke I. Systematic modelling of wind turbine dynamics and earthquake loads on wind turbines. European Wind Energy Conference & Exhibition. Athens, Greece 2006.
- [17] Nuta E. Seismic analysis of steel wind turbine towers in the Canadian environment [Thesis (M A Sc)]: University of Toronto; 2010.
- [18] Jonkman JM, Buhl Jr ML. FAST user's guide. Golden, CO: National Renewable Energy Laboratory; 2005.
- [19] Jonkman JM, Butterfield S, Musial W, Scott G. Definition of a 5-MW reference wind turbine for offshore system development: National Renewable Energy Laboratory Golden, CO; 2009.
- [20] Laino DJ, Hansen AC. User's guide to the wind turbine aerodynamics computer software AeroDyn: National Renewable Energy Laboratory (U.S.); 2002.
- [21] Asareh M-A, Volz JS. Evaluation of Aerodynamic and Seismic Coupling for Wind Turbines Using Finite Element Approach. ASME 2013 International Mechanical Engineering Congress and Exposition. San Diego, California, USA: American Society of Mechanical Engineers; 2013. p. V04BTA041.
- [22] Asareh M-A, Prowell I. Seismic Loading for FAST. Contract. 2011;303:275-3000.
- [23] Atik LA, Abrahamson N. An improved method for nonstationary spectral matching. Earthquake Spectra. 2010;26:601-17.
- [24] Hancock J, Watson-Lamprey J, Abrahamson NA, Bommer JJ, Markatis A, McCoy E et al. An improved method of matching response spectra of recorded earthquake ground motion using wavelets. Journal of Earthquake Engineering. 2006;10:67-89.
- [25] Jonkman BJ. TurbSim user's guide: version 1.50. Golden, CO: National Renewable Energy Laboratory; 2009.
- [26] ASCE/AWEA. Recommended practice for compliance of large onshore wind turbine support structures. Reston, VA: ASCE/AWEA RP2011; 2012.

- [27] Agbayani NA. A Technical Overview of ASCE/AWEA RP2011: Recommended Practice for Compliance of Large Land-Based Wind Turbine Support Structures. Structures Congress 2014. p. 1759-70.
- [28] ATC. Quantification of building seismic performance factors. Report No FEMA-P695. Redwood City, CA: Applied Technology Council; 2009.
- [29] ASCE-7-10. Minimum design loads for buildings and other structures. ASCE/SEI 7-10. Reston, Virginia: American Society of Civil Engineers; 2010.
- [30] Asareh M-A, Prowell I. A Simplified Approach for Implicitly Considering Aerodynamics in the Seismic Response of Utility Scale Wind Turbines. 53rd AIAA/ASME/ASCE/AHS/ASC Structures, Structural Dynamics and Materials Conference: American Institute of Aeronautics and Astronautics; 2012.
- [31] Valamanesh V, Myers A. Aerodynamic Damping and Seismic Response of Horizontal Axis Wind Turbine Towers. Journal of Structural Engineering. 2014;140:04014090.

III. FRAGILITY ANALYSIS OF A 5-MW NREL WIND TURBINE CONSIDERING AERO-ELASTIC AND SEISMIC INTERACTION USING FINITE ELEMENT METHOD

ABSTRACT

With the improvements and advances made in the field of renewable energy, this alternative method has become competitive with more traditional sources of energy generation techniques, including hydro power or fossil fuels. This has led to construction of wind turbines in areas prone to seismic activity. To increase the power production from wind energy, wind turbines have increased in size and mass, which makes them more vulnerable to lateral loads such as seismic induced forces, wind loads, and in the case of offshore wind turbines, wave loads. For this reason, computational analysis in the field are recently focusing on considering the interaction between lateral loads to present more realistic and cost effective designs. In this paper, the nonlinear dynamic behavior of a 5-MW NREL wind turbine is evaluated considering different earthquake and wind intensities using a newly developed finite element model. The model is first calibrated and verified with simplified models using modal and static pushover analysis. Engineering Demand Parameters (EDP) and Intensity Measures (IM) are then obtained from nonlinear Incremental Dynamic Analysis (IDA) and used to assess the probability of exceeding different Damage States (DS) using fragility curves. From the findings in this research, it is shown that earthquake loads have considerable effects on the design and analysis of wind turbines.

Keywords: Finite element analysis; Wind turbine; Aerodynamic-seismic interaction; Incremental Dynamic Analysis (IDA); Engineering Demand Parameters (EDP); Intensity Measure (IM); Damage State (DS); Fragility analysis

1. INTRODUCTION

For an efficient large scale application of wind energy, the cost of construction of wind turbines must be relatively near or less than the traditional methods of energy production, such as hydro power or fossil fuels. Using traditional methods for power production can lead to some drawbacks that include carbon emissions, hazardous waste disposal, high construction and maintenance costs, and potential for damaging ecosystems. With the rapid advancements in the recent decade in the wind energy industry, several countries in the world have focused their resources to take advantage of the power that can be generated from wind. According to recently published DOE report [1], by taking advantage of the growth in the wind technology industry and also by using the complete potential of the offshore wind from the east and west coasts of the US, it is predicted that by the end of year 2030, the estimated value of energy production using wind will reach 300GW, which is 20% of the total energy produced in this country. In the year 2013 this value is estimated to be 61GW and rapidly increasing.

The power that is generated from wind is proportional to the wind speed, and rotor diameter [2]. For this reason, to achieve the optimum power from the wind, rotor diameter has to increase in size. A larger rotor results in a higher mass at the top of the tower which will require a steel tower with higher load demands as discussed in [3, 4]. Modern wind turbines are utilized with advanced control systems to enhance power production and to meet safety requirements in case of harsh environmental conditions. The blade pitch control system is responsible for controlling the aerodynamic load applied to the turbine. In case of a severe wind condition, the blade pitch control system will feather (rotate) the blades to decrease the lift forces produced on the blades and prevent the system from sustaining damage [5, 6].

Recently, with the growth in the wind energy industry, various wind farms have been constructed in regions prone to high seismic activities. It is important to note that, as a coincidence, most of the regions in the world with high potential in wind resources also have a high seismic hazard [3, 7]. These regions include, the Pacific Rim which contains the west coast of the United States, Japan, and the east coast of Asia. Modern turbines have increased in size and mass which leads to a decrease in natural frequency and for

this reason they become more vulnerable to earthquake motions. Therefore, the interaction between earthquake, aerodynamic, and operational loading conditions is important in accurately determining ultimate demand for wind turbine tower structures.

The interaction between wind and earthquake and their effects on wind turbines is not yet well understood. Most of the research in this field considers multibody dynamic linear models with limited degrees of freedom [8, 9] without considering earthquake excitation. There are three documents that provide direct guidelines for seismic design of wind turbines [10-12]. In these guidelines, wind turbines are represented in frequency domain and treated as a SDOF system. The structure is assumed to be linear, even in extreme load cases. IEC [10] and GL [11] rely on local building codes in the absence of specific provisions. The most recent publication is the ASCE/AWEA guideline for the design and permitting of large wind turbine support structures [13] which begins to address nonlinear response for large wind turbines. For buckling analysis, it is mentioned that a procedure that considers material and geometrical nonlinearity would be acceptable to obtain the design loads of the support structure.

Recently, with the advances in computational tools, researchers have started to consider the importance of seismic load for an operational wind turbine. Early work by Bazeos, et al. [14] and Lavassas, et al. [15] include consideration of seismic loading of wind turbines by focusing on the loading of the tower. These simplified models assume the tower top components (nacelle and rotor) to be a lumped mass for prototype 450-kW and 1MW turbines with 38 m and 44 m tall steel towers designed for installation in Greece. The authors speculate that seismic design could become critical in regions with higher seismic hazard and less favorable soil conditions. Witcher [16] presented an overview of the GH Bladed [17] seismic module for a two megawatt upwind turbine with 80 m rotor diameter and 60 m tower height and considers the response of the structure in three different load cases of parked, operational, and earthquake induced emergency shutdown. The significance of time domain analysis and the effects of aerodynamic damping were emphasized in this work. Prowell, et al. [18] conducted experimental work on a 65 KW Nordtank wind turbine using the large high performance outdoor shake table available in University of California at San Diego. Earthquake motions were applied in two horizontal directions and the modal characteristics and dynamic behavior of this

turbine was obtained. This work also concluded that the importance of considering seismic demand increases as the turbines grow in capacity. Ishihara and Sawar [19] and Haenler [20] also studied the effects of aerodynamic and seismic loads using simplified methods.

More recently, an extensive investigation into the seismic response of a 1.65-MW Vestas turbines was conducted using ANSYS by Nuta, et al. [21]. The authors developed fragility curves by performing incremental dynamic analysis and considering different intensity measures, damage measures, and damage states. Seismic fragility analysis of the 5-MW offshore platform was also conducted by Kim et al. [22] with the consideration of soil-pile interactions using the properties of the soil layers. Stress at yielding, allowable stress, displacement at yielding, and allowable displacement were the damage criteria used to calculate the probability of failure in fragility analysis. However, in these two studies, aerodynamic loading was not considered in the analysis.

In this paper, fragility analysis of a 5-MW NREL [23] wind turbine considering aerodynamic and seismic load interaction is considered using finite element analysis. The structural and material properties of the studied turbine are described and the FE model is then calibrated and verified with the previous experimental and numerical research done in terms of modal analysis and natural frequencies. A suite of earthquake ground motion is selected and scaled for simulation on the FE model. Different wind intensities are also selected and applied as aerodynamic loads on the blade elements of the model in each time step. Fragility analysis are performed in the last step using different intensity measures (IM), engineering demand parameters (EDP), and damage states (DS) to reflect the nonlinear behavior of the turbine tower in different loading conditions.

2. PROPERTIES OF 5-MW NREL WIND TURBINE

The 5-MW NREL wind turbine model is intended to serve as a standard model for conceptual studies of modern multi megawatt offshore and onshore wind turbines. The definition of this turbine is described in detail in the report published in the National Wind Technology Center (NWTC) by Jonkman et al. [23]. Some of the properties of this turbine are presented in Table 1 in Paper I. The total mass of different components of the model is approximately 700 metric tons. Tower height and rotor diameter are 87.6 m and 126 m, respectively. From the fore-aft and side-side natural frequencies of the tower, it is concluded that the structure is quite flexible which will result in more sensitivity to lateral loading. Turbine tower material is made from HSS circular section A709 steel with a yield stress of 55 ksi (380 MPa) according to ASCE/AWEA [13] that mentions the consideration of high strength steel material for wind turbine towers. The turbine tower diameter and thickness reduce linearly along the height of the tower.

The finite element model is developed from the 5-MW NREL standard onshore reference turbine model descriptions published by the NWTC for the FAST code [24] using the commercial finite element program ABAQUS [25]. The tower is modeled according to the geometric properties using eight node quadratic shell elements. Material used for the tower has an elastic modulus of 210 GPa, Poisson ratio of 0.3, density of 8500 kg/m^3 , and yield stress of 380 MPa. The density is above the typical steel value of 7850 kg/m^3 to account for paint, bolts, welds, and flanges that are not accounted for in the tower thickness data [23]. Table 1 shows the structural properties of the 5-MW NREL wind turbine. According to the recent research done on the effects of aerodynamic damping on the response of wind turbine structures in idle condition (non-operational turbine) the corresponding Rayleigh damping ratio is predicted to be between 0.5%-1% of the critical damping [4, 16, 26]. A damping ratio of 5% is also considered to be used to contain the equivalent aerodynamic damping along with structural damping in the operational condition of a turbine. ABAQUS automatically distributes the mass of the tower between the tower nodes with the given material density for tower shell elements.

Table 1. Structural properties of the 5-MW NREL Wind Turbine

Base Diameter	6 m
Base Thickness	0.027 m
Top Diameter	3.87 m
Top Thickness	0.019 m
Density	8500 kg/m ³
E (Young's modulus)	210 GPa
Poisson ratio	0.3
Yield stress	380 MPa
E _b (Blade Young's modulus)	13.1 GPa

Mass of the components in the nacelle is distributed between different nodes of the defined geometry so that the center of mass for this section will correlate with the turbine specifications. Having a larger stiffness relative to the other components (tower and blades), a rigid body constraint was considered for the nacelle and drive shaft. The main purpose of this rigid body is to transfer the resultant aerodynamic loads from the rotor to the turbine tower. Figure 1 shows the configuration of the finite element model used for simulations herein. Blade beam elements are extruded in Figure 1 according to their structural properties.

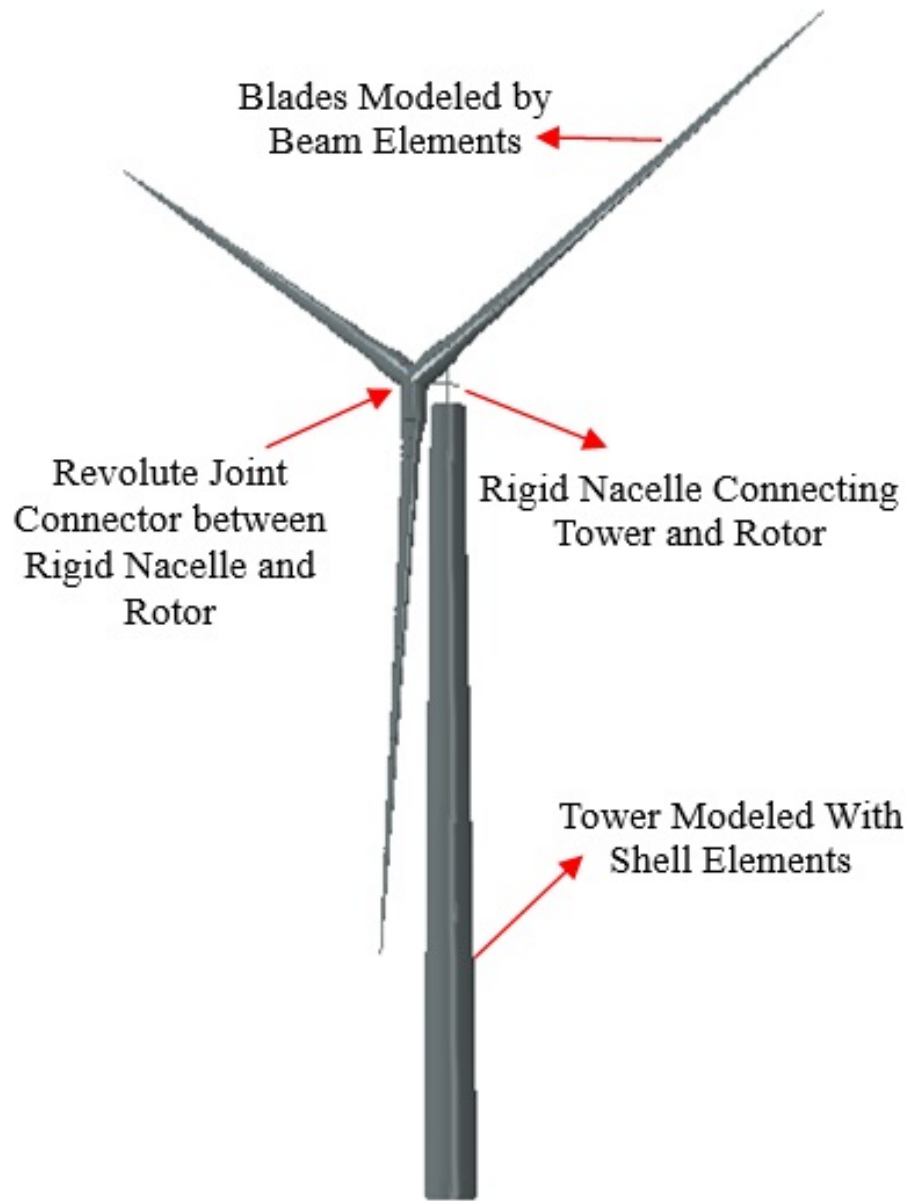


Figure 1. Configuration of the developed finite element model

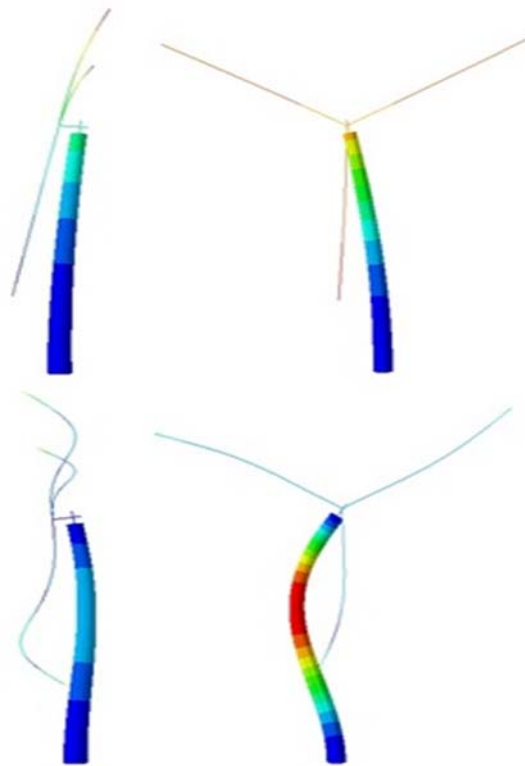
The blades are modeled using the stiffness properties of different sections of the airfoils that were considered in the reference turbine specifications. A generalized beam section is used for different elements of each blade. These properties include the area, moment of inertia along two axes, and polar moment of inertia. This paper mainly

focuses on the nonlinear behavior of the turbine tower; therefore, the blades were modeled as linear beam elements to decrease simulation time and data capacity. The material used for blades has a Young's modulus of 13.1 GPa and a shear modulus of 8 GPa. The mass of the blades is given as lumped mass distributed between each node of the blade. The blades center of mass is located approximately near the root as the blade gets lighter near the tip. Orientation of the blade beams are modified so that the strong axis of the blade is alongside the edge wise direction of the blade. The nodes of the tower top section are coupled with the nacelle rigid body so that they can move together. A revolte joint connector is used between the nacelle and rotor so that the rotor can rotate freely in the axis of rotation relative to the drive shaft of the turbine.

In order to calibrate the finite element model and validate the mass and stiffness distributions through different components, modal analysis is performed and the mode shapes are compared with the multi-body dynamic models generated in FAST [24] and MD ADAMS using linearization analysis and a model developed in OpenSees[4, 27]. The results show that the mass of the tower for all four models is 347 metric tons and the mass of the complete model is 697 metric tons. The center of mass for all models is located at 64 m above ground level. The comparison of natural frequencies for the four models is shown in Table 2. The fore-aft and side-side mode shapes for the developed model in ABAQUS are shown in Figure 2. As observed, the blades contribute in the first and second tower modes. A seismic module developed by Asareh and Prowell [28] for FAST was used to calibrate the finite element model. The results are discussed in a previous publication by the authors of this paper [29] which show good agreement between the linear dynamic analysis of the FE model and the multibody dynamic model developed in FAST.

Table 2. Natural frequencies of different modes for four models

#	Mode	FAST	ADAMS	OpenSees	ABAQUS
1	1st Tower Fore-Aft	0.32	0.32	0.32	0.32
2	1st Tower Side-Side	0.31	0.32	0.31	0.31
3	1st Blade Flap-Wise Yaw	0.67	0.63	0.65	0.63
4	1st Blade Flap-Wise Pitch	0.67	0.67	0.67	0.66
5	1st Blade Collective Flap	0.70	0.70	0.68	0.69
6	1st Blade Edgewise Pitch	1.08	1.07	1.02	1.05
7	1st Blade Edgewise Yaw	1.09	1.09	1.10	1.07
8	2nd Blade Flap-wise Yaw	1.93	1.65	1.78	1.70
9	2nd Blade Flap-wise Pitch	1.92	1.86	1.91	1.83
10	2nd Blade collective flap	2.02	1.96	1.92	1.93
11	2nd Tower Fore-Aft	2.90	2.86	2.76	2.78
12	2nd Tower Side-Side	2.94	2.94	2.95	2.83

Figure 2. Tower fore-aft and side-side 1st and 2nd mode shapes

A static pushover analysis is also conducted to observe the nonlinear behavior of the shell elements of the turbine tower. This procedure is done using displacement control analysis that is gradually applied in the fore-aft direction at the reference point of the rigid nacelle. The base nodes of the turbine are also coupled in the center of the section so that the reaction loads from the base are summed up in a single node. It is observed that failure starts to occur when the top displacement reaches 2.2 m and the maximum plastic moment of the turbine tower is approximately 250 MN-m which agrees with the calculations in the ASCE/AWEA guideline for obtaining the maximum plastic moment of the tower. Figure 3 shows a graphical realization of the pushover analysis. Tower failure occurs at a point approximately 20 m above the base of the structure. Figure 4 shows the displacement moment relationship obtained with the pushover analysis. The gradual decay in moment demand can be seen after the turbine has failed.

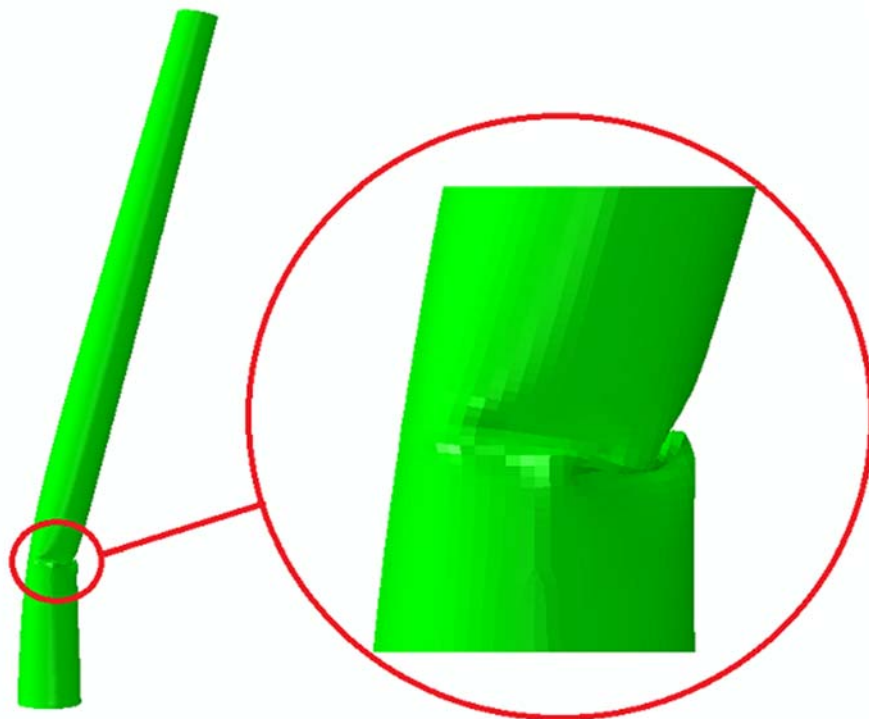


Figure 3. Graphical representation of the pushover analysis for the finite element model

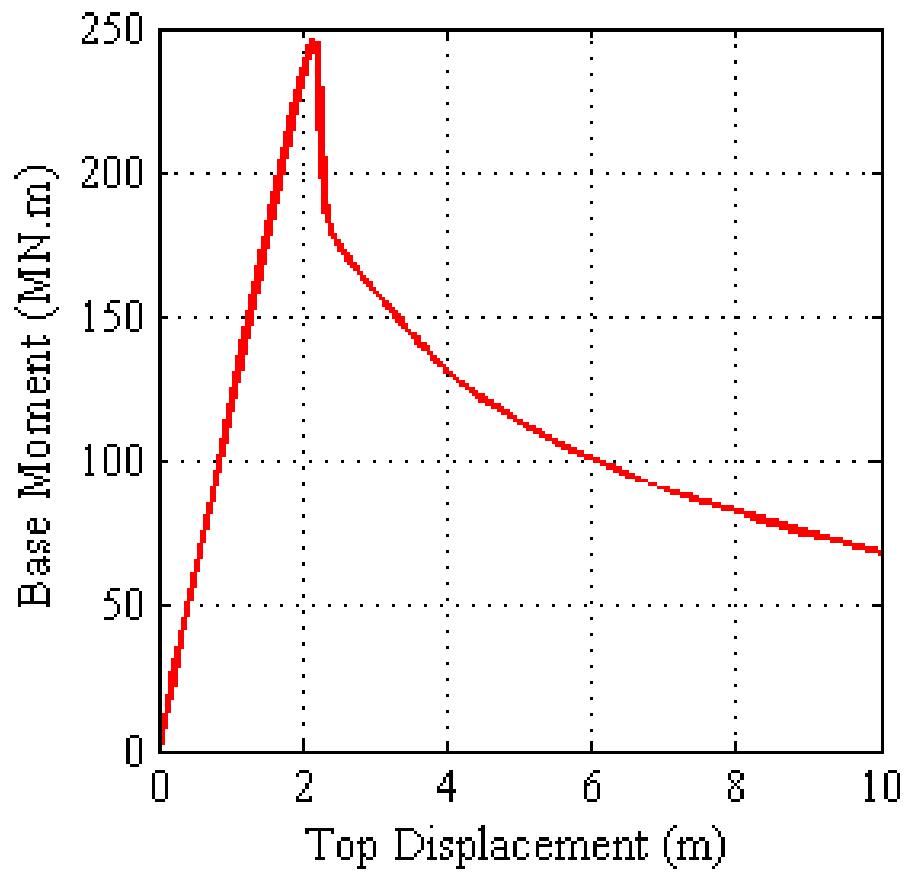


Figure 4. Base moment and top displacement relationship for pushover analysis

3. SELECTED GROUND MOTIONS AND AERODYNAMIC LOADS FOR NONLINEAR ANALYSIS

A suite of 22 earthquake motions, each consisting of two independent horizontal components, are considered for the nonlinear dynamic simulations. These ground motion records constitute the far-field record set presented in the FEMAP695 report from the Applied Technology Council (ATC) [30]. For each motion, the horizontal component is swapped in the fore-aft and side-side direction to reduce bias caused by relative orientation making each record being used twice in the simulations. The square root of sum of the squares (SRSS) of spectral displacement considering the first natural period of the structure and 5% damping for each record is shown in Figure 8 in Paper I. The resulting mean of the spectral displacements (shown in red) is scaled to conform with the requirements for three dimensional excitation presented in ASCE 7-10 [31] for a site with a one second spectral response acceleration (S_1) of 0.55g (shown in black), typical for a class B site located in Northern California. The mean of the SRSS of spectral displacements is also scaled such that it matches the displacement design spectrum for that location at the first natural period of the structure ($T = 3.22$ sec). Table 2 in Paper I presented the properties and spectral acceleration and displacements for the selected 22 earthquakes.

In order to obtain the blade aerodynamic loads, the AeroDyn code [32] was modified to be used simultaneously with ABAQUS to calculate the normal, tangential, and pitch moment forces from the wind field and assign them to each node of the blades in the finite element model in each time step. Eight wind fields were considered for the simulations done herein. Wind fields with mean wind speeds of 2.5, 3.5, 4.0, 6.0, 7.0, 8.0, 9.0, and 10.0 m/s were generated in the stochastic, full-field, turbulent wind simulation program TurbSim [33], that produces output files that can be read by AeroDyn. An IEC turbulence level B was used to generate 150 second duration wind fields in TurbSim. The generated wind fields are calculated using a specific hub-height wind speed which will have a mean wind speed of the given hub-height wind speed with some fluctuations over time. These short term variations in mean wind speed in different directions through time will result in turbulence that will influence the design loading of the blades. The airfoil

properties for the blades of the 5-MW NREL turbine were given to AeroDyn along with the 150 second wind fields generated with TurbSim. AeroDyn uses blade element momentum theory to obtain the normal, tangential, and pitch moment for each element of the blade using the airfoil properties, angle of attack, and the drag and lift loads caused by the wind field. The resulting loads obtained for each element of the three blades were stored and used as input values for the finite element model along with the mentioned earthquake ground motions.

4. NONLINEAR DYNAMIC ANALYSIS

The selected 44 ground motions and 8 wind speeds were assigned to the finite element model and a nonlinear dynamic analysis was performed. Simulation time for the analysis was considered to be the time duration of the wind speed data which was 150 seconds. The earthquake load was applied at the start of the 20th second to allow dissipation of the initial transient behavior of the blades and wind loads so that it would not interfere with the interaction of wind and seismic loads. It was ultimately decided to convert the acceleration ground motion to displacement time history by integration because applying acceleration time history directly resulted in severe convergence difficulties. The displacement time history was applied to the coupled base nodes at a point in the center of the section base with a fix support. It was later verified that the acceleration experienced at the base of the tower was indeed the same as the original acceleration time history of each record. As previously stated, the damping ratio considered for an operational turbine was taken as 5% of the critical damping ratio [4]. It was assigned to the finite element model as the Rayleigh mass and stiffness proportional damping coefficients in terms of the first and second modes of the tower. After the end of the earthquake record duration, the simulations continue to the end of the 150th second with only the aerodynamic load acting on the turbine which attenuated through time because of the structural damping in the system.

One of the main design driven parameters in for analysis and cost estimation of wind turbine tower and foundation design is the maximum base moment of the structure. Figure 5 shows the maximum base moment of the turbine for the simulated earthquakes for three different wind conditions. The intensity measures selected to show these properties of the earthquake motions are the Peak Ground Displacement (PGD) and Spectral Displacement considering the fundamental period of the structure and a 5% damping ratio, $S_d(T_1, 5\%)$. A linear regression of each set of simulations for the three wind speeds is also shown in this figure. As observed, $S_d(T_1, 5\%)$ serves as a better intensity measure for evaluating the moment data. This is because $S_d(T_1, 5\%)$ contains the properties of the structure and is related to the fundamental period of the turbine. However, peak ground displacement is solely related to the earthquake and does not have

any specific relationship with the properties of the simulated structure. It is also shown that with the increase in wind intensity, the maximum base moment increases due to the increase in the aerodynamic loads.

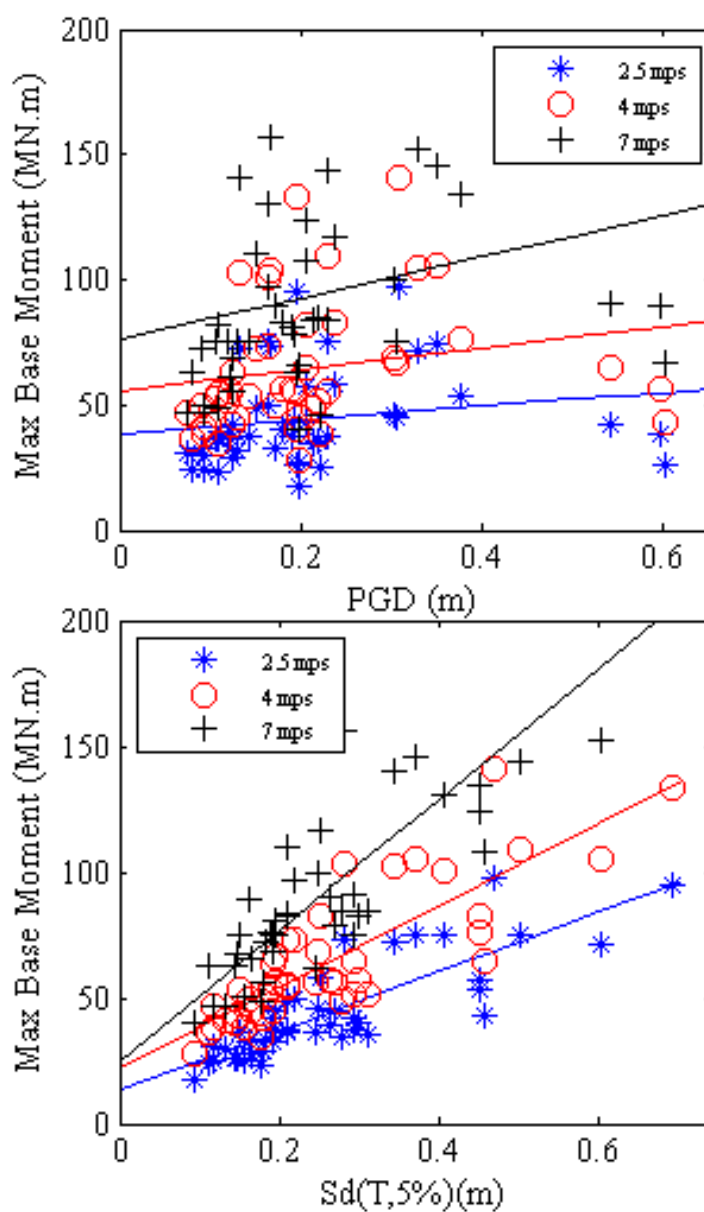


Figure 5. Maximum base moment of 5-MW turbine for 44 earthquake motions and three wind speeds

Engineering Demand Parameters (EDP) or Damage Measures (DM) were chosen to compare the response of the structure under the effects of wind and earthquake in the finite element model. EDPs included peak stress, peak of the tower top displacement, peak rotation, and residual deformation of tower top at the end of the earthquake record. Table 3 shows the square root of sum of the squares of EDPs obtained for the 44 earthquakes in the case of a 7 m/s wind speed. This shows the relation between two different intensity measures corresponding to the earthquake and the response of the structure in each case. Figure 6 to Figure 9 present for different damage measures for three wind speeds in terms of the spectral displacement of each earthquake. From the results shown in the following figures, it can be concluded that the wind load has a smaller effect on the structure than the earthquake forces applied to the base of the structure. Although there is a slight increase in the trend of damage measures as the aerodynamic load assigned to the blade elements increases. It is also determined that for the set of earthquakes and wind loads (44×7 simulations) subjected to the structure, none of them have reached the yielding stress of the tower. In the worst case scenario when the wind speed is 10 m/s and the earthquake intensity is the strongest (Earthquake #5) the resulting maximum stress achieved is 367.7 MPa which is approximately 3% lower than the yield stress of the assigned material. Figure 7 shows a less dispersed distribution of the data (peak rotation) in relation to other damage measures assessed for this model.

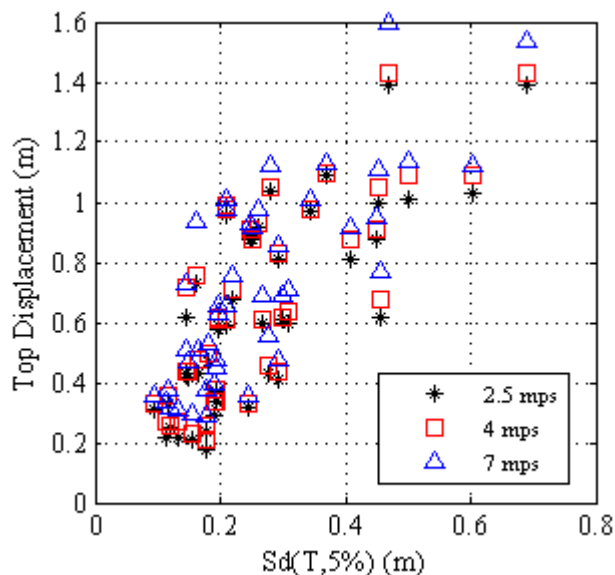


Figure 6. Peak tower top displacement for 44 earthquake simulations in three wind scenarios

Table 3. SRSS values of engineering demand parameters for 44 earthquakes and 7 m/s wind speed

#	Time Duration	$S_a(T,5\%)$	$S_d(T,5\%)$	Peak Displacement (m)	Peak Rotation (Rad)	Residual Deformation (m)	Peak Stress (MPa)
1	29.99	0.09	0.24	0.41	0.0130	0.17	68.61
2	19.98	0.12	0.31	0.60	0.0139	0.25	94.95
3	55.90	0.14	0.37	0.95	0.0169	0.18	102.80
4	45.31	0.13	0.33	0.95	0.0156	0.29	175.18
5	99.92	0.32	0.84	2.22	0.0415	0.83	320.34
6	39.03	0.20	0.52	1.32	0.0231	0.75	256.21
7	40.99	0.10	0.27	0.61	0.0133	0.20	111.12
8	40.96	0.13	0.33	0.67	0.0145	0.26	111.15
9	27.18	0.19	0.50	1.50	0.0228	0.54	277.70
10	30.00	0.13	0.34	1.39	0.0158	0.37	108.31
11	44.00	0.15	0.39	1.26	0.0182	0.32	204.53
12	27.96	0.08	0.22	0.72	0.0117	0.36	74.36
13	39.95	0.08	0.21	0.51	0.0116	0.20	85.03
14	39.95	0.13	0.33	0.77	0.0162	0.42	99.99
15	53.99	0.20	0.51	1.08	0.0200	0.42	217.89
15	40.00	0.14	0.37	0.95	0.0164	0.35	132.45
17	22.30	0.21	0.53	1.36	0.0266	0.48	233.72
18	36.00	0.06	0.15	0.52	0.0086	0.30	68.31
19	90.00	0.24	0.62	1.60	0.0285	0.46	280.35
20	90.00	0.08	0.22	1.19	0.0149	0.20	70.21
21	28.00	0.26	0.67	1.58	0.0296	0.60	250.34
22	36.34	0.07	0.18	0.44	0.0103	0.18	73.81

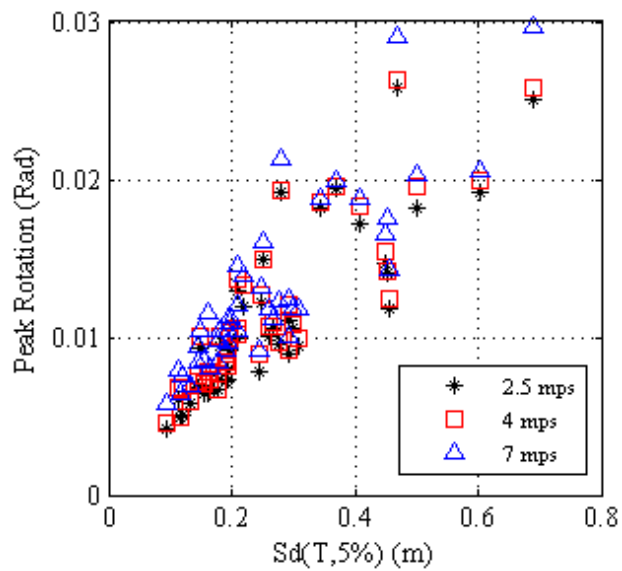


Figure 7. Peak rotation for 44 earthquake simulations in three wind scenarios

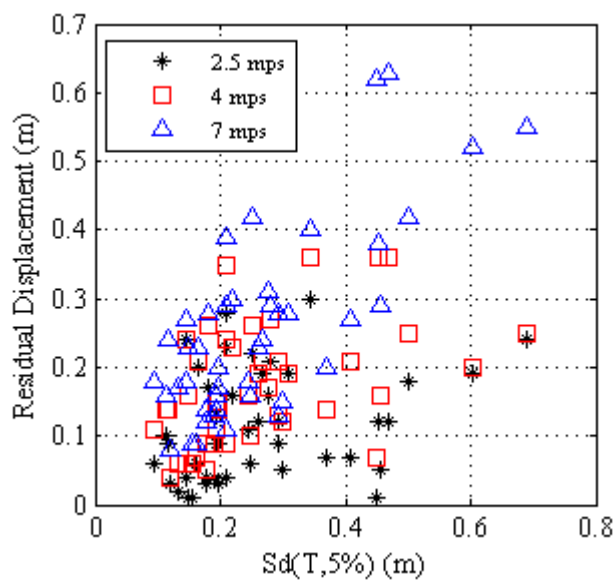


Figure 8. Residual deformation for 44 earthquake simulations in three wind scenarios

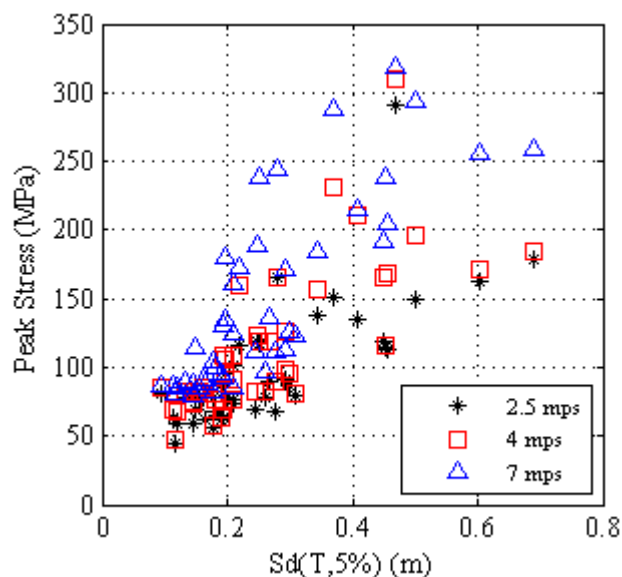


Figure 9. Peak stress for 44 earthquake simulations in three wind scenarios

In order to evaluate the probability of failure of the structure, a dynamic pushover analysis (better known as Incremental Dynamic Analysis) was implemented on the earthquake data. The 44 ground motions were applied with magnification factors of 1, 2, 4, 6, 8, 10, 12, and 14 and analyzed with the seven sets of wind speed. Simulations with magnification factor of one and wind speeds were already discussed previously and are the realistic earthquake and wind state. The other 6 magnification factors resulted in 2156 set of simulations in total for the finite element model of the turbine (44 earthquakes \times 7 wind speeds \times 7 earthquake magnification factors). These factors were considered to take into account the fragility of structure for all intensities of the selected ground motions. For instance the structure would fail in the 4th magnification factor if the earthquake has a high intensity measure and vice versa. It would also relate to the intensity of the wind load applied.

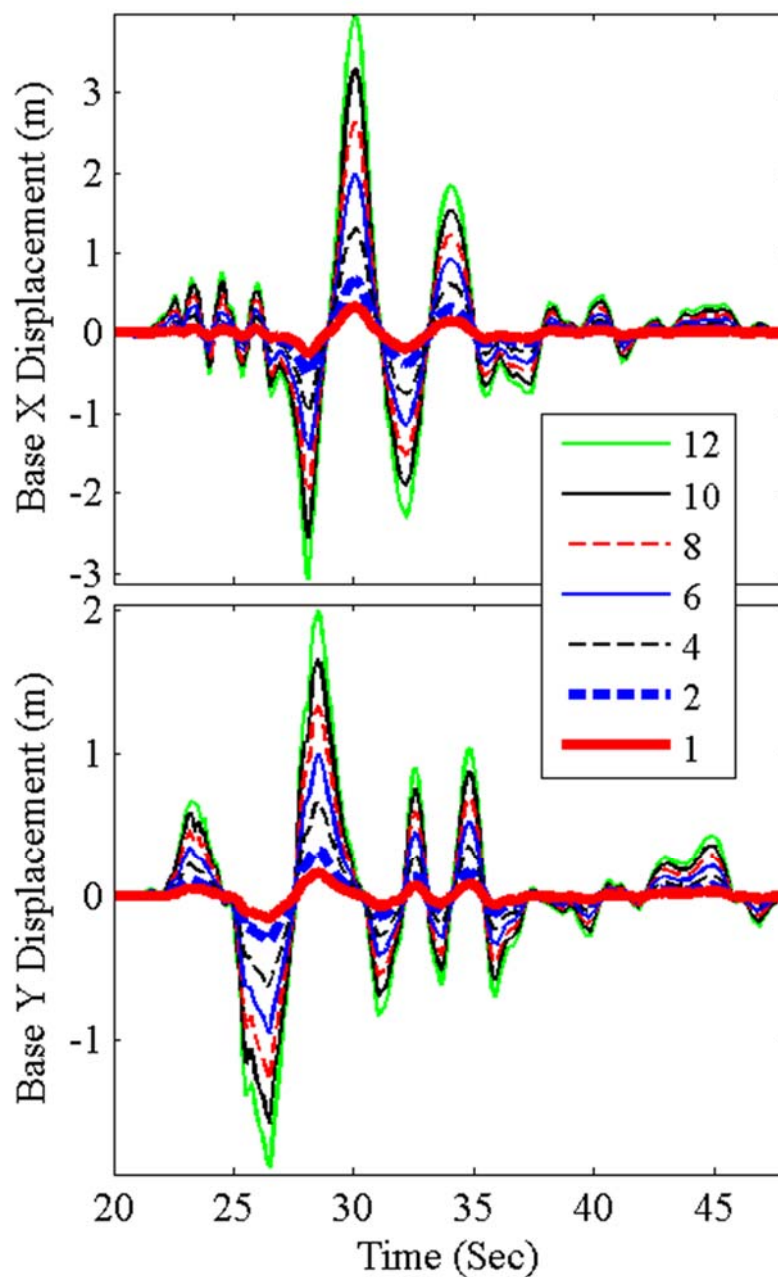


Figure 10. Displacement time history of earthquake #18 applied with different magnification factors to the base of the turbine model in wind speed 2.5 m/s

The selected earthquake would cause structural failure in the 2nd magnification factor if the intensity of the wind is approximately near the rated wind speed of the turbine where the maximum moment demand is achieved (10-12 m/s). Although it was

mentioned that the earthquake load is more dominant than the aerodynamic load in the case of large utility scaled turbines. Figure 10 illustrates one of the displacement time histories with different magnification factors applied at the base of the turbine. As can be seen, the original earthquake has a PGD of less than 0.5 m in both directions but with a 12 magnification factor, the PGD of the presented earthquake would reach 3.5 m in fore-aft direction and 2 m in the side-side direction. Figure 11 also shows the peak base moment for the 44 earthquake ground motion scenarios with different magnification factors for a constant wind speed in terms of peak ground acceleration. As observed, PGA of the amplified earthquakes has reached up to 6 m/s². Base moment of different earthquakes follows a linear increase until the maximum moment capacity of the turbine tower where the moment remains approximately constant through the largest magnification factor when the turbine has failed.

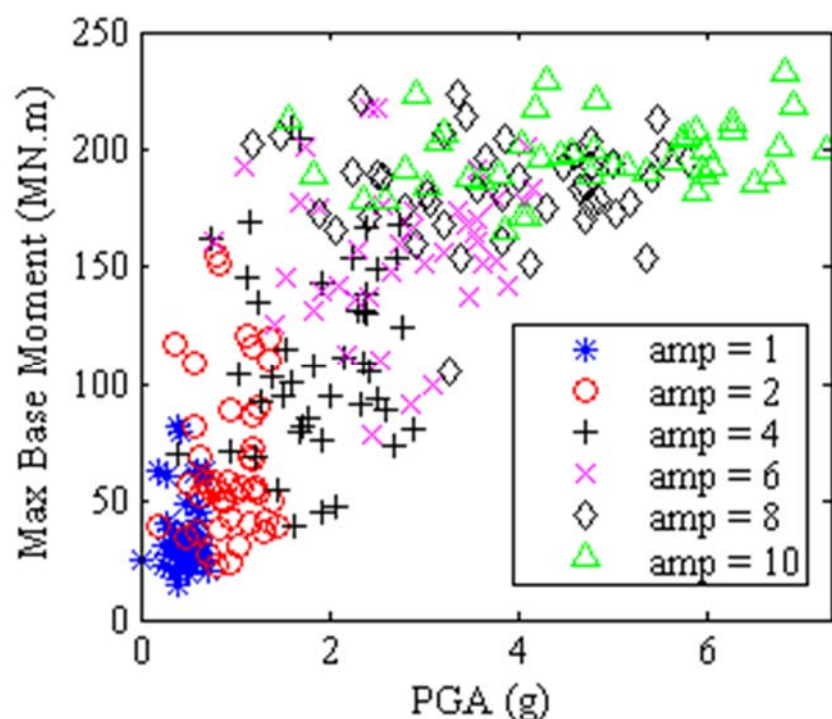


Figure 11. Peak base moment for 44 earthquakes with various amplifications for wind speed 2.5 m/s

The displacement time history for top of the tower can be used to evaluate severe nonlinear effects or turbine buckling through different simulations. As an example, the tower top displacement history for different magnification factors of earthquake #7 and wind speed of 7 m/s is shown in Figure 12. It is observed that the structure fluctuates around the center for the case of 1 and 4 magnification factor and the structure still acts linearly. The nonlinear effects start to increase in magnification factors of 8, 10, and 12 when the drifts from the center point increase. The dot in the graph represents when the turbine has buckled in the 12th magnification factor. Buckling was assessed by observing high rates of displacement and rotation along the height of the tower for each simulation.

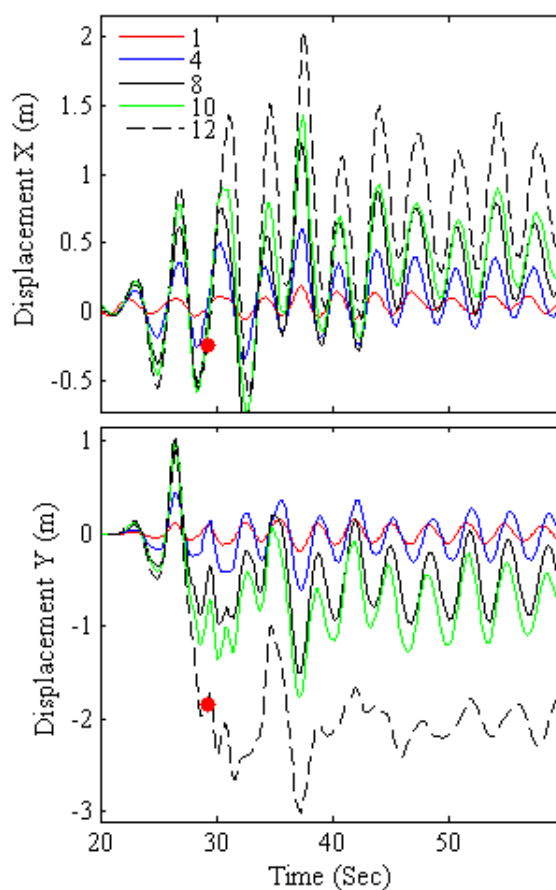


Figure 12. Tower top displacement for earthquake #7 with wind speed of 7 m/s in terms of different magnification factors

Figure 13 shows the peak displacement relative to the 10th ground motion in different heights of the tower for wind intensity of 9 m/s. As observed buckling can be evaluated in terms of sudden changes in the displacement along the height of the tower. In this case buckling has occurred in the 8, 10, 12, and 14 amplifications of the earthquake. A code was written to obtain turbine buckling for different earthquake and wind loading scenarios using sudden changes in displacement and rotation along the height of the tower.

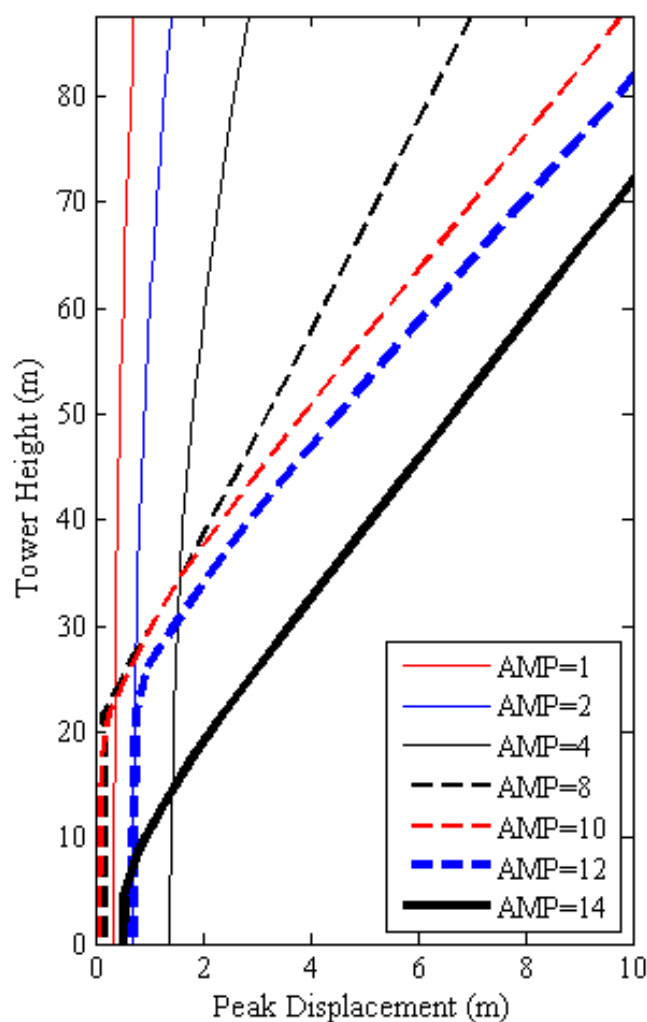


Figure 13. Peak displacement in terms of different elevations of the tower for earthquake #10 and wind speed 9 m/s

The information will be used later for fragility analysis of this structure. Figure 14 shows the buckling behavior of the structure in different wind speeds and earthquake spectral displacements. Each dot in the figure represents a simulation carried out on the finite element model. The black dots represent a scenario which the turbine has not failed through the analysis. A red x-mark represents simulations that buckling has occurred. It can be noted from this figure that wind speed also has a small effect in the failure of the turbine in case of wind and seismic simultaneous loading.

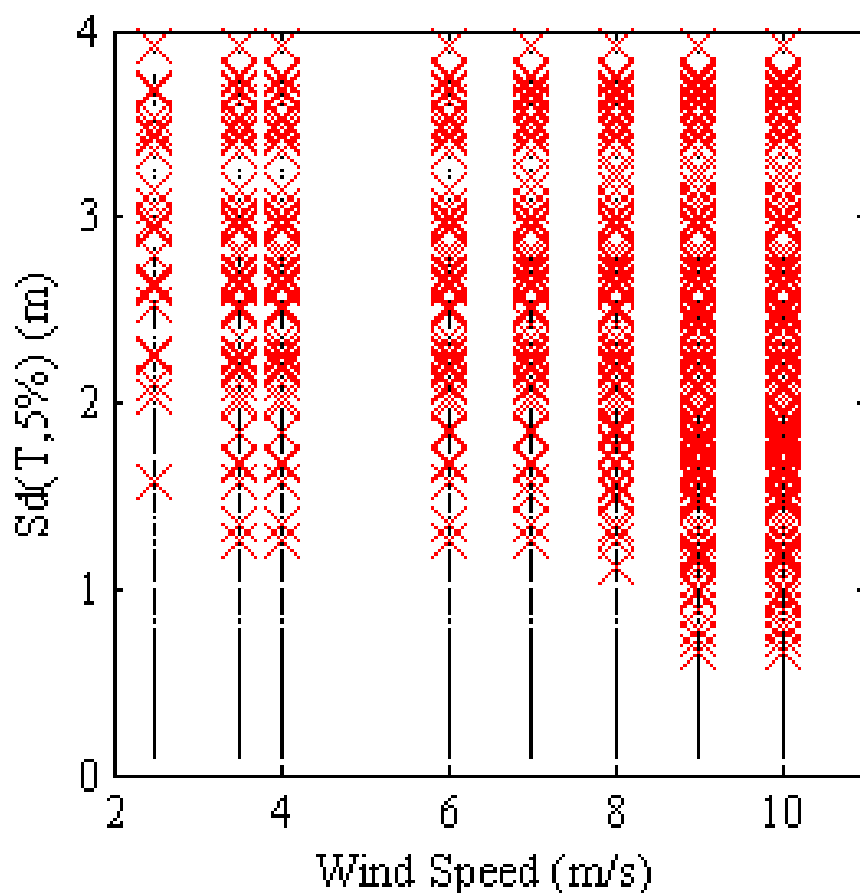


Figure 14. Buckling of the tower for all simulations with different earthquake intensities and wind speeds

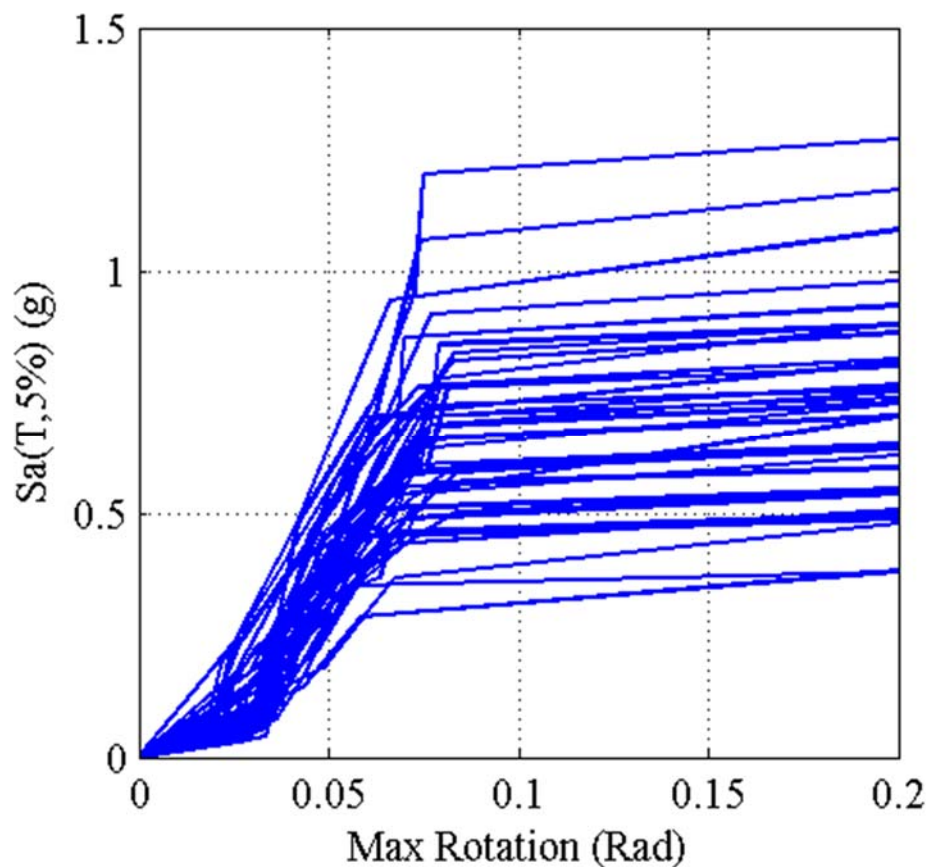


Figure 15. IDA curves for maximum rotation relative to the spectral acceleration for 10 m/s wind speed

Figure 15 shows the IDA analysis considering maximum rotation, as the structure's damage measure and spectral acceleration, as the earthquake's intensity measure for wind speed of 10 m/s. The straight lines at the end of all earthquakes shows that the rotation has a sudden increase which shows the failure of the turbine. The mean of the IDA analysis for maximum rotation in terms of spectral acceleration of the magnified earthquakes is shown for all wind speed simulations in Figure 16. It can be predicted that with the increase in wind intensity, the maximum rotation is reached sooner resulting in a lower spectral acceleration. Another observation, as mentioned before, is that the effects of aerodynamic loads on the structure are smaller compared to the earthquake loads with magnified intensities.

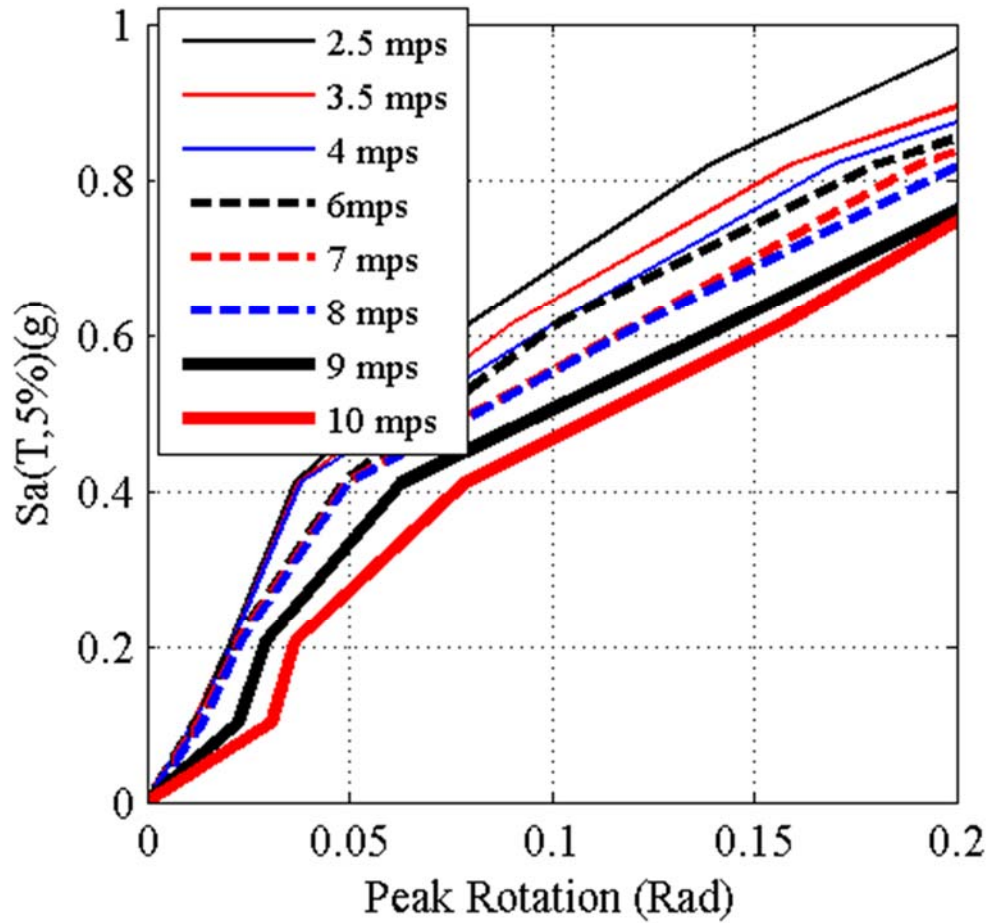


Figure 16. Mean of the IDA curves for maximum rotation relative to the spectral acceleration for all wind speed

The results from the IDA analysis on different engineering demand parameters and intensity measures of wind and earthquake is used in the next section to conduct fragility analysis of the turbine structure.

5. FRAGILITY ANALYSIS OF THE 5-MW WIND TURBINE

Fragility analysis of civil structures is usually done by assigning different Damage States (DS) to the response of various engineering demand parameters considering different intensity measures that relate to the loading condition of the structure (in this case, wind and earthquake loads). The cumulative distribution function of a lognormal distribution is shown to evaluate the probability of exceedance of a certain damage state in terms of different intensity measures. It is usually defined using the equation

$$F_{DS}(IM) = \Phi \left[\frac{\ln\left(\frac{IM}{\mu_{IM}}\right)}{\sigma_{IM}} \right] \quad (1)$$

where IM is the intensity measure of earthquake (PGA, PGD, S_a , or S_d); μ_{IM} and σ_{IM} are, respectively, the mean and log standard deviation of the intensity measure; $\Phi(\cdot)$ is the cumulative distribution function of standard normal variable; and DS is the damage level assigned to a certain damage measure or engineering demand parameter. The fragility ranges from 0.0 to 1.0 according to the probability of failure. If fragility is equal to 0, then there is almost no failure probability, while if it reaches 1, then there is a certain likelihood of failure. Because the exact pattern and intensity of the loads that can be experienced by the structure is unknown, artificial event histories that can include all major scenarios in the response of the structure should be covered. The incremental dynamic analysis that were conducted in the previous section are the artificial loading events that can be used for fragility analysis of this structure.

To estimate the fragility of the turbine structure, damage states should be defined depending on different demand parameters of the turbine that are relevant to different hazard levels ranging from emergency shutdown to total collapse and failure of the structure. The damage states assigned to this wind turbine are shown in Table 4. The first and second damage states (DS_1 and DS_2) are related to any excessive displacement or rotation which would cause loss of efficiency in power generation. In modern utility scale wind turbines this case is also known as earthquake induced emergency shutdown. If the displacement exceeds 1.25% height of the tower in the simulations, the corresponding IM

is used for fragility analysis. Excessive rotation on top of the tower might lead to loss of efficiency in the power generated in the rotor and might also cause collision between the blades and the tower. Two other damage states defined here, are when the stress in any point of the tower exceeds the yield stress of the material (DS₄), and when the residual deformation at the top of the tower exceeds 1% of the tower height (DS₃). The first two damage states do not necessarily correspond to tower failure. They are just safety precautions that have to be taken into account in case of an earthquake excitation. DS₄ is the start of nonlinear behavior in the turbine tower and the last damage state is the complete loss of the tower, or when buckling has occurred. The probability of exceeding this damage state is lower or less likely to happen compared to the other damage states. The log of the mean of the resulting intensity measures related to specified damage state, and the standard deviation of the log of each intensity measure were used to obtain the fragility curves for damage states. Figure 17 shows the fragility curves for different damage states with respect to the spectral acceleration of the set of earthquakes with the selected magnification factors for 2.5 m/s wind speed. Because of the high natural period of structure, spectral accelerations that would exceed a certain damage state would be quite low.

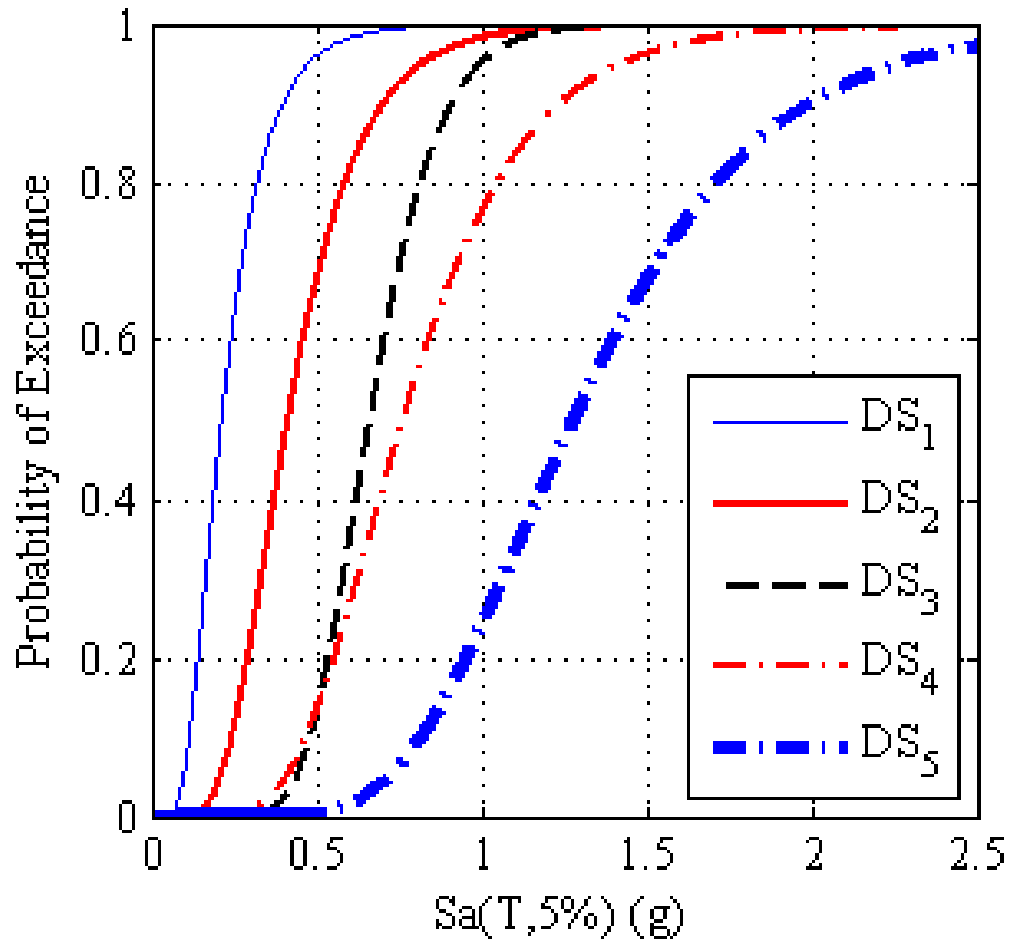


Figure 17. Fragility Curve for different damage states of the 5-MW NREL wind turbine for 2.5 m/s wind speed

Table 4. Damage states considered for fragility analysis

Damage State	Description
DS ₁	1.25%H top displacement
DS ₂	5° Rotation at tower top
DS ₃	1%H Residual deformation
DS ₄	Yield Stress (F_y)
DS ₅	Buckling (Loss of tower)

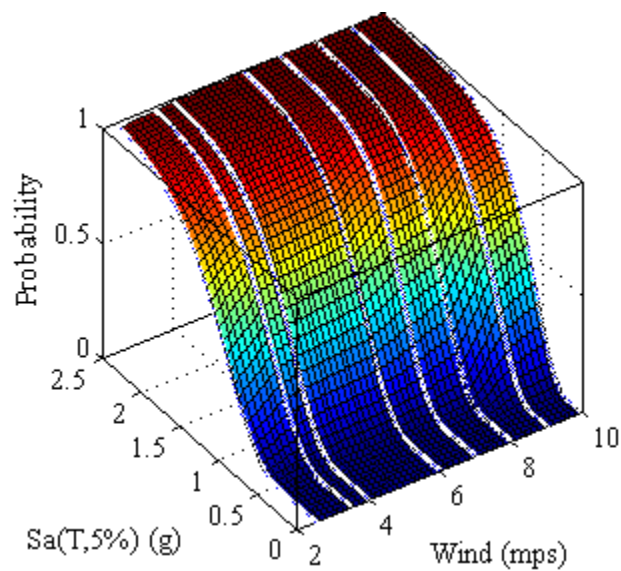


Figure 18. Fragility curve in with respect to spectral acceleration and wind intensity for DS₅

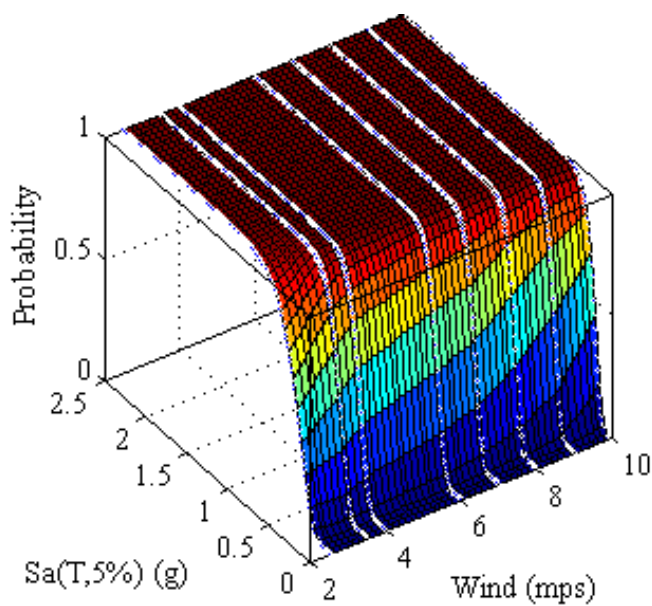


Figure 19. Fragility curve in with respect to spectral acceleration and wind intensity for DS₂

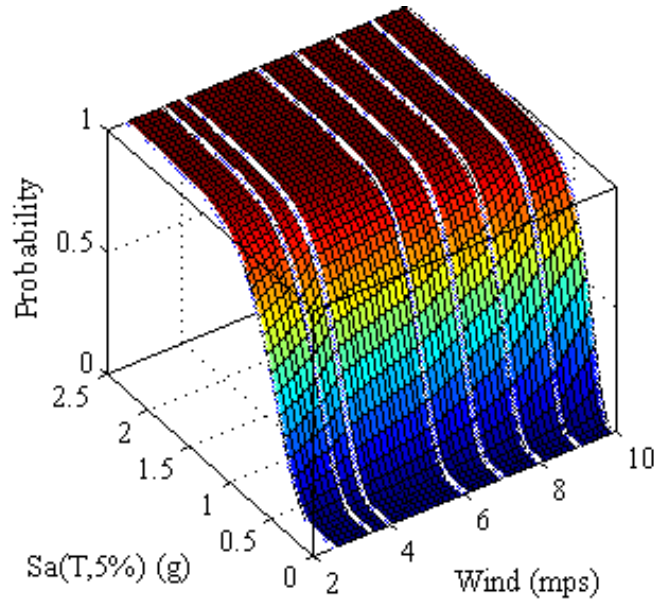


Figure 20. Fragility curve in with respect to spectral acceleration and wind intensity for DS₄

To consider the effects of wind intensities in the fragility analysis, a three dimensional representation of the fragility curves is shown for 3 damage states in terms of the simulated wind speeds and earthquake spectral acceleration. Figure 18 shows the mentioned fragility curve for probability of exceeding buckling (DS₅).

It is shown that probability of exceeding this damage state has a small increase when wind speed reaches at some value near the rated wind speed of the turbine. But the effect of wind is shown to be less significant compared to the induced earthquake loads. Figure 19 and Figure 20 show the same representation for probability of exceeding the rotation damage state (DS₂), and probability of exceeding yield stress in the tower (DS₄), respectively. The same trend can be observed concerning wind intensity effects in these damage states.

6. CONCLUSIONS

Fragility analysis for a 5-MW NREL wind turbine considering different intensities of ground motion and wind speeds was evaluated by developing a finite element model that consisted of different components of the structure. The model was calibrated and verified using modal, static pushover, and linear dynamic analysis with a previously developed multi-body dynamics model. A suite of earthquake ground motions were selected and scaled using the design spectrum of a specific site considering the fundamental period of the structure. Aerodynamic loads were calculated by modifying the AeroDyn code to obtain normal, tangential, and pitch moment forces for the three blades at each time step. Aerodynamic loads generated from wind fields with different mean wind speeds were then applied to the blades of the finite element model along with earthquake motion applied to the base of the turbine. From the observed response of the structure in base moment, peak displacements and rotations, and stress analysis, it was concluded that the tower design is acceptable in the case of simultaneous earthquake and wind loads applied with different intensities. In the worst case scenario of high wind and earthquake intensity, the peak stress in the tower would not reach the yield stress of the tower material.

In the next step, the fragility of the structure was evaluated using earthquake intensities that were scaled with different magnification factors. Incremental dynamic analysis was implemented using the obtained earthquake records and the previously mentioned wind intensities. It was shown that when the turbine reaches the maximum moment capacity, the moment demand would remain constant in high magnification factors of ground motion intensity, showing failure in the tower. Engineering demand parameters were calculated for the simulated model, including peak top displacement, peak rotation, maximum yield stress, and residual deformation at tower top. The corresponding intensity measure for each EDP was also obtained to be used in the fragility analysis of the structure in the final step. Turbine tower failure due to buckling was also assessed for different wind intensities and earthquake magnifications. It was concluded that tower would fail in lower earthquake intensities if the aerodynamic loading applied is near the rated wind speed of the turbine. It is also concluded that the

effect of wind loads on the tower is less significant compared to earthquake loads.

To perform fragility analysis on the wind turbine model, different damage states corresponding to engineering demand parameters were introduced. The maximum tower top displacement and peak tower top rotation were introduced in relation with seismic induced emergency shutdown of the tower for the safety of the turbine when there is loss of efficiency in power generation during operation. The other damage measures relate to the occurrence of nonlinearity or complete loss of the tower. As can be speculated, the probability of exceeding buckling or yielding in a simultaneous application of wind and earthquake is less likely to arise but the probability of occurrence of the top displacement or rotation in an event is more apparent. It is also concluded that the probability of exceeding all damage states has a small increase as the wind intensity reaches near the rated wind speed of the turbine but the difference is insignificant compared to the earthquake loads applied to the wind turbine structure.

7. ACKNOWLEDGEMENT

The authors gratefully acknowledge the support of National Renewable Energy Laboratory (NREL) that provided the grant with contract No. DE-AC36-08GO28308, and the help of Dr. Jason Jonkman and Dr. Ian Prowell, as the technical monitors for developing seismic module for FAST. This code was developed by the authors in the first stages of the work and was used here for verification purposes.

REFERENCES

- [1] Lindenberg S, Smith B, O'Dell K, 20% wind energy by 2030, National Renewable Energy Laboratory (NREL), US Department of Energy, Renewable Energy consulting Services, Energetics Incorporated, 2008.
- [2] Hau E, Wind turbines : fundamentals, technologies, application, economics, 2nd ed., Berlin ; New York: Springer, 2006.
- [3] Prowell I, Veers P, Assessment of wind turbine seismic risk: Existing literature and simple study of tower moment demand, in, Albuquerque, NM: Sandia National Laboratories, 2009.
- [4] Asareh MA, Prowell I, A Simplified Approach for Implicitly Considering Aerodynamics in the Seismic Response of Utility Scale Wind Turbines, in: 53rd AIAA/ASME/ASCE/AHS/ASC Structures, Structural Dynamics and Materials Conference: American Institute of Aeronautics and Astronautics, 2012.
- [5] Mensah AF, Duenas-Osorio L, Prowell I, Asareh MA, Probabilistic Combination of Earthquake and Operational Loads for Wind Turbines, in: 15th World Conference on Earthquake Engineering, Lisbon, Portugal, 2012.
- [6] Altay O, Taddei F, Butenweg C, Klinkel S, Vibration Mitigation of Wind Turbine Towers with Tuned Mass Dampers, in: Wind Turbine Control and Monitoring: Springer, 2014, pp. 337-373.
- [7] Prowell I, Veletzos M, Elgamal A, Restrepo J, Experimental and numerical seismic response of a 65 kW wind turbine, Journal of Earthquake Engineering, 13 2009 1172-1190.
- [8] Ahlström A, Simulating dynamical behaviour of wind power structures, in: Department of Mechanics, Stockholm: Royal Institute of Technology, 2002.
- [9] Gebhardt C, Preidikman S, Jørgensen MH, Massa J, Non-linear aeroelastic behavior of large horizontal-axis wind turbines: A multibody system approach, International Journal of Hydrogen Energy, 37 2012 14719-14724.
- [10] IEC, IEC 61400-1 Ed. 3: Wind Turbines - Part 1: Design Requirements, in, Geneva, Switzerland: International Electrotechnical Commission, 2005.
- [11] GL, Guidelines for the certification of wind turbines, in, Hamburg, Germany: Germanischer Lloyd, 2003.
- [12] Risø-DNV, Guidelines for Design of Wind Turbines, in, Copenhagen, Denmark: Wind Energy Department of Risø National Laboratory and Det Norske Veritas, 2001.

- [13] Agbayani NA, A Technical Overview of ASCE/AWEA RP2011: Recommended Practice for Compliance of Large Land-based Wind Turbine Support Structures, in: Structures Congress 2014: ASCE, 2014, pp. 1759-1770.
- [14] Bazeos N, Hatzigeorgiou GD, Hondros ID, Karamaneas H, Karabalis DL, Beskos DE, Static, seismic and stability analyses of a prototype wind turbine steel tower, *Engineering Structures*, 24 2002 1015–1025.
- [15] Lavassas I, Nikolaidis G, Zervas P, Efthimiou E, Doudoumis IN, Baniotopoulos CC, Analysis and design of the prototype of a steel 1-MW wind turbine tower, *Engineering Structures*, 25 2003 1097–1106.
- [16] Witcher D, Seismic analysis of wind turbines in the time domain, *Wind Energy*, 8 2005 81–91.
- [17] Bossanyi EA, *Bladed for Windows User Manual*, in, Bristol, UK: Garrad Hassan and Partners, 2000.
- [18] Prowell I, An experimental and numerical study of wind turbine seismic behavior, in: University of California, San Diego, 2011.
- [19] Ishihara T, Sawar MW, Numerical and theoretical study on seismic response of wind turbines, in: European Wind Energy Conference and Exhibition, Brussels, Belgium: European Wind Energy Association, 2008.
- [20] Haenler M, Ritschel U, Warnke I, Systematic modelling of wind turbine dynamics and earthquake loads on wind turbines, in: European Wind Energy Conference & Exhibition, Athens, Greece, 2006.
- [21] Nuta E, Seismic analysis of steel wind turbine towers in the Canadian environment, in: University of Toronto, 2010.
- [22] Kim DH, Lee SG, Lee IK, Seismic fragility analysis of 5 MW offshore wind turbine, *Renewable Energy*, 65 2014 250-256.
- [23] Jonkman JM, Butterfield S, Musial W, Scott G, Definition of a 5-MW reference wind turbine for offshore system development, in: Report No NREL/TP-500-38060, Golden, CO.: National Renewable Energy Laboratory, 2009.
- [24] Jonkman JM, Buhl Jr. ML, FAST user's guide, in, 2005.
- [25] Hibbitt, Karlsson, Sorensen, ABAQUS/Standard user's manual: Hibbitt, Karlsson & Sorensen, 2001.
- [26] Valamanesh V, Myers A, Aerodynamic damping and seismic response of horizontal axis wind turbine towers, *Journal of Structural Engineering*, 140 2014.
- [27] Mazzoni S, McKenna F, Fenves GL, *Open System for Earthquake Engineering*

- Simulation User Manual, in, Berkeley, CA.: Pacific Earthquake Engineering Research Center, 2006.
- [28] Asareh MA, Prowell I, Seismic Loading for Fast, in, Golden, CO: National Renewable Energy Laboratory, 2011.
- [29] Asareh M-A, Volz JS, Evaluation of Aerodynamic and Seismic Coupling for Wind Turbines Using Finite Element Approach, in: ASME 2013 International Mechanical Engineering Congress and Exposition: American Society of Mechanical Engineers, 2013, pp. V04BT04A041-V004BT004A041.
- [30] ATC, Quantification of building seismic performance factors, in: Report No FEMA-P695, Redwood City, CA: Applied Technology Council, 2009.
- [31] ASCE-7-10, Minimum design loads for buildings and other structures, in: ASCE/SEI 7-10, Reston, Virginia: American Society of Civil Engineers, 2010.
- [32] Laino DJ, Hansen AC, User's guide to the wind turbine aerodynamics computer software AeroDyn, in: National Renewable Energy Laboratory (U.S.), 2002.
- [33] Jonkman BJ, TurbSim user's guide: version 1.50, in, Golden,CO: National Renewable energy Laboratory, 2009.

SECTION

2. CONCLUSIONS AND FUTURE WORK

The objectives of this study were developed and presented in three different steps and the results of the analyses conducted were presented in the sections “Paper I”, “Paper II”, and “Paper III”. Several reports and conference papers were also published for the preliminary research leading to the work presented here which were cited in the submitted papers.

The first objective of the research was to develop a seismic module which could be compiled with the aero-elastic simulation tool FAST. FAST is an open source, publicly available code for design and analysis of wind turbines under aerodynamic loads available in National Renewable Energy Laboratory (NREL) website. The developed seismic module added capabilities consisting subroutines for applying user-defined and synthetically generated ground motion by mounting a damped actuator at the base of the wind turbine in three translational directions. The updated code is being widely used and cited by researchers in the field of wind turbine industry since 2011.

The code also incorporates motion handling procedure subroutines such as baseline correction (for ground motions containing residual velocity or displacement) and response spectral matching analysis (when the ground motion needs to be scaled according to a specific design spectrum related to a location) that can be called by modifying the variables in the seismic input file. The seismic code and user’s manual can be downloaded from the NREL website. A second version of the code was also modified in 2012 according to the suggestions and recommendation by the users which included modifications stated in the change log also available in the website. Verifications of the code were done by the experimental work done by Prowell (2011) by applying earthquake loads to a full scale turbine mounted on the shake table in UC San Diego.

Seismic module for FAST is used in the other steps of the work for evaluating the effects of aerodynamic damping, and blade pitch control system on the response of wind turbine in different operational scenarios when different wind and seismic intensities are applied to the turbine. It is also used for evaluating the effects of seismic and

aerodynamic load coupling on the power generation of wind turbines in different operational conditions of 1) idling, 2) normal operation, and 3) seismic induced emergency shutdown. Simulations of an idling scenario of the turbine subjected to base shaking without consideration of aerodynamic, are also compared to conventional FE simulations using OpenSees. A method was developed using FE models for implicit consideration of aerodynamic damping to obtain the resulting loads from load combinations available in different turbine specific guidelines. It was shown that in the absence of aerodynamic loads (or idling condition), a total value of 1% structural damping is required to provide a good estimate for the 5-MW NREL model when simulated in conventional FE simulation tools more common in civil engineering. The structural damping required in the operational condition is estimated to reach 5% when the effects of aerodynamic damping need to be considered in the system.

Linear load combinations of seismic and operational loads with two different load factors of one and 0.75 are achieved from the individual wind and earthquake simulations. These combinations are compared with the results obtained from coupled simulations. This comparison shows that the load factor of one for earthquake and wind load is an overestimation in the design of wind turbines because the effect of aerodynamic damping during the operation of structure will considerably reduce the moment demand of these structures. Therefore, the 0.75 load factors are considered to be a better estimate of seismic and aerodynamic loads for design and analysis of wind turbines.

In the second step of the research, the effects of seismic and aerodynamic load interaction on the power generation and structural response of 5-MW NREL wind turbine is evaluated. The seismic code was used for the wind turbine model using different wind and earthquake scenarios. The results obtained in this part of the research, are shown to evaluate power generation and structural dynamic characteristics without the involvement of earthquake at the first step. In the next steps, the normal operation of the wind turbine model in the first step was compared with three operational conditions of idling, running, and seismic induced emergency shutdown with the consideration of earthquake loads. Power generation formulations were obtained for different conditions using statistical methods in different operational scenarios considering various intensity measures from

the earthquake and wind loads that were applied to the structure. The effects of pitch control system and aerodynamic damping caused by the interaction of these loads was also shown in different simulation conditions.

It was concluded that power generated in normal operational condition without the consideration of seismic forces will reach the capacity of turbine at the rated wind speed of the turbine and will remain constant by controlling the constant torque produced by active pitch control system until the cut-off wind speed that will transition the turbine operation from normal to idling. Power generation for running mode with earthquake loads involved was the same as the normal operation of turbine without seismic loads. However a 30% decrease in power generation was observed when shutdown was triggered in the time the acceleration at the top of the tower reaches 2 m/s^2 . No power was generated in the idling case because the blades were completely feathered and rotor was not moving. Moment and shear forces obtained from normal operation of the turbine without earthquake loads were also evaluated and reach their maximum value at the rated wind speed of the turbine and gradually decrease as the turbine blades begin to feather. Moment and shear forces in the presence of earthquake loading were significantly increased in comparison with normal turbine operation without earthquake but changed in a similar pattern in relation with rated wind speed. Moment and shear forces for the idling load case remained relatively constant at all wind speeds because no aerodynamic load was involved and the demand solely relied on earthquake forces in this condition.

An 11% decrease in moment demand was observed in the emergency shutdown case in relation with running condition when the turbine was subjected to earthquake loads. The difference in shear loads in these two cases were relatively smaller. Moment demand envelopes along the elevation of the turbine tower in cases where earthquake activities were involved show the involvement of higher modes in comparison with normal operation of the turbine without seismic excitation. Another conclusion from the results presented in this part of the research was that the interaction between earthquake loads and aerodynamic loads will result in a moment demand value which is 34% smaller than the addition of the loads as a linear combination which show the effect of aerodynamic damping on seismic loads applied to the structure. This effect has resulted in moment demands smaller than the bending capacity of the turbine.

In the last part of the research a finite element model of the 5-MW NREL turbine structure using beam elements for blades and shell elements for the turbine tower was developed and calibrated with the FAST code and previous FE models generated. A suite of earthquake ground motion was selected and scaled for simulation on the FE model. Different wind intensities were also selected and applied as aerodynamic loads on the blade elements of the model in each time step. Fragility analysis was performed in the last step using different intensity measures (IM), engineering demand parameters (EDP), and damage states (DS) to reflect the nonlinear behavior of the turbine tower in different loading conditions.

From the observed response of the structure in base moment, peak displacements and rotations, and stress analysis, it was concluded that the tower design is acceptable in the case of simultaneous earthquake and wind loads applied with different intensities. In the worst case scenario of high wind and earthquake intensity, the peak stress in the tower would not reach the yield stress of the tower material. Incremental dynamic analysis was implemented using the obtained earthquake records and the different wind intensities. It was shown that when the turbine reaches the maximum moment capacity, the moment demand would remain constant in high magnification factors of ground motion intensity, showing failure in the tower. Engineering demand parameters were calculated for the simulated model, including peak top displacement, peak rotation, maximum yield stress, and residual deformation at tower top. The corresponding intensity measure for each EDP was also obtained to be used in the fragility analysis of the structure in the final step. Turbine tower failure due to buckling was also assessed for different wind intensities and earthquake magnifications. It was concluded that tower would fail in lower earthquake intensities if the aerodynamic loading applied is near the rated wind speed of the turbine. It is also concluded that the effect of wind loads on the tower is less significant compared to earthquake loads.

Different damage states corresponding to engineering demand parameters were introduced to correspond to a certain damage level for wind turbines. The maximum tower top displacement and peak tower top rotation were introduced in relation with seismic induced emergency shutdown of the tower for the safety of the turbine when there is loss of efficiency in power generation during operation. The other damage

measures relate to the occurrence of nonlinearity or complete loss of the tower. As speculated, the probability of exceeding buckling or yielding in a simultaneous application of wind and earthquake was less likely to arise but the probability of occurrence of the top displacement or rotation in an event was more apparent. It was also concluded that the probability of exceeding all damage states had a small increase as the wind intensity reached near the rated wind speed of the turbine but the difference was insignificant compared to the earthquake loads applied to the wind turbine structure.

The wind power industry could significantly benefit from more experimental models of different sizes of utility scale wind turbines. Future work could also incorporate the effects of different soil conditions, foundation types, and turbine models where dynamic characteristics have not been assessed. Further studies exploring the implications of temperature, wind speed, turbulence, and other factors would assist in developing a more complete understanding of the variability of assumed dynamic responses. Results from these efforts can be used to further the design and construction of offshore wind turbines. The interaction between waves, current, and wind loads is an important consideration and should be investigated in the future. Different support structures already used in the oil industry have to be evaluated for the use in offshore wind industry, including monopiles, jackets, and tripods for shallow water wind farms. For deep water wind farms, floating support structures, which have been shown to be a cost effective and reliable support structure method for harnessing wind energy, should be investigated. Hurricane induced loads and the coupled influences of wind, wave, and current on an offshore wind turbine during hurricanes that could affect the power production of an entire offshore wind farm would also need to be evaluated. Soil-pile-structure interactions for offshore wind turbines and the effects of considering the soil in the dynamic response of the structure is also an important aspect that needs to be considered in the future.

For numerical analysis and considering nonlinear effects of these structures, improvements in considering composite models for blades and using those in a full system model which requires more computational time could be evaluated. For cost optimization purposes, considering concrete towers instead of steel towers and its effect on the dynamic response and design demands of the structure can also be studied.

APPENDIX A.

SEISMIC MODULE INPUT FILE DESCRIPTION

The source code for seismic module, developed by the author can be found in the National Renewable energy Laboratory (NREL) webpage <https://nwtc.nrel.gov/Seismic>. This is a FORTRAN file named *UserPtfmLd_Seismic.f90* that can be compiled with the core program of FAST. When FAST is compiled with this module, another input file is required from the user for the definition of the seismic input properties. An example of the seismic input file is shown below.

```

-----
----- FAST INPUT FILE -----
-----
FAST: Seismic loading parameters
1          SeismicMode          - variable specifying the type
of motion (1 = user-defined or 2 = synthetic Motion) for the platform
"..\El_CentroX.dat"  PtfmXMotionFn  - Name of file containing
motion in the X direction for the platform
"..\El_CentroY.dat"  PtfmYMotionFn  - Name of file containing
motion in the Y direction for the platform
"                  PtfmZMotionFn  - Name of file containing
motion in the Z direction for the platform
1          PtfmMotionType       - Type of motion specified:
1=acceleration; 2=velocity; and 3=displacement
9.80665     PtfmMotionFactor     - Factor to convert the
specified motion to units of m for displacement, m/s for velocity, and
m/s^2 for acceleration
12.0        ActFreq             - The frequency of the
"actuator" used to calculate base forces
65.0        ActDamp             - The damping value for the
"actuator" used to calculate base forces
400.0       EqDelay             - The number of seconds to
delay the start of the earthquake
123456789   SynRandomSeedX1     - First random seed of
Synthetic Motion for X direction [-2147483648 to 2147483647] (-)
[unused when SeismicMode=1]
1011121314  SynRandomSeedX2     - Second random seed of
Synthetic Motion for X direction [-2147483648 to 2147483647] (-)
[unused when SeismicMode=1]
-223456789  SynRandomSeedY1     - First random seed of
Synthetic Motion for Y direction [-2147483648 to 2147483647] (-)
[unused when SeismicMode=1]
2111121314  SynRandomSeedY2     - Second random seed of
Synthetic Motion for Y direction [-2147483648 to 2147483647] (-)
[unused when SeismicMode=1]
1123456789  SynRandomSeedZ1     - First random seed of
Synthetic Motion for Z direction [-2147483648 to 2147483647] (-)
[unused when SeismicMode=1]
-1011121314 SynRandomSeedZ2     - Second random seed of
Synthetic Motion for Z direction [-2147483648 to 2147483647] (-)
[unused when SeismicMode=1]
0.0         SynRMSAmpX          - The RMS amplitude used for
synthetic motion in X direction in m/s^2 [unused when SeismicMode=1]
0.0         SynRMSAmpY          - The RMS amplitude used for

```

```

synthetic motion in Y direction in m/s^2 [unused when SeismicMode=1]
0.0          SynRMSAmpZ      - The RMS amplitude used for
synthetic motion in Z direction in m/s^2 [unused when SeismicMode=1]
0.0          SynDuration     - Duration of the synthetic
motion in seconds [unused when SeismicMode=1]
"           SynInitRampFnX   - Initial ramping file name
for synthetic motion in X direction [unused when SeismicMode=1]
"           SynInitRampFnY   - Initial ramping file name
for synthetic motion in Y direction [unused when SeismicMode=1]
"           SynInitRampFnZ   - Initial ramping file name
for synthetic motion in Z direction [unused when SeismicMode=1]
"           SynFinalRampFnX  - Final ramping file name for
synthetic motion in X direction [unused when SeismicMode=1]
"           SynFinalRampFnY  - Final ramping file name for
synthetic motion in X direction [unused when SeismicMode=1]
"           SynFinalRampFnZ  - Final ramping file name for
synthetic motion in X direction [unused when SeismicMode=1]
False       BLineCorrection  - Variable specifying if
motion should be baseline corrected [used when PtfmMotionType=1]
False       TgtResponse      - variable specifying if
spectral matching should be performed on motion [used when
PtfmMotionType=1]
"           TgtResFnX        - Target response file name in
X direction [used when PtfmMotionType=1 & TgtResponse = True]
"           TgtResFnY        - Target response file name in
Y direction [used when PtfmMotionType=1 & TgtResponse = True]
"           TgtResFnZ        - Target response file name in
Z direction [used when PtfmMotionType=1 & TgtResponse = True]
4           nPass            - Integer specifying the
number of passes in spectral matching [used when PtfmMotionType=1 &
TgtResponse = True]
400         MaxIter          - Integer specifying maximum
number of iterations in each pass for spectral matching [used when
PtfmMotionType=1 & TgtResponse = True]
5           SMTol            - Tolerance used for spectral
matching [used when PtfmMotionType=1 & TgtResponse = True]
35.0        MaxFreq          - Maximum frequency up to
which spectral matching is performed [used when PtfmMotionType=1 &
TgtResponse = True]
1,35.0      FreqMatch12     - Two frequencies which
clarify the frequency range for spectral matching in 1st pass [used
when PtfmMotionType=1 & TgtResponse = True]
END of FAST input file (the word "END" must appear in the first 3
columns of this last line).
-----

```

Seismic input parameters are specified in a separate configuration file similar to how parameters are defined for the tower, platform, and other portions of the model. This document details the input parameters needed for seismic analysis and describes the function of each one. The configurations for seismic input have essentially the same format as other configuration files for FAST.

Aside from the seismic configuration file which is required for seismic analysis,

some additional input files are needed in different simulation conditions. For conducting a seismic analysis with user-defined input motion, the user has to provide the motion files for each direction and define the file paths in the seismic configuration file. For generating synthetic motion, the user has to provide the initial and final ramps in input files and define the paths in the configuration file. For each of the horizontal and vertical directions, the user can include a different initial and final ramping file or a similar file can be used for all directions. Finally, for spectral matching analysis, the user needs to provide an additional target spectrum input file in each direction which will be used to match the response of the user-defined or synthetic motion with the target spectrum.

SeismicMode [1 or 2]

This switch determines if the user wants to provide a base motion time history or informing FAST to generate a synthetic time series. To perform a user-defined time history, set *SeismicMode* to “1”. A setting of “2” will result in a synthetically generated time history for each of the 3 loading directions (2 – horizontal and 1 – vertical). Other values are not valid and will result in aborting execution of the simulation.

PtfmXMotionFn, PtfmYMotionFn, and PtfmZMotionFn: Platform X/Y/Z Motion Filename [Quoted String]

These are the full or relative path of the files containing the base motion time history data provided by the user. The user can specify any of the three files needed for the analysis. This file name must contain fewer than 100 characters and must be enclosed in apostrophes or double quotes. FAST will read these files if the value of each parameter is not null. *PtfmXMotionFn*, *PtfmYMotionFn*, and *PtfmZMotionFn* contain motion information in the tower base coordinate system X, Y, and Z direction, respectively. The values in these files should be given in two columns representing time and motion for each time-step. If a file name is omitted for a particular direction it is assumed that no loading is requested and no motion will be applied in that direction.

PtfmMotionType: The Platform Motion Type [-]

This switch will be required if *SeismicMode* is set to “1” and ground motion is user-defined. This switch will describe the type of ground motion given by the user.

Setting *PtfmMotionType* to “1” will mean that the ground motion type given by the user is in the form of acceleration. A setting of “2” and “3” will mean that the data is given to FAST in velocity and displacement, respectively. Using other values for this switch will cause FAST to abort.

PtfmMotionFactor: Platform Motion Factor [-]

This switch will be required if *SeismicMode* is set to “1” and ground motion is user-defined. This is a value for scaling the data available in *PtfmXMotionFn*, *PtfmYMotionFn*, and *PtfmZMotionFn*. Depending on the units for the data available in the input files, the user can scale them to match the units available in the model. The FAST code assumes that input motions are specified in m, m/s, and m/s² for displacement, velocity, and acceleration, respectively. This factor is applied to all three specified directions.

ActFreq: Actuator Frequency [Hz]

The frequency of the actuator used to calculate the base forces according to the input motion given to the program.

ActDamp: Actuator Damping [%]

The damping ratio assigned to the actuator to calculate the base forces. This variable is specified as a percent of the critical damping. A value of 60 to 70 percent is suggested.

EqDelay: Earthquake Delay [s]

Offset from the start of the simulation when the base shaking is to be applied to the turbine.

Model for seismic loading

Seismic loads created in a structure are the resultant of base motion that, for FAST simulations, can be prescribed as acceleration, velocity, or displacement. Using the provided base motion, a consistent set of acceleration, velocity, and displacement is calculated for each of the translational directions. To develop the required force time

history to enforce the supplied base motion time history, a damped oscillator is simulated at the base of a modeled wind turbine. Through this approach, the seismic forces required to achieve the earthquake input given by the user is calculated at each time-step. The oscillator stiffness is controlled through specification of the natural frequency through the *ActFreq* variable. It is recommended that the actuator frequency be kept at least twice the highest frequency of the turbine model being excited. The maximum frequency of a wind turbine model can be obtained by performing a linearization analysis in FAST before carrying out the seismic analysis. To obtain stable results, the time-step of the simulation (*dt*) must be kept sufficiently small. As a general rule, the simulation time-step should be at most 1/10 the period of the actuator. By assuming a relatively large damping value, and maintaining a high stiffness, the damped actuator provides an efficient way to translate the specified motion into the required force time history. The actuator damping value can be specified as a percent of critical damping using the *ActDamp* variable. A value of 60 to 70 percent is recommended. Further information detailing theory associated with motion of a damped oscillator is available in most fundamental dynamics textbooks.

Motions

Two types of motions are supported for application of base shaking in FAST: The first is explicitly provided by the user as acceleration, velocity, or displacement in each desired direction of shaking; and the second is a synthetically generated acceleration based on parameters given by the user. Both user-defined and synthetic motions can be adjusted to be compatible with a user-defined target spectrum.

For performing seismic analysis on a wind turbine, the platform's translational degrees of freedom should be set to "true" in each direction of motion applied to the structure. These variables can be found in the FAST platform file which is shown below. For example, if motion is to be applied in X, Y, and Z directions, *PtfmSgDOF*, *PtfmSwDOF*, and *PtfmHvDOF* must each be set to "true". Without further modifications to the provided analysis routines the platform's rotational degrees of freedom should be set to "False" at all times.

```

-----
FAST PLATFORM FILE
-----
FEATURE FLAGS (CONT)
-----
True   PtfmSgDOF - Platform horizontal surge translation DOF (flag)
True   PtfmSwDOF - Platform horizontal sway translation DOF (flag)
True   PtfmHvDOF - Platform vertical heave translation DOF (flag)
False  PtfmRDOF  - Platform roll tilt rotation DOF (flag)
False  PtfmPDOF - Platform pitch tilt rotation DOF (flag)
False  PtfmYDOF - Platform yaw rotation DOF (flag)
-----
INITIAL CONDITIONS (CONT)
-----
0.0    PtfmSurge - Initial or fixed horizontal surge translational
displacement of platform (meters)
0.0    PtfmSway  - Initial or fixed horizontal sway translational
displacement of platform (meters)
0.0    PtfmHeave - Initial or fixed vertical heave translational
displacement of platform (meters)
0.0    PtfmRoll  - Initial or fixed roll tilt rotational
displacement of platform (degrees)
0.0    PtfmPitch - Initial or fixed pitchtilt rotational
displacement of platform (degrees)
0.0    PtfmYaw   - Initial or fixed yaw rotational displacement of
platform (degrees)
-----
TURBINE CONFIGURATION (CONT)
-----
0.0    TwrDraft  - Downward distance from the ground level [onshore]
or MSL [offshore] to the tower base platform connection (meters)
0.0    PtfmCM    - Downward distance from the ground level [onshore]
or MSL [offshore] to the platform CM (meters)
0.0    PtfmRef   - Downward distance from the ground level [onshore]
or MSL [offshore] to the platform reference point (meters)
-----
MASS AND INERTIA (CONT)
-----
7.0e5  PtfmMass   - The mass of the foundation (kg)
0.0    PtfmRIner - The rotational inertial of the foundation for
rolling (km*m^2)
0.0    PtfmPIner - The rotational inertial of the foundation for
pitching (km*m^2)
0.0    PtfmYIner - The rotational inertial of the foundation for
yawing (km*m^2)
-----
PLATFORM LOADING
-----
1      PtfmLdMod - Platform loading model {0: none, 1: user-defined
from routine UserPtfmLd} (switch)

```

For FAST to conduct seismic analysis, *PtfmLdMod* should be set to 1 so that FAST can call the subroutines available in the user defined platform loading file containing the seismic properties of the simulation.

User specified input motion

A user specified input motion is indicated by switching *SeismicMode* to 1 and defining the path of each input file using the three parameters *PtfmXMotionFn*,

PtfmYMotionFn, and *PtfmZMotionFn* which represent the user specified motion in horizontal x axis, y axis, and vertical z axis of the inertial-frame coordinate system, respectively. The data in the motion files contain two columns which represent time in the first column and desired motion in the second column. Motion can be given in any time-step according to the recorded data that will be interpolated in terms of the time-step given to the primary FAST input file by the program. The user may provide input for FAST in terms of acceleration, velocity, or displacement by defining the type of user specified input motion using *PtfmMotionType*. A scale factor, *PtfmMotionFactor*, with a default of 1.0 is used to adjust the amplitude of the specified input motion. This factor may be used to correct input to the assumed units (m/s^2 , m/s , and m for acceleration, velocity, and displacement respectively) or to otherwise scale the input amplitude to any desired level. If the user provides an input motion with residual drifts in displacement and velocity time histories, baseline correction can be applied in the simulation by switching on *BLineCorrection* parameter in the seismic input file which will be explained in the following sections. As mentioned earlier, it is recommended that the user review the resulting platform acceleration, velocity, and displacement following simulations to ensure expected behavior. These values can be recorded platform motion variables in the main FAST output file.

Synthetic motions

In addition to a user-specified motion, generation of synthetic motion is supported by setting *SeismicMode* to 2. A full description of variables used by synthetic motions simulations is provided at the end of this section. Generation of the synthetic motion starts by creating sequence of random numbers with zero mean and unit variance of the specified length (*SynDuration*). The generation motion is then scaled so that the resulting root mean square (RMS) amplitude matches the specified amplitude, for each direction. To adjust the generated synthetic motion to more closely resemble an earthquake motion, which generally builds from low amplitude shaking to a period of strong motion and then decays again, an initial and final ramp may be specified for each direction. The ramps are specified in a separate file as a single time and amplitude pair separated by a space on each line. Amplitudes of any value are acceptable, but it is suggested that initial ramps

monotonically increase from zero to one and final ramps monotonically decrease from one to zero. The ramps are applied by interpolating between specified time/amplitude pairs and then multiplied by the synthetic motion. This process results in a motion, which more closely resembles observed earthquake time histories, but often modification of the response spectrum is desirable to adjust the frequency content of the synthetic motion. This can be achieved by specification of a target response spectrum to alter the frequency content of the synthetic time histories, described below. As always in seismic simulations, it is recommended that the resulting platform motion be recorded through capture of the appropriate variables in the main FAST output file. Further, without baseline correction synthetically generated motions will most likely result in residual velocities and displacements.

SynRandomSeedX1, SynRandomSeedY1, SynRandomSeedZ1, SynRandomSeedX2, SynRandomSeedY2, and SynRandomSeedZ2: Synthetic Motion Random Seeds [-]

This value will be required if *SeismicMode* is set to “2”. This value is used to generate randomized data for synthetic motion. *SynRandomSeed* is the seed number for the random number generator.

SynRMSAmpX, SynRMSAmpY, and SynRMSAmpZ: Synthetic Motion RMS Amplitude [m/s²]

These values are required if *SeismicMode* is set to “2”. This variable is used to specify the RMS amplitude (m/s²) of the synthetically generated motion in each direction. The RMS amplitude is calculated prior to application of initial and final ramps. Further, the final amplitude may be influenced by motion modification to conform to a target response spectrum. If no motion is desired in a particular direction, simply set the RMS amplitude for that direction to 0.

SynDuration: Synthetic Motion Duration [s]

This value indicates the duration of the generated synthetic time history. Duration is independent of *EqDelay*.

SynInitRampFnX, SynInitRampFnY, and SynInitRampFnZ: Synthetic Motion Initial Ramp Filename [-]

This is the full path to a file containing time and amplitude pairs used to specify an initial ramp to be applied to the synthetically generated motion in each of the three possible loading directions. Each line consists of two floating point numbers separated by a space. The first number is the time in seconds. The second is the multiplication factor used to scale the motion. It is recommended that values monotonically increase from zero to one, but this is not enforced. For intermediate time values not specified, a scale factor is calculated through linearly interpolating between given values. If a ramp file name is omitted, no ramp is applied to the generated motion.

SynFinalRampFnX, SynFinalRampFnY, and SynFinalRampFnZ: Synthetic Motion Final Ramp Filename [-]

This is the full path to a file containing time and amplitude pairs used to specify a final ramp to be applied to the synthetically generated motion in each of the three possible directions. It is formatted as the *InitRampFn* file. It is recommended that values in this file monotonically decrease from one to zero, but such behavior is not enforced. If a ramp file name is omitted, no ramp is applied to the generated motion.

Motion handling

This section explains how the specified user-defined or synthetic ground motions can be manipulated. There are two types of dealing with a ground motion in FAST. The first method of motion modification is baseline correction, in which a ground motion that has residual drifts in velocity or displacement time history is adjusted to eliminate these artifacts. The second modification procedure is to adjust the motion to be compatible with a target response spectrum. Both user-defined and synthetic motion can be adjusted to conform within a desired tolerance of a target response spectrum. Though the method used for adjusting a motion to conform to a target spectrum will not create additional residual velocity or displacement, motions that originally result in residual velocity or displacement should still be corrected. A brief description of each type of motion handling is available in the following sections.

Baseline Correction

If the user provides an input motion or uses a synthetic motion that shows residual drifts in its displacement and velocity, baseline correction may be performed to remove these numerical artifacts. Baseline correction is performed by fitting a second-order polynomial fit to the calculated displacement. The resulting polynomial is subtracted from the displacement time series to eliminate residual drifts in the displacement. Finally the updated velocity and acceleration time histories are calculated using the corrected displacement time history.

BLineCorrection: Base Line Correction [T/F]

This is a flag which lets the user decide whether baseline correction is needed for the input data files or not. If *BLineCorrection* is set to “True”, motions are corrected for all of the three axes.

Target spectrum

The response of an initial ground motion can be matched with a user-provided target response spectrum. Many approaches are available for matching the response of an initial time history to a desired response spectrum. The tapered cosine wavelet method implemented in the 2009 version of RspMatch (also known as RspMatch09) and documented in Atik and Abrahamson is supported for use in the FAST code. This approach strategically adds a tapered cosine wavelet to the acceleration time history that has the effect of reducing the discrepancy between the actual and target response spectrum. Over previous approaches, this procedure provides numerous advantages including: numerical efficiency; eliminating the need for additional baseline correction; and improved preservation the non-stationary characteristics of the original motion. For more information about the process of spectral matching, the user can refer to Atik and Abrahamson. Variables required for modification of the motion response spectrum are described below. For using the target spectrum capabilities of FAST, the executable file of the RspMatch program has to be copied in the same folder as the FAST executable file and *TgtResponse* flag is set to “True” in the seismic configuration file.

TgtResponse: Target Response Spectrum [-]

This is a flag indicating if the user needs to match the time history with a target response spectrum. This flag is usually true when a synthetic motion is created and *SeismicMode* is set to “2”.

TgtResFnX, TgtResFnY, and TgtResFnZ: Target Response Spectrum Filename [-]

This is the full or relative path of the files containing a target response spectrum given by the user for each direction of loading. The format of this file is described in the target spectrum section below. If a null value is provided for any direction, no modification of motions will be made in that direction.

nPass: Number of Passes [-]

This value is only used if *TgtResponse* is set to “True”, and FAST is required to match a time history with a response spectrum. This is an integer showing the number of adjustment passes that are required for different frequency ranges to make the synthetic motion match the target response spectrum. A default of “4” is acceptable for all cases.

MaxIter: Maximum Number of Iterations [-]

This value is only used if *TgtResponse* is set to “True”. This is an integer showing the maximum number of iterations for spectral matching in each pass. A default number of 20 can be given to this value.

Tol: Tolerance [%]

This value is only used if *TgtResponse* is set to “True”. This value is the tolerance for maximum mismatch in fraction of target and it is typically set to 0.05 for 5% maximum deviation from the target spectrum.

MaxFreq: Maximum Frequency [Hz]

This value is only used if *TgtResponse* is set to “True”. This value indicates the maximum frequency up to which spectral matching is performed.

FreqMatch12: Frequency Match 1 and 2 [Hz]

This value is only used if *TgtResponse* is set to “True”. Two frequencies which clarify the frequency range for spectral matching which are separated by commas. Spectral matching for a certain pass is performed for all frequencies between *freqMatch1* and *freqMatch2*.

FAST input file

The FAST input file is the main file that contains properties of the generator, the path to the tower and blade properties, the path file for the aerodynamic properties, and other controls of the simulation. The output information needed from the simulation can also be requested by the user at the end of the FAST input file.

```

-----
----- FAST INPUT FILE -----
----- SIMULATION CONTROL -----
False      Echo          - Echo input data to "echo.out" (flag)
3          ADAMSPrep       - ADAMS preprocessor mode {1: Run FAST, 2: use
FAST as a preprocessor to create an ADAMS model, 3: do both} (switch)
1          AnalMode     - Analysis mode {1: Run a time-marching
simulation, 2: create a periodic linearized model} (switch)
3          NumBl       - Number of blades (-)
500.00     TMax           - Total run time (s)
0.005     DT           - Integration time step (s)
----- TURBINE CONTROL -----
0          YCMode     - Yaw control mode {0: none, 1: user-defined
from routine UserYawCont, 2: user-defined from Simulink} (switch)
9999.9     TYCon      - Time to enable active yaw control (s) [unused
when YCMode=0]
1          PCMode     - Pitch control mode {0: none, 1: user-defined
from routine PitchCntrl, 2: user-defined from Simulink} (switch)
0.0        TPCOn      - Time to enable active pitch control (s)
[unused when PCMode=0]
2          VSContrl   - Variable-speed control mode {0: none, 1:
simple VS, 2: user-defined from routine UserVSCont, 3: user-defined
from Simulink} (switch)
9999.9     VS_RtGnSp   - Rated generator speed for simple variable-
speed generator control (HSS side) (rpm) [used only when VSContrl=1]
9999.9     VS_RtTq     - Rated generator torque/constant generator
torque in Region 3 for simple variable-speed generator control (HSS
side) (N-m) [used only when VSContrl=1]
9999.9     VS_Rgn2K    - Generator torque constant in Region 2 for
simple variable-speed generator control (HSS side) (N-m/rpm^2) [used
only when VSContrl=1]
9999.9     VS_SlPc     - Rated generator slip percentage in Region 2
1/2 for simple variable-speed generator control (%) [used only when
VSContrl=1]
2          GenModel   - Generator model {1: simple, 2: Thevenin, 3:

```

```

user-defined from routine UserGen} (switch) [used only when VSContrl=0]
True      GenTiStr    - Method to start the generator {T: timed using
TimGenOn, F: generator speed using SpdGenOn} (flag)
True      GenTiStp    - Method to stop the generator {T: timed using
TimGenOf, F: when generator power = 0} (flag)
9999.9    SpdGenOn    - Generator speed to turn on the generator for
a startup (HSS speed) (rpm) [used only when GenTiStr=False]
0.0       TimGenOn    - Time to turn on the generator for a startup
(s) [used only when GenTiStr=True]
9999.9    TimGenOf    - Time to turn off the generator (s) [used only
when GenTiStp=True]
1         HSSBrMode   - HSS brake model {1: simple, 2: user-defined
from routine UserHSSBr} (switch)
9999.9    THSSBrDp    - Time to initiate deployment of the HSS brake
(s)
9999.9    TiDynBrk    - Time to initiate deployment of the dynamic
generator brake [CURRENTLY IGNORED] (s)
9999.9    TTPBrDp(1)  - Time to initiate deployment of tip brake 1
(s)
9999.9    TTPBrDp(2)  - Time to initiate deployment of tip brake 2
(s)
9999.9    TTPBrDp(3)  - Time to initiate deployment of tip brake 3
(s) [unused for 2 blades]
9999.9    TBDepISp(1) - Deployment-initiation speed for the tip brake
on blade 1 (rpm)
9999.9    TBDepISp(2) - Deployment-initiation speed for the tip brake
on blade 2 (rpm)
9999.9    TBDepISp(3) - Deployment-initiation speed for the tip brake
on blade 3 (rpm) [unused for 2 blades]
9999.9    TYawManS    - Time to start override yaw maneuver and end
standard yaw control (s)
9999.9    TYawManE    - Time at which override yaw maneuver reaches
final yaw angle (s)
0.0       NacYawF     - Final yaw angle for yaw maneuvers (degrees)
9999.9    TPitManS(1) - Time to start override pitch maneuver for
blade 1 and end standard pitch control (s)
9999.9    TPitManS(2) - Time to start override pitch maneuver for
blade 2 and end standard pitch control (s)
9999.9    TPitManS(3) - Time to start override pitch maneuver for
blade 3 and end standard pitch control (s) [unused for 2 blades]
9999.9    TPitManE(1) - Time at which override pitch maneuver for
blade 1 reaches final pitch (s)
9999.9    TPitManE(2) - Time at which override pitch maneuver for
blade 2 reaches final pitch (s)
9999.9    TPitManE(3) - Time at which override pitch maneuver for
blade 3 reaches final pitch (s) [unused for 2 blades]
0.0       B1Pitch(1)  - Blade 1 initial pitch (degrees)
0.0       B1Pitch(2)  - Blade 2 initial pitch (degrees)
0.0       B1Pitch(3)  - Blade 3 initial pitch (degrees) [unused for 2
blades]
0.0       B1PitchF(1) - Blade 1 final pitch for pitch maneuvers
(degrees)
0.0       B1PitchF(2) - Blade 2 final pitch for pitch maneuvers
(degrees)
0.0       B1PitchF(3) - Blade 3 final pitch for pitch maneuvers
(degrees) [unused for 2 blades]

```

```

----- ENVIRONMENTAL CONDITIONS -----
9.80665 Gravity - Gravitational acceleration (m/s^2)
----- FEATURE FLAGS -----
True FlapDOF1 - First flapwise blade mode DOF (flag)
True FlapDOF2 - Second flapwise blade mode DOF (flag)
True EdgeDOF - First edgewise blade mode DOF (flag)
False TeetDOF - Rotor-teeter DOF (flag) [unused for 3 blades]
True DrTrDOF - Drivetrain rotational-flexibility DOF (flag)
True GenDOF - Generator DOF (flag)
True YawDOF - Yaw DOF (flag)
True TwFADOF1 - First fore-aft tower bending-mode DOF (flag)
True TwFADOF2 - Second fore-aft tower bending-mode DOF (flag)
True TwSSDOF1 - First side-to-side tower bending-mode DOF
(flag)
True TwSSDOF2 - Second side-to-side tower bending-mode DOF
(flag)
True CompAero - Compute aerodynamic forces (flag)
False CompNoise - Compute aerodynamic noise (flag)
----- INITIAL CONDITIONS -----
0.0 OopDefl - Initial out-of-plane blade-tip displacement
(meters)
0.0 IPDefl - Initial in-plane blade-tip deflection
(meters)
0.0 TeetDefl - Initial or fixed teeter angle (degrees)
[unused for 3 blades]
0.0 Azimuth - Initial azimuth angle for blade 1 (degrees)
12.1 RotSpeed - Initial or fixed rotor speed (rpm)
0.0 NacYaw - Initial or fixed nacelle-yaw angle (degrees)
0.0 TTDspFA - Initial fore-aft tower-top displacement
(meters)
0.0 TTDspSS - Initial side-to-side tower-top displacement
(meters)
----- TURBINE CONFIGURATION -----
63.0 TipRad - The distance from the rotor apex to the blade
tip (meters)
1.5 HubRad - The distance from the rotor apex to the blade
root (meters)
1 PSpnElN - Number of the innermost blade element which
is still part of the pitchable portion of the blade for partial-span
pitch control [1 to BldNodes] [CURRENTLY IGNORED] (-)
0.0 UndSling - Undersling length [distance from teeter pin
to the rotor apex] (meters) [unused for 3 blades]
0.0 HubCM - Distance from rotor apex to hub mass
[positive downwind] (meters)
-5.01910 OverHang - Distance from yaw axis to rotor apex [3
blades] or teeter pin [2 blades] (meters)
1.9 NacCMxn - Downwind distance from the tower-top to the
nacelle CM (meters)
0.0 NacCMyn - Lateral distance from the tower-top to the
nacelle CM (meters)
1.75 NacCMzn - Vertical distance from the tower-top to the
nacelle CM (meters)
87.6 TowerHt - Height of tower above ground level [onshore]
or MSL [offshore] (meters)
1.96256 Twr2Shft - Vertical distance from the tower-top to the
rotor shaft (meters)

```

```

    0.0      TwrRBHt    - Tower rigid base height (meters)
   -5.0     ShftTilt   - Rotor shaft tilt angle (degrees)
    0.0     Delta3     - Delta-3 angle for teetering rotors (degrees)
[unused for 3 blades]
   -2.5     PreCone(1) - Blade 1 cone angle (degrees)
   -2.5     PreCone(2) - Blade 2 cone angle (degrees)
   -2.5     PreCone(3) - Blade 3 cone angle (degrees) [unused for 2
blades]
    0.0     AzimBlUp   - Azimuth value to use for I/O when blade 1
points up (degrees)
----- MASS AND INERTIA -----
    0.0     YawBrMass  - Yaw bearing mass (kg)
  240.00E3  NacMass    - Nacelle mass (kg)
   56.78E3  HubMass    - Hub mass (kg)
    0.0     TipMass(1) - Tip-brake mass, blade 1 (kg)
    0.0     TipMass(2) - Tip-brake mass, blade 2 (kg)
    0.0     TipMass(3) - Tip-brake mass, blade 3 (kg) [unused for 2
blades]
  2607.89E3 NacYIner   - Nacelle inertia about yaw axis (kg m^2)
   534.116  GenIner    - Generator inertia about HSS (kg m^2)
  115.926E3 HubIner    - Hub inertia about rotor axis [3 blades] or
teeter axis [2 blades] (kg m^2)
----- DRIVETRAIN -----
   100.0    GBoxEff    - Gearbox efficiency (%)
    94.4    GenEff     - Generator efficiency [ignored by the Thevenin
and user-defined generator models] (%)
    97.0    GBRatio    - Gearbox ratio (-)
False      GBRevers   - Gearbox reversal {T: if rotor and generator
rotate in opposite directions} (flag)
  28.1162E3 HSSBrTqF   - Fully deployed HSS-brake torque (N-m)
    0.6     HSSBrDT    - Time for HSS-brake to reach full deployment
once initiated (sec) [used only when HSSBrMode=1]
           DynBrkFi    - File containing a mech-gen-torque vs HSS-
speed curve for a dynamic brake [CURRENTLY IGNORED] (quoted string)
  867.637E6 DTTorSpr   - Drivetrain torsional spring (N-m/rad)
    6.215E6 DTTorDmp   - Drivetrain torsional damper (N-m/(rad/s))
----- SIMPLE INDUCTION GENERATOR -----
  9999.9    SIG_SlPc    - Rated generator slip percentage (%) [used
only when VSContrl=0 and GenModel=1]
  9999.9    SIG_SySp    - Synchronous (zero-torque) generator speed
(rpm) [used only when VSContrl=0 and GenModel=1]
  9999.9    SIG_RtTq    - Rated torque (N-m) [used only when VSContrl=0
and GenModel=1]
  9999.9    SIG_PORT    - Pull-out ratio (Tpullout/Trated) (-) [used
only when VSContrl=0 and GenModel=1]
----- THEVENIN-EQUIVALENT INDUCTION GENERATOR -----
  9999.9    TEC_Freq    - Line frequency [50 or 60] (Hz) [used only
when VSContrl=0 and GenModel=2]
  9998     TEC_NPol    - Number of poles [even integer > 0] (-) [used
only when VSContrl=0 and GenModel=2]
  9999.9    TEC_SRes    - Stator resistance (ohms) [used only when
VSContrl=0 and GenModel=2]
  9999.9    TEC_RRes    - Rotor resistance (ohms) [used only when
VSContrl=0 and GenModel=2]
  9999.9    TEC_VLL    - Line-to-line RMS voltage (volts) [used only
when VSContrl=0 and GenModel=2]

```



```

9999.9      TEC_SLR      - Stator leakage reactance (ohms) [used only
when VSContrl=0 and GenModel=2]
9999.9      TEC_RLR      - Rotor leakage reactance (ohms) [used only
when VSContrl=0 and GenModel=2]
9999.9      TEC_MR       - Magnetizing reactance (ohms) [used only when
VSContrl=0 and GenModel=2]
----- PLATFORM -----
      1      PtfmModel    - Platform model {0: none, 1: onshore, 2: fixed
bottom offshore, 3: floating offshore} (switch)
"NRELOffshrbaseline5MW_Onshore_Ptfm.dat"      PtfmFile    - Name of
file containing platform properties (quoted string) [unused when
PtfmModel=0]
----- TOWER -----
      20      TwrNodes    - Number of tower nodes used for analysis (-)
"NRELOffshrbaseline5MW_Tower_Onshore.dat"      TwrFile      - Name of
file containing tower properties (quoted string)
----- NACELLE-YAW -----
9028.32E6   YawSpr       - Nacelle-yaw spring constant (N-m/rad)
      19.16E6   YawDamp    - Nacelle-yaw damping constant (N-m/(rad/s))
      0.0      YawNeut    - Neutral yaw position--yaw spring force is
zero at this yaw (degrees)
----- FURLING -----
False       Furling      - Read in additional model properties for
furling turbine (flag)
           FurlFile      - Name of file containing furling properties
(quoted string) [unused when Furling=False]
----- ROTOR-TEETER -----
      0      TeetMod     - Rotor-teeter spring/damper model {0: none, 1:
standard, 2: user-defined from routine UserTeet} (switch) [unused for 3
blades]
      0.0     TeetDmpP    - Rotor-teeter damper position (degrees) [used
only for 2 blades and when TeetMod=1]
      0.0     TeetDmp     - Rotor-teeter damping constant (N-m/(rad/s))
[used only for 2 blades and when TeetMod=1]
      0.0     TeetCDmp    - Rotor-teeter rate-independent Coulomb-damping
moment (N-m) [used only for 2 blades and when TeetMod=1]
      0.0     TeetSSStP   - Rotor-teeter soft-stop position (degrees)
[used only for 2 blades and when TeetMod=1]
      0.0     TeetHStP    - Rotor-teeter hard-stop position (degrees)
[used only for 2 blades and when TeetMod=1]
      0.0     TeetSSSp    - Rotor-teeter soft-stop linear-spring constant
(N-m/rad) [used only for 2 blades and when TeetMod=1]
      0.0     TeetHSSp    - Rotor-teeter hard-stop linear-spring constant
(N-m/rad) [used only for 2 blades and when TeetMod=1]
----- TIP-BRAKE -----
      0.0     TBrConN     - Tip-brake drag constant during normal
operation, Cd*Area (m^2)
      0.0     TBrConD     - Tip-brake drag constant during fully-deployed
operation, Cd*Area (m^2)
      0.0     TpBrDT      - Time for tip-brake to reach full deployment
once released (sec)
----- BLADE -----
"NRELOffshrbaseline5MW_Blade.dat"      BldFile(1)  - Name of file
containing properties for blade 1 (quoted string)
"NRELOffshrbaseline5MW_Blade.dat"      BldFile(2)  - Name of file
containing properties for blade 2 (quoted string)

```

```

"NREOffshrbaseline5MW_Blade.dat"          BldFile(3) - Name of file
containing properties for blade 3 (quoted string) [unused for 2 blades]
----- AERODYN -----
"NREOffshrbaseline5MW_AeroDyn.ipt"        ADFile      - Name of file
containing AeroDyn input parameters (quoted string)
----- NOISE -----
      NoiseFile - Name of file containing aerodynamic noise
input parameters (quoted string) [used only when CompNoise=True]
----- ADAMS -----
"NREOffshrbaseline5MW_ADAMSSpecific.dat"  ADAMSFile   - Name of file
containing ADAMS-specific input parameters (quoted string) [unused when
ADAMSPrep=1]
----- LINEARIZATION CONTROL -----
"NREOffshrbaseline5MW_Linear.dat"         LinFile     - Name of file
containing FAST linearization parameters (quoted string) [unused when
AnalMode=1]
----- OUTPUT -----
True          SumPrint - Print summary data to "<RootName>.fsm" (flag)
True          TabDelim - Generate a tab-delimited tabular output file.
(flag)
"ES10.3E2"   OutFmt    - Format used for tabular output except time.
Resulting field should be 10 characters. (quoted string) [not checked
for validity!]
      0.0      TStart    - Time to begin tabular output (s)
      1        DecFact   - Decimation factor for tabular output {1:
output every time step} (-)
      1.0      SttsTime  - Amount of time between screen status messages
(sec)
-3.09528     NcIMUxn    - Downwind distance from the tower-top to the
nacelle IMU (meters)
      0.0      NcIMUyn    - Lateral distance from the tower-top to the
nacelle IMU (meters)
      2.23336   NcIMUzn    - Vertical distance from the tower-top to the
nacelle IMU (meters)
      1.912     ShftGagL  - Distance from rotor apex [3 blades] or teeter
pin [2 blades] to shaft strain gages [positive for upwind rotors]
(meters)
      0         NTwGages  - Number of tower nodes that have strain gages
for output [0 to 9] (-)
      TwrGagNd - List of tower nodes that have strain gages [1
to TwrNodes] (-) [unused if NTwGages=0]
      3         NBlGages  - Number of blade nodes that have strain gages
for output [0 to 9] (-)
      5,9,13    BldGagNd  - List of blade nodes that have strain gages [1
to BldNodes] (-) [unused if NBlGages=0]
      OutList   - The next line(s) contains a list of output
parameters. See OutList.txt for a listing of available output
channels, (-)
"PtfmTDxi, PtfmTDyi, PtfmTDzi" - Output for platform displacement
"PtfmTVxi, PtfmTVyi, PtfmTVzi" - Output for platform velocity
"PtfmTAXi, PtfmTAYi, PtfmTAzi" - Output for platform acceleration
"YawBrFxp, YawBrFyp, YawBrFzp" - Fore-aft shear, side-to-side shear,
and vertical forces at the top of the tower (not rotating with nacelle
yaw)
"YawBrMxp, YawBrMyp, YawBrMzp" - Side-to-side bending, fore-aft
bending, and yaw moments at the top of the tower (not rotating with

```

```
nacelle yaw)
"TwrBsFxt, TwrBsFyt , TwrBsFzt" - Fore-aft shear, side-to-side shear,
and vertical forces at the base of the tower (mudline)
"TwrBsMxt , TwrBsMyt , TwrBsMzt" - Side-to-side bending, fore-aft
bending, and yaw moments at the base of the tower (mudline)
END of FAST input file (the word "END" must appear in the first 3
columns of this last line).
```

APPENDIX B.

ABAQUS-AERODYN-FAST LINK THROUGH MATLAB

The finite element model of 5-MW wind turbine developed in ABAQUS was calibrated using modal analysis with previous models tested with other previously used FE codes or multi-body dynamic procedures as presented in Paper III. Aerodynamic loads were applied to the finite element model by modifications done in AeroDyn. The AeroDyn source code was modified using FORTRAN to return normal, tangential, and pitch moment of each segment of the three blades. Each blade consisted of 17 aerodynamic segments. The timesteps were set to match the dynamic simulation timestep of the whole model including earthquake that was given to ABAQUS for coupled simulations. AeroDyn consists of compiling 5 source code files. The modifications were done in the AeroSubs.f90. This file contains subroutines for calculation and output parameters of an input wind on the blades of a wind turbine. The Modified part of the AeroSubs.f90 are shown below which gives the output aerodynamic loads of the three blades in different time steps of the simulation.

```

!*****
!*****Element Force Calculations*****
SUBROUTINE ELEMFRFC (PSI, RLOCAL, J, IBlade, VNROTOR2, VT, VNW, &
                   VNB, DFN, DFT, PMA, Initial)
! Calculates the aerodynamic forces on the three
! blade elements. Inputs include all velocities.
! Normal and tangential forces and pitch moment forces.
! They are returned in the element output .dat file.
! *****
! First use other subroutines in other files
USE                               Airfoil
USE                               ElOutParams
USE                               Blade
USE                               Element
USE                               ElemInflow
USE                               InducedVel
USE                               Rotor
USE                               Switch
USE                               Wind
IMPLICIT NONE
! Define input Variables
REAL(ReKi), INTENT(OUT)           :: DFN
REAL(ReKi), INTENT(OUT)           :: DFT
REAL(ReKi), INTENT(OUT)           :: PMA
REAL(ReKi), INTENT(IN)            :: PSI
REAL(ReKi), INTENT(IN)            :: RLOCAL
REAL(ReKi), INTENT(IN)            :: VNB
REAL(ReKi), INTENT(IN)            :: VNROTOR2
REAL(ReKi), INTENT(IN)            :: VNW
REAL(ReKi), INTENT(INOUT)         :: VT
INTEGER, INTENT(IN)                :: J
INTEGER, INTENT(IN)                :: IBlade   ! Blade Number

```

```

LOGICAL,   INTENT(IN)       :: Initial
! Local Variables
REAL(ReKi) :: CDA
REAL(ReKi) :: CLA
REAL(ReKi) :: CMA
REAL(ReKi) :: CPHI
REAL(ReKi) :: PHI
REAL(ReKi) :: QA
REAL(ReKi) :: ReNum
REAL(ReKi) :: SPHI
REAL(ReKi) :: Vinduced
REAL(ReKi) :: VN
! Check for being at the center of rotation.
! If we are at the center of rotation, the induction equations
! are undefined, so let's just USE zeros.

IF ( RLOCAL < 0.01 ) THEN
  A (J,IBLADE) = 0.0
  AP(J,IBLADE) = 0.0
ELSEIF( DYNINFL .AND. R * REVS < 2.0 ) THEN
  A (J,IBLADE) = 0.0
  AP(J,IBLADE) = 0.0
  DYNINIT = .TRUE.!Reinitialize if we begin using dynamic inflow again
ELSE
! Get induction factor = A using static airfoil coefficients
  IF ( WAKE .AND. .NOT. Initial) THEN

! USE dynamic inflow model to find A
    CALL VINDINF( J, IBlade, RLOCAL, VNW, VNB, VT, PSI )
  ELSE
! USE momentum balance to find A
    CALL VIND( J, IBlade, RLOCAL, VNROTOR2, VNW, VNB, VT )
! Apply skewed-wake correction, if applicable
    IF( SKEW ) CALL VNMOD( J, IBlade, RLOCAL, PSI )
  ENDIF
  ELSE
! Ignore the wake calculation entirely
    A (J,IBLADE) = 0.0
    AP(J,IBLADE) = 0.0
  ENDIF
ENDIF
Vinduced = VNW * A(J,IBLADE)
VN = VNW + VNB - Vinduced
SumInfl = SumInfl + Vinduced * RLOCAL * DR(J)
! Get the angle of attack
PHI = ATAN2( VN, VT )
ALPHA(J,Iblade) = PHI - PITNOW
CALL MPI2PI ( ALPHA(J,Iblade) )
W2(J,Iblade) = VN * VN + VT * VT
! Get the Reynold's number for the element
! Returns Reynold's number x 10^6
IF (Reynolds) MulTabLoc = ReNum
! Get lift coefficient from dynamic stall routine if desired
! note that the induced velocity was calculated
! using the static CL, not the dynamic CL

```

```

IF ( DSTALL ) THEN
! USE BEDDOES dynamic stall model
  IF (Initial) THEN ! USE static data on first pass
    CALL BEDINIT (J, IBlade, ALPHA(J,IBlade))
    CALL CLCD( ALPHA(J,IBlade), CLA, CDA, CMA, NFOIL(J), ErrStat )
  ELSE
    CALL BEDDOES( W2(J,IBlade), J, IBlade, ALPHA(J,IBlade), CLA, CDA,
      CMA)
  ENDIF
ELSE
! Don't USE dynamic stall model
  CALL CLCD( ALPHA(J,IBlade), CLA, CDA, CMA, NFOIL(J), ErrStat )
ENDIF
QA      = 0.5 * RHO * W2(J,IBlade) * DR(J) * C(J)
CPHI    = COS( PHI )
SPHI    = SIN( PHI )
DFN     = ( CLA * CPHI + CDA * SPHI ) * QA
DFT     = ( CLA * SPHI - CDA * CPHI ) * QA
IF ( PMOMENT ) THEN
  PMA = CMA * QA * C(J)
ELSE
  PMA = 0.
  CMA = 0.
ENDIF
! Save values at appropriate station for blade 1
IF ( IBLADE == 1 ) THEN
  IF ( ElPrList(J) > 0 ) THEN
    AAA ( ElPrList(J) ) = A (J,IBLADE)
    AAP ( ElPrList(J) ) = AP(J,IBLADE)
    ALF ( ElPrList(J) ) = ALPHA(J,IBlade) * R2D
    CDD ( ElPrList(J) ) = CDA
    CLL ( ElPrList(J) ) = CLA
    CMM ( ElPrList(J) ) = CMA
    CNN ( ElPrList(J) ) = CLA * COS(ALPHA(J,IBlade)) + CDA *
      SIN(ALPHA(J,IBlade))
    CTT ( ElPrList(J) ) = -CDA * COS(ALPHA(J,IBlade)) + CLA *
      SIN(ALPHA(J,IBlade))
    DFNSAV ( ElPrList(J) ) = DFN
    DFTSAV ( ElPrList(J) ) = DFT
    DynPres( ElPrList(J) ) = 0.5 * RHO * W2(J,IBlade)
    PITSAV ( ElPrList(J) ) = PITNOW * R2D
    PMM ( ElPrList(J) ) = PMA
    ReyNum ( ElPrList(J) ) = ReNum
  ENDIF
ENDIF
IF ( IBLADE == 2 ) THEN
  IF ( ElPrList(J) > 0 ) THEN
    AAA ( ElPrList(J) ) = A (J,IBLADE)
    AAP ( ElPrList(J) ) = AP(J,IBLADE)
    ALF ( ElPrList(J) ) = ALPHA(J,IBlade) * R2D
    CDD ( ElPrList(J) ) = CDA
    CLL ( ElPrList(J) ) = CLA
    CMM ( ElPrList(J) ) = CMA
    CNN ( ElPrList(J) ) = CLA * COS(ALPHA(J,IBlade)) + CDA *
      SIN(ALPHA(J,IBlade))
    CTT ( ElPrList(J) ) = -CDA * COS(ALPHA(J,IBlade)) + CLA *

```

```

                                SIN(ALPHA(J,IBlade))
    DFNSAV ( ElPrList(J) )      = DFN
    DFTSAV ( ElPrList(J) )      = DFT
    DynPres( ElPrList(J) )      = 0.5 * RHO * W2(J,IBlade)
    PITSAV ( ElPrList(J) )      = PITNOW * R2D
    PMM     ( ElPrList(J) )      = PMA
    ReyNum  ( ElPrList(J) )      = ReNum
  ENDIF
ENDIF
IF ( IBLADE == 3 ) THEN
  IF ( ElPrList(J) > 0 ) THEN
    AAA     ( ElPrList(J) )      = A (J,IBLADE)
    AAP     ( ElPrList(J) )      = AP(J,IBLADE)
    ALF     ( ElPrList(J) )      = ALPHA(J,IBlade) * R2D
    CDD     ( ElPrList(J) )      = CDA
    CLL     ( ElPrList(J) )      = CLA
    CMM     ( ElPrList(J) )      = CMA
    CNN     ( ElPrList(J) )      = CLA * COS(ALPHA(J,IBlade)) + CDA *
                                SIN(ALPHA(J,IBlade))
    CTT     ( ElPrList(J) )      = -CDA * COS(ALPHA(J,IBlade)) + CLA *
                                SIN(ALPHA(J,IBlade))

    DFNSAV ( ElPrList(J) )      = DFN
    DFTSAV ( ElPrList(J) )      = DFT
    DynPres( ElPrList(J) )      = 0.5 * RHO * W2(J,IBlade)
    PITSAV ( ElPrList(J) )      = PITNOW * R2D
    PMM     ( ElPrList(J) )      = PMA
    ReyNum  ( ElPrList(J) )      = ReNum
  ENDIF
ENDIF
RETURN
END SUBROUTINE ELEMFRG
!*****
!*****End of Element Force Calculations subroutine *****

```

The element forces were then stored in Hierarchical Data Format (HDF5) designed to store and organize large amounts of numerical data. For all wind simulations, after calculation of the forces on blade elements is complete, the following program in MATLAB is used to change the large .dat output file to a more compressed hdf5 file. The codes to save and load hdf5 files in MATLAB are shown below.

```

% Save data to hdf5 time series data file.
function savehdf5(fileName, dataMatrix, sampleFreq, desc, units,...
    location, metaData)
% Save data to hdf5 time series data file.
%   savehdf5(fileName, dataMatrix, deltaT, desc, units, metaData)
%   fileName   : File name text.
%   dataMatrix : N x M time series data matrix (M channels of N data
%               points)
%   sampleFreq : Sample interval (optional; default = 0.0).
%   desc       : Channel descriptors text cell.
%   units      : Channel units text cell

```



```

% location    : The path to the data in the hdf5 file (default is /)
% metaData    : Extra numeric information to be stored describing each
%              channel
%% input argument checking
if ~exist('fileName','var')
    error('File name is a mandatory input to savehdf5.')
end
if ~exist('dataMatrix','var')
    error('Data is a mandatory input to savehdf5.')
end
if ~exist('sampleFreq','var')
    sampleFreq = 0;
end
if ~exist('desc','var')
    desc = [];
end
if ~exist('units','var')
    units = [];
end
if ~exist('location','var')
    location = '/';
end
[numPoints,channels] = size(dataMatrix);
if strcmp(desc{1},'Time')
    dset = dataMatrix;
    storedUnits = units;
    storedChannelName= desc;
else
    dset = zeros(numPoints, channels+1);
    storedUnits = cell(1,channels+1);
    storedChannelName= cell(1,channels+1);
    storedUnits{1}='s';
    storedChannelName{1}='Time';
    dset(:,1)=(0:1/sampleFreq:(numPoints-1)/sampleFreq)';
    dset(:,2:end)=dataMatrix;
    for iChannel = 1:channels
        storedUnits{iChannel+1}=units{iChannel};
        storedChannelName{iChannel+1}=desc{iChannel};
    end
end
if length(location) == 1
    dset_details.Location = location;
else
    dset_details.Location = location{iChannel};
end
dset_details.Name = 'Data';
if strcmp(dset_details.Location, '/')
    fullPath = sprintf('%s%s',dset_details.Location,...
        dset_details.Name);
else
    fullPath = sprintf('%s%s%s',dset_details.Location, '/',...
        dset_details.Name);
end
attr = storedUnits;
attr_details.Name = 'Units';
attr_details.AttachedTo = fullPath;

```

```

attr_details.AttachType = 'dataset';
attr2 = sampleFreq;
attr2_details.Name = 'Sample Rate';
attr2_details.AttachedTo = fullPath;
attr2_details.AttachType = 'dataset';
attr3 = storedChannelName;
attr3_details.Name = 'Channel Name';
attr3_details.AttachedTo = fullPath;
attr3_details.AttachType = 'dataset';
hdf5write(fileName, dset_details, dset, ...
    attr_details, attr, attr2_details, attr2,...
    attr3_details, attr3);
%% Save the extra metadata
numBadSegmentBlocks = 0;
if exist('metaData','var')
    numExtraAttribs = size(metaData,1);
    for iAttrib = 1:numExtraAttribs
        if strcmp(metaData{iAttrib,1},'Bad Segment')
            numBadSegmentBlocks = numBadSegmentBlocks + 1;
            numExtraAttribs = size(metaData,2)-1;
            extraAttr = cell(1,numExtraAttribs);
            for iValue = 1:numExtraAttribs
                if size(metaData{iAttrib,iValue+1},1) == 2
                    extraAttr{iValue}=sprintf('%f%s%f',...
                        metaData{iAttrib,iValue+1}(1),'-',...
                        metaData{iAttrib,iValue+1}(2));
                else
                    extraAttr{iValue}=sprintf('%f',...
                        metaData{iAttrib,iValue+1});
                end
            end
            extraAttrDetails.Name = sprintf('%s%i',...
                metaData{iAttrib,1},' - ',numBadSegmentBlocks);
            extraAttrDetails.AttachedTo = fullPath;
            extraAttrDetails.AttachType = 'dataset';
            hdf5write(fileName, ...
                extraAttrDetails, extraAttr, 'WriteMode', 'append');
        elseif ~strcmp(metaData{iAttrib,1},'Units') && ...
            ~strcmp(metaData{iAttrib,1},'Display Name')
            numExtraAttribs = size(metaData,2)-1;
            extraAttr = zeros(numExtraAttribs,1);
            for iValue = 1:numExtraAttribs
                extraAttr(iValue)=metaData{iAttrib,iValue+1};
            end
            extraAttrDetails.Name = metaData{iAttrib,1};
            extraAttrDetails.AttachedTo = fullPath;
            extraAttrDetails.AttachType = 'dataset';
            hdf5write(fileName, ...
                extraAttrDetails, extraAttr, 'WriteMode', 'append');
        end
    end
end
end
end

```

To Load the hdf5 files, the following function was generated in MATLAB:

```

% Load data to hdf5 time series data file.
function [dataMatrix, sampleFreq, desc, units, metaData ] = ...
    loadhdf5(fileName, location)
% Load data to hdf5 time series data file.
% [dataMatrix, sampleFreq, desc, units, location] = ...
%   loadhdf5(fileName)
%
%   fileName : File name text.
%   dataMatrix : N x M time series data matrix (M channels of N data
%               points)
%   sampleFreq : Sample interval (optional; default = 0.0).
%   desc       : Channel descriptors text cell.
%   units      : Channel units text cell
%   metaData   : Extra information about the data
%   location   : The path to the data in the hdf5 file (default is /)
sampleFreq=1;
% input argument checking
if ~exist('fileName','var')
    error('File name is a mandatory input to loadhdf5.')
end
if ~exist('location','var')
    location = '/';
end
hinfo = hdf5info(fileName);
if strcmp(location, '/')
    dataSet = hinfo.GroupHierarchy.Datasets;
else
    error('Currently only / is supported as a location.')
    % Note to self: write recursive function that finds the dataSet
end
numChannels = length(hinfo.GroupHierarchy.Datasets);
if numChannels == 1
    dataMatrix = hdf5read(dataSet);
    numChannels = size(dataMatrix,2);
    fullName = dataSet.Name;
    numAttribures = ...
        length(dataSet(1).Attributes);
    numExtraAtters = 0;
    extraAtterIndexes=zeros(1,numAttribures);
    for iAttribute = 1:numAttribures
        atterName = dataSet.Attributes(1,iAttribute).Name;
        if strcmp([fullName '/Units'],atterName)
            unitsh5=...
                hdf5read(dataSet.Attributes(1,iAttribute));
        elseif strcmp([fullName '/Sample Rate'],atterName)
            sampleFreq =...
                dataSet.Attributes(1,iAttribute).Value;
        elseif strcmp([fullName '/Channel Name'],atterName)
            desch5 =...
                hdf5read(dataSet.Attributes(1,iAttribute));
        else
            numExtraAtters = numExtraAtters+1;
            extraAtterIndexes(numExtraAtters)=iAttribute;
        end
    end
end

```

```

end
units = cell(1,numChannels);
desc = cell(1,numChannels);
for iChannel = 1:numChannels
    units{iChannel}=unitsh5(iChannel).Data;
    desc{iChannel}=desch5(iChannel).Data;
end
metaData = cell(numExtraAtters,numChannels+1);
for iExtraAtter = 1:numExtraAtters
    iAttribute = extraAtterIndexes(iExtraAtter);
    tempName = dataSet.Attributes(1,iAttribute).Name;
    splitExtraAtterName = tab_split(tempName, '/');
    extraAtterName = splitExtraAtterName{end};
    if length(extraAtterName) >= 11 && ...
        strcmp('Bad Segment',extraAtterName(1:11))
        extraAtterName = 'Bad Segment';
    end
    metaData{iExtraAtter,1}=extraAtterName;
    curData = hdf5read(dataSet.Attributes(1,iAttribute));
    for iChannel = 1:numChannels
        try
            metaData{iExtraAtter,iChannel+1} = ...
                curData(iChannel).Data;
        catch ME
            metaData{iExtraAtter,iChannel+1} = ...
                curData(iChannel);
        end
    end
end
else
    % Deal with old format file with a data series for each channel
    desc = cell(1,numChannels);
    units = cell(1,numChannels);
    for iChannel = 1:numChannels
        fullName = dataSet(1,iChannel).Name;
        desc{iChannel} = fullName(2:end);
        numAttribures = ...
            length(dataSet(1,iChannel).Attributes);
        for iAttribute = 1:numAttribures
            atterName =
dataSet(1,iChannel).Attributes(1,iAttribute).Name;
            if strcmp([fullName '/Units'],atterName)
                units{iChannel}=...
dataSet(1,iChannel).Attributes(1,iAttribute).Value.Data;
            elseif strcmp([fullName '/Sample Rate'],atterName)
                curSampRate = ...
                    dataSet(1,iChannel).Attributes(1,iAttribute).Value;
                if iChannel ==1
                    sampleFreq =curSampRate;
                else
                    if sampleFreq ~= curSampRate
                        error('%s%i%s%i%s','File has multipe sample
                            rates',...
                            sampleFreq, ' and ', curSampRate, '.');
                    end
                end
            end
        end
    end
end

```

```
        end
    end
end
curDat = hdf5read(dataSet(iChannel));
if iChannel ==1
    dataMatrix= zeros(length(curDat),numChannels);
end
dataMatrix(:,iChannel)=curDat;
end
end
```

The next step was to convert the aerodynamic load files for each blade to readable input files for ABAQUS. This was done by using the following MATLAB code which read the hdf5 files for different winds and saved the normal, tangential, and pitch moment files for each element of the blade in different files.

```
% Make ABAQUS wind force files for different elements of blade3
inputFileName = sprintf('%s','NRELOffshrBsline5MW_Onshore.elm');
h5filename = sprintf('%s','NRELOffshrBsline5MW_Onshore.h5');
if ~exist(h5filename,'file')
    [AeroResultDataMatrix, AeroRestulColumnNames,...
     AeroResultUnits ] = ...
    read_AD_data(inputFileName);
    AeroTimeCol = get_hash_index(AeroRestulColumnNames,'Time');
    AeroResultSampleFreq = ...
    round(1/(AeroResultDataMatrix(2,AeroTimeCol)-...
             AeroResultDataMatrix(1,AeroTimeCol)));

    % Save the file in HDF5 format so future access is faster
    % and the file size is reduced
    savehdf5(h5filename, AeroResultDataMatrix, ...
             AeroResultSampleFreq, AeroRestulColumnNames, ...
             AeroResultUnits);
    cmdString = sprintf('%s','del ',...
                        inputFileName);
    system(cmdString,'-echo');
else
    % Read the HDF5 format file
    [AeroResultDataMatrix, ~, AeroRestulColumnNames, ...
     AeroResultUnits ] = ...
    loadhdf5(h5filename);
end

% FAST File manipulation
FASTinputFileName = sprintf('%s','NRELOffshrBsline5MW_Onshore.out');
FASTh5filename = sprintf('%s','FASTNRELOffshrBsline5MW_Onshore.h5');
if ~exist(FASTh5filename,'file')
    [FASTResultDataMatrix, FASTRestulColumnNames,...
     FASTResultUnits ] = ...
    read_AD_data(FASTinputFileName);
    FASTTimeCol = get_hash_index(FASTRestulColumnNames,'Time');
    FASTResultSampleFreq = ...
    round(1/(FASTResultDataMatrix(2,FASTTimeCol)-...
             FASTResultDataMatrix(1,FASTTimeCol)));

    % Save the file in HDF5 format so future access is faster
    % and the file size is reduced
    savehdf5(FASTh5filename, FASTResultDataMatrix, ...
             FASTResultSampleFreq, FASTRestulColumnNames, ...
             FASTResultUnits);
    cmdString = sprintf('%s','del ',...
                        FASTinputFileName);
    system(cmdString,'-echo');
else
    % Read the HDF5 format file
    [FASTResultDataMatrix, ~, FASTRestulColumnNames, ...
```

```

FASTResultUnits ] = ...
loadhdf5(FASTh5filename);

end
time = get_hash_index(AeroRestulColumnNames, 'Time');
Time_FAST = get_hash_index(FASTRestulColumnNames, 'Time');
BaseNameFT19 = 'ForcT0';
BaseNameFT1017 = 'ForcT';
BaseNameFN19 = 'ForcN0';
BaseNameFN1017 = 'ForcN';
BaseNameMP19 = 'Pmont0';
BaseNameMP1017 = 'Pmont';
ColumnNamesFT = cell (1,17);
ColumnNamesFN = cell (1,17);
ColumnNamesMP = cell (1,17);
ColumnNamesFTout = cell (1,17);
ColumnNamesFNout = cell (1,17);
ColumnNamesMPout = cell (1,17);
for i=1:17
    if i>=1 && i<=9
        ColumnNamesFT{i} = sprintf('%s%i',BaseNameFT19,i);
        ColumnNamesFN{i} = sprintf('%s%i',BaseNameFN19,i);
        ColumnNamesMP{i} = sprintf('%s%i',BaseNameMP19,i);
    else
        ColumnNamesFT{i} = sprintf('%s%i',BaseNameFT1017,i);
        ColumnNamesFN{i} = sprintf('%s%i',BaseNameFN1017,i);
        ColumnNamesMP{i} = sprintf('%s%i',BaseNameMP1017,i);
    end
end
for i = 1:17
    ColumnNamesFTout {i} =
sprintf('%s%s%s',ColumnNamesFT{i},'_blade3','.out');
    ColumnNamesFNout {i} =
sprintf('%s%s%s',ColumnNamesFN{i},'_blade3','.out');
    ColumnNamesMPout {i} =
sprintf('%s%s%s',ColumnNamesMP{i},'_blade3','.out');
end
FT = zeros(1,17);
FN = zeros(1,17);
MP = zeros(1,17);
for i=1:17
    FT(i) = get_hash_index(AeroRestulColumnNames, ColumnNamesFT{i});
    FN(i) = get_hash_index(AeroRestulColumnNames, ColumnNamesFN{i});
    MP(i) = get_hash_index(AeroRestulColumnNames, ColumnNamesMP{i});
end
Len = length (AeroResultDataMatrix (:,time));
Time = AeroResultDataMatrix (:,time);
Time_FAST = FASTResultDataMatrix (:,Time_FAST);
FTTime = cell (17,1);
FNTime = cell (17,1);
MPTime = cell (17,1);
for i=1:17
    FTTime {i,1} = zeros (Len,2);
    FNTime {i,1} = zeros (Len,2);
    MPTime {i,1} = zeros (Len,2);
end
for i=1:17

```

```

FTTime {i,1}(:,1) = Time(:,1);
FNTime {i,1}(:,1) = Time(:,1);
MPTime {i,1}(:,1) = Time(:,1);
FTTime {i,1}(:,2) = (AeroResultDataMatrix (:,FT(i)));
FNTime {i,1}(:,2) = (AeroResultDataMatrix (:,FN(i)));
MPTime {i,1}(:,2) = (AeroResultDataMatrix (:,MP(i)));
end
Time2 = (0:0.001:max(Time(:,1)))';
FTTime1 = cell (17,1);
FNTime1 = cell (17,1);
MPTime1 = cell (17,1);
for i=1:17
    FTTime1 {i,1}(:,1) = Time2(:,1);
    FNTime1 {i,1}(:,1) = Time2(:,1);
    MPTime1 {i,1}(:,1) = Time2(:,1);
    FTTime1 {i,1}(:,2) = (interp1(Time(:,1), AeroResultDataMatrix
(:,FT(i)), Time2(:,1)));
    FNTime1 {i,1}(:,2) = (interp1(Time(:,1), AeroResultDataMatrix
(:,FN(i)), Time2(:,1)));
    MPTime1 {i,1}(:,2) = (interp1(Time(:,1), AeroResultDataMatrix
(:,MP(i)), Time2(:,1)));
end
% ----- Output files -----
for i = 1:17
    fid =fopen(ColumnNamesFTout {i}, 'w');
    fprintf(fid,'%10.6e , %10.4e, \r\n', (FTTime1 {i,1}));
    fclose(fid);
    fid =fopen(ColumnNamesFNout {i}, 'w');
    fprintf(fid,'%10.6e , %10.4e, \r\n', (FNTime1 {i,1}));
    fclose(fid);
    fid =fopen(ColumnNamesMPout {i}, 'w');
    fprintf(fid,'%10.6e , %10.4e, \r\n',(MPTime1 {i,1}));
    fclose(fid);
end

```

The earthquake and wind files were then used as an input for the finite element model in ABAQUS as amplitudes using the following command in the .inp file in the dynamic loading step of the analysis. This is only shown for one wind force in this appendix because the input file for ABAQUS was too long.

```

*Amplitude, name=ForcN01_Blade1, INPUT=ForcN01_blade1.out
** Name: Blade1_Node1_FN   Type: Concentrated force
*Cloud, op=NEW, follower, amplitude=ForcN01_Blade1
_PickedSet357, 3, -1.

```

ABAQUS was then simulated through MATLAB parallel simulations for all earthquakes using a specific wind speed with the following code.

```

% Run parallel simulations for 44 earthquakes and wind 2.53 mps
iGM_Names = cell(22,2);
iGM_Names {1,1} = 'MUL009_0.0020_value.dat';
iGM_Names {1,2} = 'MUL279_0.0020_value.dat';

```



```

iGM_Names {2,1} = 'LOS000_0.0020_value.dat';
iGM_Names {2,2} = 'LOS270_0.0020_value.dat';
iGM_Names {3,1} = 'BOL000_0.0020_value.dat';
iGM_Names {3,2} = 'BOL090_0.0020_value.dat';
iGM_Names {4,1} = 'HEC000_0.0020_value.dat';
iGM_Names {4,2} = 'HEC090_0.0020_value.dat';
iGM_Names {5,1} = 'H-DLT262_0.0020_value.dat';
iGM_Names {5,2} = 'H-DLT352_0.0020_value.dat';
iGM_Names {6,1} = 'H-E11140_0.0020_value.dat';
iGM_Names {6,2} = 'H-E11230_0.0020_value.dat';
iGM_Names {7,1} = 'NIS000_0.0020_value.dat';
iGM_Names {7,2} = 'NIS090_0.0020_value.dat';
iGM_Names {8,1} = 'SHI000_0.0020_value.dat';
iGM_Names {8,2} = 'SHI090_0.0020_value.dat';
iGM_Names {9,1} = 'DZC180_0.0020_value.dat';
iGM_Names {9,2} = 'DZC270_0.0020_value.dat';
iGM_Names {10,1} = 'ARC000_0.0020_value.dat';
iGM_Names {10,2} = 'ARC090_0.0020_value.dat';
iGM_Names {11,1} = 'YER270_0.0020_value.dat';
iGM_Names {11,2} = 'YER360_0.0020_value.dat';
iGM_Names {12,1} = 'CLW-LN_0.0020_value.dat';
iGM_Names {12,2} = 'CLW-TR_0.0020_value.dat';
iGM_Names {13,1} = 'CAP000_0.0020_value.dat';
iGM_Names {13,2} = 'CAP090_0.0020_value.dat';
iGM_Names {14,1} = 'G03000_0.0020_value.dat';
iGM_Names {14,2} = 'G03090_0.0020_value.dat';
iGM_Names {15,1} = 'ABBAR--L_0.0020_value.dat';
iGM_Names {15,2} = 'ABBAR--T_0.0020_value.dat';
iGM_Names {16,1} = 'B-ICC000_0.0020_value.dat';
iGM_Names {16,2} = 'B-ICC090_0.0020_value.dat';
iGM_Names {17,1} = 'B-POE270_0.0020_value.dat';
iGM_Names {17,2} = 'B-POE360_0.0020_value.dat';
iGM_Names {18,1} = 'RIO270_0.0020_value.dat';
iGM_Names {18,2} = 'RIO360_0.0020_value.dat';
iGM_Names {19,1} = 'CHY101-E_0.0020_value.dat';
iGM_Names {19,2} = 'CHY101-N_0.0020_value.dat';
iGM_Names {20,1} = 'TCU045-E_0.0020_value.dat';
iGM_Names {20,2} = 'TCU045-N_0.0020_value.dat';
iGM_Names {21,1} = 'PEL090_0.0020_value.dat';
iGM_Names {21,2} = 'PEL180_0.0020_value.dat';
iGM_Names {22,1} = 'A-TMZ000_0.0020_value.dat';
iGM_Names {22,2} = 'A-TMZ270_0.0020_value.dat';
length_Name = cell(22,2);
for i=1:22
    for j=1:2
        length_Name{i,j} = char(iGM_Names{i,j});
    end
end
Analysis_Names = cell(22,2);
for i=1:22
    Analysis_Names{i,1} = sprintf('%s%s%s',length_Name{i,1}(1:end-17),'_', length_Name{i,2}(1:end-17));
    Analysis_Names{i,2} = sprintf('%s%s%s',length_Name{i,2}(1:end-17),'_', length_Name{i,1}(1:end-17));
end
Command = cell(44,1);

```

```
command = reshape(Analysis_Names,44,1);
for i=1:44
    Command{i,1} = sprintf('%s%s', 'abaqus inter j=',command{i,1});
end
matlabpool(4)
tic
% Run a for loop in parallel
parfor i=1:44
    A = char(Command{i,1});
    system(A)
end
matlabpool close
toc
```

VITA

Mohammad-Amin Asareh was a Structural Engineering PhD student in Civil, Architectural, and Environmental Department at the Missouri University of Science and Technology (Missouri S&T). In May, 2015, he received his PhD in Structural Engineering from Missouri University of Science and Technology. He was born in Ahwaz, Iran. He Attended Khajeh Nassir University of Technology in Tehran from 2001 to 2005 and received his B.S. degree in Civil Engineering. In 2005 he was granted to study in the same university and earned his M.S. degree in Structural Engineering working on the nonlinear dynamic behavior of jacket type offshore platforms considering soil-structure interaction. He joined Missouri S&T in 2009 to pursue his PhD. During his PhD program he worked on several projects dealing with programing and developing codes, finite element simulations, structural dynamics, and high performance computing on bridge foundations and wind turbine structures.